Fuzzy and Sliding Mode Controller Based Performance Analysis for Maximum Power Point Tracking of Photovoltaic Systems for Water Pumping Applications

LETA GETACHEW JALETA

A Thesis Submitted To

Department of Electrical Power and Control Engineering

School of Electrical Engineering and Computing

Presented in Partial Fulfillment of the Requirement for the Degree of Master's in Electrical Power and Control Engineering (Control Engineering)

Office of Graduate Studies

Adama Science and Technology University

March, 2023

Adama, Ethiopia

Fuzzy and Sliding Mode Controller Based Performance Analysis for Maximum Power Point Tracking of Photovoltaic Systems for Water Pumping Applications

LETA GETACHEW JALETA

Advisor: TAFESSE ASRAT ABERA (PhD)

A Thesis Submitted to

Department of Electrical Power and Control Engineering

School of Electrical Engineering and Computing

Presented in Partial Fulfillment of the Requirement for the Degree of Master's in Electrical Power and Control Engineering (Control Engineering)

Office of Graduate Studies

Adama Science and Technology University

March, 2023

Adama, Ethiopia

DECLARATION

I hereby declare that this master's thesis, entitled “Fuzzy and Sliding Mode Controller Based Performance Analysis for Maximum Power Point Tracking of Photovoltaic Systems for Water Pumping Applications" is my original work. That is, it has not been submitted for the award of any academic degree, diploma, or certificate at any other university. All sources of materials that are used for this thesis have been duly acknowledged through citation.

Leta Getachew		
Name of Student	Signature	Date

RECOMMENDATION OF ADVISOR

I, the advisor of this thesis, hereby certify that I have read the revised version of the thesis entitled "Fuzzy and Sliding Mode Controller Based Performance Analysis for Maximum Power Point Tracking of Photovoltaic Systems for Water Pumping Applications" prepared under my guidance by Leta Getachew Jaleta. Therefore, I recommend the submission of the revised version of the thesis to the department following the applicable procedures.

Tafesse Asrat Abera (PhD)

Advisor name	Signature	Date

APPROVAL OF BOARD OF EXAMINERS

I the advisors of the thesis entitled "Fuzzy and Sliding Mode Controller Based Performance Analysis for Maximum Power Point Tracking of Photovoltaic Systems for Water Pumping Applications" and developed by Leta Getachew Jaleta, hereby certify that the recommendation and suggestions made by the board of examiners are appropriately incorporated into the final version of the thesis.

____________________	_______________	____________
Advisor	Signature	Date

We, the undersigned, members of the Board of Examiners of the thesis by Leta Getachew Jaleta, have read and evaluated the thesis entitled " Fuzzy and Sliding Mode Controller Based Performance Analysis for Maximum Power Point Tracking of Photovoltaic Systems for Water Pumping Applications" and examined the candidate during an open defense. This is, therefore, to certify that the thesis is accepted for partial fulfillment of the requirement of the degree of Master of Science in Control Engineering.

______________________	______________________	________________
Chairperson	Signature	Date
______________________	______________________	________________
Internal Examiner	Signature	Date
Dr Beteley Teka	______________________	04-05-2023
External Examiner	Signature	Date

Finally, approval and acceptance of the thesis are contingent upon submission of its final copy to the Office of Postgraduate Studies (OPGS) through the Department Graduate Council (DGC) and School Graduate Committee (SGC).

________________________	_____________	__________
Department Head	Signature	Date
________________________	_____________	__________
School Dean	Signature	Date
________________________	_____________	__________
Office of Postgraduate Studies, Dean	Signature	Date

ACKNOWLEDGMENTS

First and foremost, I would like to express my deep gratitude to Almighty God for providing me with the chance and direction to accomplish my objective, as well as for his love and mercy that have kept me going during this difficult but thrilling journey.

Secondly, I would like to express my special thanks to my advisor, **Dr. Tafesse Asrat,** for giving me the opportunity to conduct research under his guidance and supervision. I received motivation, comments, encouragement, and continuous guidance from him during my graduate studies.

I am extending my thanks to the Oromia Water and Energy Office, Addis Ababa, for their willingness to give me sources that are related to my thesis.

TABLE OF CONTENTS

DECLARATION i
RECOMMENDATION OF ADVISOR ii
APPROVAL OF BOARD OF EXAMINERS iii
ACKNOWLEDGMENTS iv
LIST OF TABLES ix
LIST OF FIGURES x
LIST OF ACRONYMS xii
LIST OF ABBREVIATIONS xiii
ABSTRACT xv
CHAPTER ONE 1
INTRODUCTION 1
1.1 Background of the Study 1
1.2 Background of Photovoltaic Pumping System 4
1.3 Working Principle of Solar Water Pumps 4
1.3.1 Type of Water Pump Systems 5
1.4 Brushless DC Motor 6
1.5 Statement of the Problem 7
1.6 Objectives of the Thesis 8
1.6.1 General Objective of the Thesis 8
1.6.2 Specific Objectives of the Thesis 8
1.7 Scope of the Thesis 8
1.8 Limitation 9
1.9 Significances of the Thesis 9
1.10 Motivation 9
1.11 Thesis Outline 10

CHAPTER TWO **11**
LITERATURE REVIEW **11**
2.1 General Theory and Background 11
2.2 Reviews of Other Related Work 12
2.3 Stand-alone, Grid and Hybrid Photovoltaic Systems 15
2.4 Photovoltaic Models 16
2.5 Conventional Techniques for MPPT of A PV System 17
2.6 Classification of MPPT Techniques 17
2.6.1 Offline Technique 18
2.7 Perturb and Observe (P&O) 20
2.8 Convergence Speed 21
CHAPTER THREE **23**
MODELLING AND DESIGN OF SOLAR MPPT ALGORITHM **23**
3.1 METHEDOLOGY 23
3.2 WATER PUMPING SYSTEM DESIGN 23
3.3 Power Source for Pumps 24
3.4 Design population and daily water demand 25
3.4.1 Determination of Hydraulic power 25
3.4.2 Pump Selection 30
3.4.3 PV Panel Structure 31
3.4.4 Water Storage versus Battery Storage 31
3.4.5 AC versus DC pump 31
3.5 Relationship among PV Cell, Module and Array 32
3.5.1 Photovoltaic Cell 32
3.5.2 Photovoltaic Module 32
3.5.3 Photovoltaic Array 33
3.6 Working Principle of PV Cell 33

3.7 MODELING OF PHOTOVOLTAIC SYSTEM 34
3.7.1 Photovoltaic Characteristics under Varying Irradiances 37
3.7.2 I-V and P-V Characteristics under Varying Temperatures 38
3.8 Effects of Partial Shading on PV or Mismatch Factors 39
3.9 Identification of PV Model Parameters 40
3.10 Maximum Power Point Tracking Controller 44
3.11 Performance specifications of MPPT control algorithm 44
3.11.1 Dynamic Response...45
3.11.2 Steady-State Error...45
3.11.3 Tracking Efficiency 45
3.12 DC-DC Converter Used for the MPPT System 45
3.12.1 Boost Converter 46
3.12.2 Boost Converter Design...47
3.13 Perturb and Observation Based MPPT Technique 49
3. 14 Fuzzy Maximum Power Point Tracking Method 52
3.14.1 Rules of Fuzzy Logic Controller 53
3.14.2 Fuzzy Logic Controller Structure 54
3.15 Sliding Mode Controller Based Solar MPPT 57
3. 16 Fuzzy Sliding Mode Control Algorithm..60
3.17 Design of BLDC Motor for Solar Water Pumping System 61
3.17.1 Mathematical Model of a Brushless Direct Current Motor 62
CHAPTER FOUR **65**
RESULTS AND DISCUSSIONS **65**
4.1 Photovoltaic System Modeling Using MATLAB/Simulink........................65
4.2 Effect of Irradiance on the Performance of a PV Module 65
4.3 Effect of the Temperature on the Performance of a PV Module 66
4.4 Current and Power Curves under Partial Shading 67

4.5 Simulation Result of P and O with in different Disturbances.....................68
4.6 Simulation of FLC Solar MPPT at Constant Irradiation and Temperature 71
4.6.1 Simulation of the System at Variable Irradiation 73
4.7 Simulation Results of Sliding Mode Controller at Uniform Temperature and Irradiation 74
4.8 Simulation Result of a Fuzzy Sliding Mode Controller 78
4.9 Simulation Result of BLDC Motor 85
CHAPTER FIVE 87
CONCLUSION AND RECOMMENDATION 87
5.1 CONCLUSION 87
5.2 RECOMMENDATIONS AND FUTURE WORKS 88
ACKNOWLEDGMENTS..89
REFERENCES...90
APPENDIXES 96

LIST OF TABLES

Table 1.1 Comparison between water pumping systems powered by PV and diesel generator .3
Table 1.2 The Advantages and Disadvantages of the Motors 7
Table 2.1 General description of Solar MPPT algorithm and its limitations 22
Table 3.1 Water requirement assumptions in a day per person in a family and animals(Note, n.d.) 26
Table 3.2 Single solar data sheet 41
Table 3.3 Electrical characteristics data of PV module taken from the datasheet.....................42
Table 3.4 The Proposed Module and Array Value 43
Table 3.5 Boost Converter Parameters 48
Table 3.6 Control Actions for Various Operating Points in the P & O Method 49
Table 3.7 Fuzzy Rule Base Table 55
Table 4.1 Efficiency of Perturb and Observe Algorithm Temperature 71
Table 4.2 Performance of FLC at different Irradiation and at 25^0C...74
Table 4.3 Performance of SMC at different Irradiation and at 25^0C..77
Table 4.4 Performance of FSMC under different Irradiation and at 25^0C 81
Table 4.5 Performance of FSMC under different Temperature and at 1000W/m^2 83
Table 4.6 The performance MPPT algorithms at 25^0C and 1000W/m^2 84
Table 4.7 The performance of MPPT algorithms at different temperature and irradiance 84

LIST OF FIGURES

Figure 1. 2 Photovoltaic Pumping System(Khazane & Tissir, 2018) 5
Figure 2.1 Parallel Series Connection Of Solar System (Brahmi et al., 2018) 11
Figure 2.2 Basic Structure of PV Cell(Sethy & Maity, 2010).. 16
Figure 2.3 Classification of Commonly Used MPPT Technique 18
Figure 2.4 Flowchart For Short Circuit Current Technique(Subbarao & Kalyan, 2021).......... 19
Figure 2.5 P-V Characteristics Curve of an PV Module 20
Figure 3.1 Methodology for the thesis 23
Figure 3.2 A Solar Water Pumping System with Submersible Pump 25
Figure 3.3 Numbers of Seven Series Modules and Four Parallel String of PV Array 30
Figure 3.4 Relationship among PV Cell, Module and Array 33
Figure 3.5 Equivalent Circuit Model of a Solar Cell... 34
Figure 3.6 The Semiconductor of Converting Light Energy.. 37
Figure 3.7 I-V and P-V characteristics at constant temperature STC 25^0C 37
Figure 3.8 I-V and P-V at constant Irradiance 1000W/m^2 but at different temperature 38
Figure 3.9 Shaded PV Cell 39
Figure 3.10 Maximum Power Point Tracking System Using FSMC(El, 2017)........................ 44
Figure 3.11 DC-DC Boost Converters(ÇELİKEL & GÜNDOĞDU, 2021)............................ 46
Figure 3.12 Matlab Simulink of Dc-to-Dc Boost Converter.. 49
Figure 3.13 Flow Chart of Perturbation and Observation 51
Figure 3.14 Matlab / Simulink of Perturbation and Observation 51
Figure 3.15 Tracking of the MPPT by FLC 53
Figure 3.16 Flow Chart of Fuzzy Logic Controller(Baramadeh et al., 2021) 54
Figure 3.17 Fuzzy Logic Control Designer of Two input and one output 56
Figure 3.18 Fuzzy Membership Functions (MFs) and Rules 57
Figure 3.19 Matlab Simulink of fuzzy logic controller... 57
Figure 3.20 Flow Chart Sliding Mode Control Algorithm of the Vref on the Controller 59
Figure 3.21 Simulink Model of Sliding Mode Controller.. 60
Figure 3.22 Simulink Model of Fuzzy-Sliding Mode Controller... 61
Figure 3.23 The equivalent circuit of BLDC Motor.. 63
Figure 3.24 Model of the BLDC Motor 64

Figure 4.1 Effect of Irradiation on the PV voltage and current output....................................66
Figure 4.2 Effect of Irradiation on PV output Power 66
Figure 4.3 Effect of Temperature on output voltage and current 67
Figure 4.4 Effect of the temperature on solar power output..67
Figure 4.5 Current and Power Curve of under Partial Shading showing Local and Global MPP 68
Figure 4.6 The PV-Voltage, PV-Current and PV- Power of P and O at 25^{o}C Respectively ...69
Figure 4.7 The Output-Voltage, Output- Power and Output-Current of P and O 70
Figure 4.8 Output current and PV-Current of FLC under uniform Irradiation 72
Figure 4.9 Output Voltage and PV-Voltage of FLC at uniform Irradiation.............................72
Figure 4.10 Output Power and PV-Power of FLC at uniform Irradiation................................73
Figure 4.11 Output Power and PV-Power of FLC at different Irradiation...............................73
Figure 4.12 Signals at Variable Irradiations 74
Figure 4.13 MPPT performance of SMC at 25^{0}C and 1000W/m^{2} 75
Figure 4.14 PV and Output-Current of SMC respectively 76
Figure 4.15 Output Voltage and PV-Voltage of SMC under uniform Irradiation 76
Figure 4.16 MPPT performance of SMC with sudden variation of irradiation........................78
Figure 4.17 MPPT performance of SMC with sudden variation of Temperature 78
Figure 4.18 MPPT Output Power of FSMC with uniform Temperature and Irradiation..........79
Figure 4.19 MPPT Output Voltage of FSMC with uniform Temperature and Irradiation 80
Figure 4.20 MPPT Output-Current of FSMC with uniform Temperature and Irradiation........80
Figure 4.21 MPPT performance of FSMC with sudden variation of irradiation 81
Figure 4.22 MPPT Voltage of FSMC with sudden variation of irradiation.............................82
Figure 4.23 MPPT Current of FSMC with sudden variation of irradiation 82
Figure 4.24 MPPT performance of FSMC with sudden variation of Temperature..................83
Figure 4.25 Rotation speed of motor 85
Figure 4.26 Back EMF 86
Figure 4.27 Electromagnetic Torque 86
Figure 4.28 Stator Current 86

LIST OF ACRONYMS

A	Ideality Factor
Cmin	Minimum Capacitor
D	Duty Cycle or Duty Ratio
E_g	Band gap Energy of Semiconductor
G	Solar Irradiation (W/m^2)
G_o	Nominal Irradiation (W/m^2)
I_{photo}	Solar Generated Current or Photo current (A)
Isc	Short-Circuit Current
I_D	Diode Current
K_i	Temperature Coefficient
$I_{r,sat}$	Reverse Saturation Current
L_{min}	Minimum Value of inductance
Lo	Lower Limit
Ns	Number of cells connected in series
Np	Number of cells connected in parallel
P	Power (w)
Rsh	Shunt Resistor
Rs	Series Resistor
T	Actual Temperature
Up	Upper Limit
V	Voltage
Voc	Open Circuit Voltage
Vref	Reference Voltage
V_T	Thermal Voltage

LIST OF ABBREVIATIONS

AC	Alternating current
ANN	Artificial Neural Network
BLDC	Brushless Direct Current Motor
CRF	Current Ripple Factor
CRV	Capacitor Ripple Voltage
DC	Direct current
EMF	ElectroMotive Force
I-V	Current-Voltage
FF	Fill Factor
FL	Fuzzy Logic
FLC	Fuzzy Logic Controller
FSMC	Fuzzy Sliding Mode Controller
IM	Induction Motor
INC	Incremental Conductance
KCL	Kirchhoff's Current Law
KVL	Kirchoff's Voltage Law
MATLAB	Matrix Laboratory
MF	Membership Function
MP	Maximum Power
MPP	Maximum Power Point
MPPT	Maximum Power Point Tracking
NB	Negative Big
NM	Negative Medium
NS	Negative Small
P and O	Perturb and Observe
PB	Positive Big
PM	Positive Medium
PS	Positive Small
PV	Photovoltaic
PVPS	Photovoltaic pumping system

SMC	Sliding Mode Controller
STC	Standard Test Condition
TDH	Total Dynamic Head
Z	Zero

ABSTRACT

The best source of energy is solar energy, which naturally regenerates itself in a short amount of time and is referred to as renewable energy or sustainable energy. The maximum power point (MPP) of solar panels, which is dependent on external parameters including temperature and irradiance, has a nonlinear voltage-current characteristic, and its maximum power point is not constant. Which maximizes the power output for a specific set of conditions is critical for water pumping systems in order to capture the maximum power from the solar panels on a continuous basis. Using a fuzzy sliding control scheme, a stand-alone photovoltaic (PV) system can achieve maximum power point tracking. The main objectives of these controllers are to increase the effectiveness of the PV power system, achieve maximum power point operation without the requirement for atmospheric condition measurement, and reduce the chattering of the sliding mode controller. The power oscillation around the operating point is a problem that most commonly affects maximum power point tracking techniques and is determined by the proposed controller. Environmental elements like varying temperatures and radiance, shadows cast by tall buildings and trees, and solar system performance all have an impact. Such varying environmental conditions affect solar cells' efficiency. To improve the efficiency of the solar system, power extraction must be optimized under all weather conditions. Using solar photovoltaic systems as a source of energy is beneficial over fossil fuels and has no environmental issues like atmospheric greenhouse gas emissions that result in acidic rain, global climate change, etc. This thesis focuses on increasing energy extraction by improving maximum PowerPoint tracking (MPPT). One of the most promising areas of photovoltaic applications is the use of photovoltaic energy as a source of energy for water pumping. From the simulation, the highest performance values for perturb and observe are 98.70%, the highest performance for a fuzzy logic controller is 99.60%, the highest performance, or efficiency sliding mode, is 99.66%, and the hybrid efficiency of a fuzz-sliding mode controller is 99.97%. Kyocera KC200G. In this thesis, 5.682 KW of power is designed for a BLDC solar water pumping system.

Keywords: DC-DC boost converter, fuzzy logic, fuzzy sliding mode control, maximum power point tracking, PV water pumping system, sliding mode control

CHAPTER ONE

INTRODUCTION

1.1 Background of the Study

The best source of energy is solar energy, which naturally regenerates itself in a short amount of time and is referred to as renewable energy or sustainable energy. One of the renewable energy sources that can offer us consistent, dependable power is solar energy. No gases or poisons are emitted into the air. Solar power systems need minimal maintenance. Solar panels can survive for 25 years with no lubrication or upkeep(Abdul-Razzaq et al., 2021).

In rural areas(Shebani & Iqbal, 2017), pumping systems are needed to pump water for domestic use, irrigating crops, watering cattle and livestock, and more. Therefore, a power source is required to operate the pumping system. Diesel pumps are frequently utilized to supply water in isolated and rural places. Diesel pumps use more fuel, have a greater impact on the environment, need special maintenance, and are less dependable. Photovoltaic water pumps(Miqoi et al., 2019) is technology of electronic power systems, as well as significant advancements in the field of solar cells, have attracted a lot of attention lately. The PV system is widely used in remote and rural areas where no public grid is available and the installation of new power lines and transformers may be costly. Water pump readings in this thesis process are one of the many applications for PV power in rural areas. Traditionally, electrical energy is produced mainly from fossil fuels and nuclear power plants. Water is essential for human life and one of the most fundamental requirements for rural development(Solomon et al., 2021).

A photovoltaic water pumping system (PVPS) contains a PV array, a pump subsystem, and storage. The storage items may be electric storage batteries, a water storage tank, or both. Solar photovoltaic (PV) systems are a source of clean and natural energy. Photovoltaic panels have a unique point that represents the most available energy, and this point depends on environmentally friendly conditions such as temperature and irradiance(Solomon et al., 2021).

Maximum power point tracking (MPPT) is required for optimal performance. Sunshine is the most important component of a PV system. Solar radiation is the term that refers to photons (or electromagnetic waves) generated by the sun. It is important to note that solar radiation is measured in units of energy(Gouws & Lukhwareni, 2012). On the other hand, solar irradiation is the solar power incident per unit area on the earth's surface in units of watts per square meter (W/m^2).

Consumers strive to offset the rise in carbon emissions and the fall in the usage of fossil fuels by using renewable energy for immediate use. Solar power generation is the most environmentally friendly alternative to conventional power systems (B. S. Kumar et al., 2020). Because it produces no emissions, pure, limitless, and is abundant, solar energy is one of the main sources of green energy. Photovoltaic energy is being used and developed more and more everywhere. One of the promising uses for solar energy is photovoltaic pumping, particularly in rural locations with a lot of insolation but no electric grid access.

A PV system's ability to reduce carbon dioxide (Co2) emissions is a huge benefit. Professionals predict that until 2040, renewable energy derived from PV systems will be the main replacement source (Narendiran, 2016).The Consumption of solar energy is rising daily. A highly pure source of energy is solar energy. After installation, it is clean and doesn't release any greenhouse emissions. It can reduce the amount of electricity produced by burning fossil fuels like coal and gas, which pollute the air, land, and water. One of the most practical uses of solar energy is water pumping.

Photovoltaic (PV) is a technology in which radiant energy from the sun is converted to direct current (DC) electricity. The most important advantages of photovoltaic systems are:

- The photovoltaic processes are completely solid state and self-contained.
- There are no moving parts and no materials consumed or emitted.
- They are non-polluting emissions.
- They require no connection to an existing power source or fuel supply.
- They may be combined with other power sources to increase system reliability.
- They can withstand severe weather conditions, including cloudy weather.
- They consume no fossil fuels - their fuel is abundant and free.

Table 1.1 Comparison between water pumping systems powered by PV and diesel generator

System type	Advantage	Disadvantage
Photovoltaic Powered system	✓ Low maintenance ✓ Reliable long life ✓ No fuel and no fumes ✓ Easy to install ✓ System is modular and ✓ closely matched to need ✓ free from pollution	✓ Relatively high initial cost ✓ Low output in cloudy weather
Diesel (or Gas) Powered System	✓ Moderate capital costs ✓ Easy to install ✓ Linear and control operation and does not depend on the weather condition	✓ Needs maintenance and Replacement ✓ Noise, fume, dirt problems ✓ High environmental pollution

Generally, photovoltaic systems operate in two different modes: off-grid and on-grid connected. As their name suggests, standalone PV systems are made to operate independently of the utility grid. These systems are composed of several components that convert solar energy into electric energy in a controlled, reliable, and efficient manner in order to supply a DC or AC load.

One of the finest solutions for supplying electricity needs in rural or isolated areas when utility power is unavailable or expensive is an off-grid PV system. Among the various off-grid PV system applications, the water pumping system is among the most alluring and promising in a variety of fields, including small-scale irrigation systems, fish farms, and the delivery of water to homes and livestock.

A technique for maximizing energy extraction from a photovoltaic (PV) power system is provided in this thesis. The maximum power of a PV module changes with temperature, solar radiation, and load. In order to enhance efficiency, PV systems employ a Maximum Power

Point Tracker (MPPT) to continuously extract the highest power and deliver it to the load. A controller and a dc-dc converter make up an MPPT. The MPPT locates the maximum power point and maintains operation there using a tracking algorithm.

1.2 Background of Photovoltaic Pumping System

Different water pumping systems use electricity and diesel to run the pumps. However, this kind of source has several drawbacks, such as environmental pollution, low reliability, high fossil fuel prices, low efficiency, and high maintenance costs(Gonal, 2016). In various remote and isolated regions, hand pumps or diesel-driven pumps are used for water supply. Diesel pumps consume fossil fuel, affect the environment, need more maintenance and are less reliable(Moussa et al., 2019). A PV pumping system is operated independently of the utility grid and is composed of several components, such as a PV array, power converters, an electrical motor, a water pump, and a storage element, which can be a battery bank or a water tank. PV pumping systems are generally installed with a battery bank and can work without chemical storage elements.

In battery-less PV pumping systems, fluid storage takes the place of batteries, and steady-state operation is dependent on the amount of power available in order to improve system reliability and lower costs (batteries are bulky, expensive, and have a limited lifespan) (Muralidhar, 2021). The PV pumping system has the ability to provide power to either AC or DC motors. Boost, Buck, and Buck Boost are a few types of single-stage DC-DC power converters that can be used with DC motor pumping systems instead of connecting the DC motor directly to the PV array. Inverter control is difficult because many control goals, such as maximum power point tracking (MPPT) and the reduction of electromechanical conversion losses, must be taken into account at once.

1.3 Working Principle of Solar Water Pumps

A solar pump's operation is based on the photovoltaic principle. When a solar pump is running, PV (photovoltaic) systems catch the radiant sun's energy and turn it into electricity. The resulting electricity was sufficient to power the entire system. Either the electricity generated by photovoltaic (PV) panels or the radiant heat produced by stored solar energy powers solar water pumps.

The solar-powered pump runs on solar electricity. It is made up of a water storage tank, a DC water pump, a solar controller (MPPT), and an array of solar panels. Solar pumping systems are an efficient way to deal with the water shortage in communities. Solar pumping devices are additionally employed in the communal water supply for irrigation.

A solar pump is a machine that raises liquid from a low level to a high level using solar energy, which is afterwards converted into electrical energy by photovoltaic panels. Solar energy or light energy strikes on photovoltaic panels, where it is transformed into DC electrical energy. Now, this DC can either power a DC motor connected to a pump or it can power an AC motor by being inverted through an inverter(W*hat Is a Solar Pump : Working & Its Applications What Is a Solar Pump*, 2021).

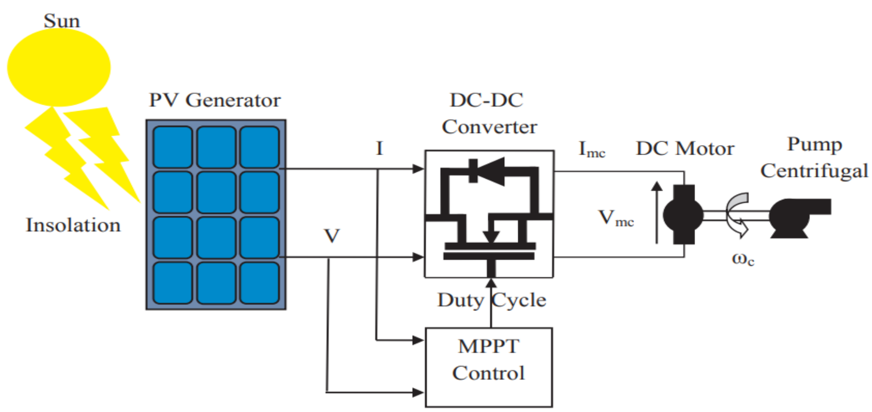

Figure 1. 1 Solar water pumping system (Khazane & Tissir, 2018)

1.3.1 Type of Water Pump Systems

Solar-powered pumps are ones that run on electricity produced by photovoltaic panels or the radiated thermal energy that is accessible from gathering sunshine, as opposed to grid electricity or diesel-powered water pumps.

Since, solar photovoltaic modules produce their own power during the day, a solar water pumping system can function independently of other systems.

There are different varieties of solar pumps available on the market. Submersible, surface, and floating water pumps can be divided into three groups according to the volume of water they need to move(Raghuwanshi & Khare, 2018).

Submersible Solar Pumps: Pumps that are submersible in water, such as those found in shallow wells and boreholes, are known as submersible solar pumps. Inside the well or borehole in these systems is where the solar water pump is located. Water is usually pumped to a water reservoir from a borehole or well, which typically has a solar array close to the top. Usually, the solar array is where the pump controller is located. The connection between the pump and pump controller is made using waterproof cables.

Surface Solar Pumps: These systems are typically used in shallow wells or boreholes and also lakes, rivers and any open water source that is near or on the surface.

1.4 Brushless DC Motor

The BLDC motor is specially designed to meet the demands of the commercial and industrial sectors. Due to their long lifespan, strong torque-to-mass ratio, low noise, and improved dependability, BLDC motors have a variety of advantages over DC and induction motors. Because there are no mechanical commutators in BLDC motors, they offer a longer lifespan and a greater dynamic response. Additionally, it is used in a variety of industrial industries due to its high efficiency and minimal maintenance costs(Nakuçi & Spahiu, 2018).

Due to their efficiency in terms of energy use, brushless DC (BLDC) motors are essential to this trend. In comparison to an induction motor, which is frequently used in solar photovoltaic (PV)-based water pumping, BLDC motors offer a high power density, high efficiency, high torque or inertia ratio, and a high power factor. Additionally, unlike an induction motor, a BLDC motor's speed is not limited by power frequency.

The motor's size is thereby lowered, while its capacity is raised(Spandana & Kanchikere, 2018). In contrast to other rotating electrical machines, BLDC motors have a comparable design and operation. It consists mostly of two components, a rotor and a stator. The other essential parts are the stator winding and permanent magnet, which are mounted on the stator and rotor, respectively. Permanent magnets are sometimes known as rotor magnets.

Table 1.2 The Advantages and Disadvantages of the Motors

Motor Type	Advantages	Disadvantages
Brushed DC Motor	Simple and efficient for small loads. No complex control circuitry Needed.	Brushes need replacing periodically. They have short service life
Brushless DC Motor	Efficient. Less maintenance required It has no brush Inverter is not required Long operating life	Electronic commutation adds extra expense and possible breakdown risk.
AC-motor	Larger range available for larger loads. Cheaper than DC-motors.	Less efficient than DC units. An inverter would be required to converter DC electricity produced by solar panels to AC. This increase complexity and cost, it reduces efficiency.

1.5 Statement of the Problem

The solar system's performance is influenced by natural factors such as temperature and radiation, as well as the shadows cast by large objects like trees and buildings. Depending on the surroundings, a solar cell's efficiency can change. To improve the total efficiency of the solar system, energy production must be enhanced under all weather conditions.

In addition, variations in temperature, solar radiation, and load affect a PV module's maximum power. In order to enhance efficiency, photovoltaic systems use a maximum power point tracker (MPPT) to continually gather the most power that a solar panel is capable of producing and then transmit it to the load. It represents maximum power is not delivered from PV source to load. So it is necessary to provide a MPPT technique to extract maximum power from PV cells.

Fuzzy and sliding mode techniques are efficient, fast, and reliable methods of tracking the maximum power point. The application of these two approaches significantly increases the system efficiency for all environmental conditions. The sliding mode technique is a very fast, and robust algorithm that works effectively under different weather conditions, but this algorithm has chattering phenomena. The efficiency of the photovoltaic system decreases as a result of chattering. In this thesis FSMC approaches uses fuzzy logic to reduce oscillation around the operating point in order to get rid of the chattering phenomenon that the sliding mode technique has. These methods control the duty ratio of a DC-DC converter to produce maximum power from the solar panel. The duty ratio of the DC-DC boost converter is controlled to optimize the design and performance of the FSMC for the MPPT PV water pumping system.

1.6 Objectives of the Thesis

1.6.1 General Objective of the Thesis

The main objective of this thesis is to Analysis Performance of Fuzzy and Sliding Mode Controller of Maximum Power Point Tracking of Photovoltaic Systems for Water Pumping Applications.

1.6.2 Specific Objectives of the Thesis

- To investigate and analyze the effects of irradiation and temperature changes on the output characteristics of the PV array.
- Implement the proposed controllers using Matlab/Simulink to test the overall system efficiency in different weather conditions.
- Compare the results of FSMC with FLC and SMC, as well as to perturb and observe under various weather conditions.
- To analyses the simulations results and make recommendation based on the finding of this thesis.

1.7 Scope of the Thesis

The scope of this thesis is to investigate how to improve the MPPT in a stand-alone PV water pumping system by using MATLAB/SIMULINK to test the overall system efficiency and compare a fuzzy-sliding mode controller. To design and simulate an efficiency controller for a

PV system capable of identifying and tracking the MPP of PV in a short time with low oscillation under all conditions. To investigate MATLAB modeling methods for PV module behavior under various environmental conditions. Compare the efficiency of a solar photovoltaic system using traditional perturb and observe maximum power point tracking techniques (MPPT) with intelligent controllers such as fuzzy logic controllers and a robust solar MPPT technique sliding mode controller with a fuzzy-sliding mode controller on Matlab software or Simulink.

1.8 Limitation

This thesis is limited to providing theoretical design, modeling, and simulations of a PV water pumping system controller with MPPT. Hardware implementation will not be included in the system.

1.9 Significances of the Thesis

- To reduce power losses caused by weather conditions and improve the efficiency of photovoltaic panels.
- Efficiency analysis of power generated by standalone solar systems under variations in atmospheric conditions.
- To extract the maximum possible power generated from photovoltaic systems under atmospheric conditions, using fuzzy logic and a sliding mode control system.
- To extract the maximum possible power from a PV array.

1.10 Motivation

The demand for water for drinking purposes is still an issue to be solved in many developing countries, mainly in rural areas. With the energy crisis and pollution caused primarily by the use of fossil fuels, this problem has found a solution in the form of a solar photovoltaic water pumping (SPVWP) system. Now, solar-powered pumps represent a growing market as they offer a better and more viable solution for off-grid areas. The water pumping system, driven by electrical motors, is a popular application of photovoltaic energy utilization. The two main constraints for using solar energy are the high initial installation cost and the low photovoltaic cell conversion efficiency. Solar photovoltaic pumping systems have become so popular not only in the agricultural sector but also for drinking water and micro-irrigation applications in developing and developed countries.

1.11 Thesis Outline

This study is organized into five chapters.

Chapter 1: An introduction, a statement of the problems, objectives, significance, scope, and limitations, as well as the significance and motivations for the proposed thesis are included.

Chapter 2: A literature review on the background of PV, MPPT algorithm techniques, and related works is discussed.

Chapter 3 describes the controller's design, the DC-DC boost converter, and the MPPT algorithm.

Chapter 4 summarizes the results of the simulation work and discussions.

Chapter 5: Finally, the conclusion and recommendation are made.

CHAPTER TWO

LITERATURE REVIEW

2.1 General Theory and Background

The MPPT control is a complex issue because, on the one hand, the PV panel will always suffer from rapid external disturbances due to the variation in weather conditions. The design of a suitable maximum power point tracking (MPPT) controller is challenging since the PV system may suffer various internal disturbances, such as load change(Derri et al., 2016).

The efficiency of solar photovoltaic (PV) energy conversion is low, and the characteristics of PV arrays are highly nonlinear and dependent on the surrounding environment. These problems must be set for the PV pumping system to function at its most effective level, therefore, an MPPT is required. To fight global warming and other issues related to fossil fuels, the majority of countries are switching to renewable energy sources like sunlight, biomass, water, and wind. Despite the fact that renewable energy is currently used in many countries, some applications and locations do not benefit from it. However, photovoltaic arrays are used for a number of purposes, such as street lighting, battery charging, and water pumping. In this situation, the load might need more power than the PV system is able to supply. In order to maximize the power generated by the PV system and obtain the required power, a power conversion system is used.

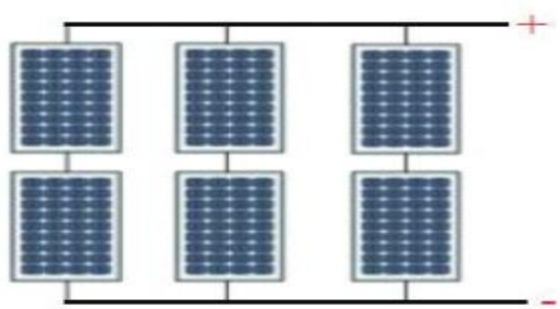

Figure 2.1 Parallel Series Connection Of Solar System (Brahmi et al., 2018)

Many researchers have investigated the use of solar energy. Solar cells are known to be inefficient; therefore, a better control mechanism is required to improve efficiency. To accomplish this, work must be done at MPP, when the power output is at its peak, which is determined by the temperature of the panels as well as the irradiance conditions. Both conditions alter during the day and differ depending on the season. Irradiation can also alter quickly as a result of changing meteorological conditions, such as passing clouds. Regardless of changes in the environment, the MPPT algorithm ensures that PV systems continue to produce maximum power.

2.2 Reviews of Other Related Work

(Kayisli, 2023) The need for renewable energy sources is increasing while the use of non-environmentally energy sources is decreasing day by day. At this point, solar energy which is a great natural energy source comes to the fore. MPPT control is performed based on sliding mode control as a robust control method. A super-twisting sliding mode controller has been developed and type 2 fuzzy set has been adapted to the system to reduce the chattering problem. The developed MPPT control algorithm is applied to a solar PV system and tested under variable irradiance conditions. Generally, many control algorithms have their own advantages and disadvantages. The chattering problem is one of the disadvantages of the SMC method in steady state.

(Chinnamayan, 2020) A conventional P&O technique measures the dc-dc converter's output power to change the voltage at the input of the converter by varying the duty cycle of the converter. MPPT technique is another technique in which a fixed percentage (71%-78%) of open circuit voltage is used as module operating voltage to extract maximum power from solar PV. Fractional Short Circuit Current MPPT technique is another technique in which a fixed percentage (78%-92%) of short circuit current is used as module operating current to extract maximum power from solar PV.

(Biadgie, 2021)An induction motor is an example of asynchronous AC machine, which consists of a stator and a rotor. A sinusoidal voltage is applied to the stator, in the induction motor, which results in an induced electromagnetic field. A current in the rotor is induced due to this field, which creates another field that tries to align with the stator field, causing the rotor to spin. In this work aim is to develop an MPPT controller based on FSMC which is the hybridization of fuzzy logic control and sliding mode control that improve system efficiency regardless of environmental condition. the limitation of this paper is one it is selected induction motor for water pumping because, induction motor requires inverter and it is complex with inverter. It is only based on fuzzy and sliding mode controller performance.

(El, 2017a)The output power of PV source is influenced by environmental factors, such as temperature and illumination; also the solar cell (I-V) characteristic is nonlinear. There is a unique point on the (I-V) or (P-V) curve of the solar array called MPP, where the entire PV system operates with maximum efficiency and produces its maximum output power. In a PV panel, MPP location is not known but can be located, either through calculation models, or by search algorithm. It is well known that SMC offer good robustness and transient performance. However due to the discontinuous control action, the chattering which is defined as the oscillations around the sliding surface exists and causes the steady state performance to degrade. Adding the Fuzzy Logic Control to the Sliding Mode Controller reduces these oscillations and gives better results.

In (Zhang et al., 2021) PV tracking has been accomplished using a variety of sophisticated techniques, including fuzzy logic control and artificial neural networks (ANN). The maximum power point technique based on neural networks, on the other hand, necessitates a large amount of representative input and output data. Insufficient data will prevent the neural network from producing the best results for the system. In addition, training takes more time due to the abundance of input and output data.

(Hahm et al., 2016a)Among all the MPPT techniques, the perturb and observe (P&O) strategy is widely used in practice because of its ease of implementation. This method is based on the perturbation of the photovoltaic system by the increase or decrease of the duty cycle, then observing the effect on the output power of PV generator.If the output power is increased due to the perturbation, this means that the operating point has moved toward nthe maximum power and, therefore, the following perturbation will be made in the same direction. But if the output power decreases, the new perturbation is made in the opposite direction. The major drawbacks of this strategy are deviation from the maximum power point during rapidly changing weather conditions. Fuzzy logic-based MPPT tracker have exposed very excellent performances under changing irradiation and temperature conditions without any knowledge of PV generator model. It requires good design to select appropriate fuzzification, inference mechanism, rule base, and defuzzification processes. The MPP tracking speed is faster with the increase in switching but voltage output and power output oscillations increases. The performances of the SMC based MPPT is high as compared to other classical techniques.

In (Singhal et al., 2021) The output characteristics of solar arrays are influenced by irradiance level, temperature, load. Through the use of MPPT technology, the MPP can increase work productivity and fully utilize solar energy resources. These days, the most popular MPPT solutions are the P&O and INC algorithms. But, the fault in this algorithm is that the oscillation is quite large at the maximum power point, so the approach fails to follow the MPP when the solar irradiance changes.

In (Singh & Mishra, 2015) Any solar pump with an electric motor can be powered by the sun. On-site solar panels that transform solar energy into direct-current (DC) electricity are used to generate electricity for the motor. A solar-powered pump needs a DC motor in order to function without the aid of other electrical components because the electrical output from a solar panel is DC in nature. For a pump using an alternating-current (AC) motor, an inverter would be necessary to convert the DC electricity generated by the solar panels to AC electricity. Most solar-powered pumps use DC motors since an AC system is more expensive, more complicated, and less efficient. This means that a DC motor is better than an AC motor.

In (Derbeli et al., 2018) Over the years, a number of MPPT techniques, such as the Perturb and Observe (P&O) algorithm and the Incremental Conductance (IC) algorithm, have been developed and are frequently used to find the maximum power point. There are additional artificial intelligence-based methodologies, such as fuzzy logic and neural network techniques. A strong controller seems to be necessary for ensuring high-accuracy tracking of the ideal location because weather conditions change frequently. The sliding mode controller has a faster tracking speed, and the strategy is still useful when the partial shading condition is changed.

In (Kchaou et al., 2017) The incremental conductance (INC) approach, which employs the features of the solar cell's power-voltage curve to locate the highest power point, is another classic method. When the slope of the power-voltage curve reaches zero, the maximum power point is reached. Under quickly varying situations, the INC can enhance tracking accuracy and dynamic performance. However, there are still some disturbances at the maximum power point. Sliding-mode control (SMC) is a strong tool for controlling uncertain systems. The system governed by sliding-mode control displays flexibility features in the face of both internal and external parameter uncertainties. In Sliding-mode control has been widely employed in power electronic equipment up to this point, and numerous algorithms based on sliding-mode control have been developed for tracking the maximum power points of power electronic equipment. Yet, its main drawback is the chattering phenomenon caused by the high-frequency switching control.

The majority of the MPPT methods outlined above are widely utilized because they are not dependent on atmospheric observations and are simple to use, but they also have the drawback of power oscillation and MPP that is brought on by a fixed perturbation step size.(El, 2017b) It is well known that SMC offers good robustness and transient performance. However, due to the discontinuous control action, chattering, defined as oscillations around the sliding surface, exists and degrades steady-state performance. According to the simulation, adding the fuzzy logic control to the sliding mode controller reduces these oscillations and gives better results.

Generally, all existing pumping systems use water storage. Some systems, on the other hand, use energy storage devices to circulate water during the night (for special applications), while others use the battery to supply a constant current to the motor (normally applicable when the solar modules are under designed for the specific solar water pumping system in order to save installation costs). Therefore, irrespective of the amount of power supplied by the solar panels, the motor will maintain a constant rotational speed.

2.3 Stand-alone, Grid and Hybrid Photovoltaic Systems

Electric power consumption has greatly increased throughout the world due to population growth, which has led to an expansion in the number of real estate developments. This has given rise to non-convectional centralized electric power sources such as hydroelectric, geothermal, fossil fuel, and nuclear power plants.

Renewable energy sources such as solar, tidal energy, biomass, and wind have emerged as an alternative to supplement the rapid rise in demand for energy. The declines in the cost of production and improvements in efficiency for photovoltaic solar cells have resulted in an increase in production, which has resulted in the availability of affordable and efficient solar modules. The demand for stand-alone, grid-connected, and hybrid photovoltaic solar systems is therefore rising exponentially. The standalone system is an independent, decentralized power source that is optimized to supply electricity for local demand. The hybrid system consists of two or more unrelated sources of electricity. It is powered by independent sources and pumped into national power grids.

2.4 Photovoltaic Models

A photovoltaic (PV) cell or module can be modeled using single diode, double diode, and triple diode equivalent circuits in an effort to understand its non-linear current-voltage (I-V) and power-voltage (P-V) characteristics. The single diode model (SDM), which has five unknown parameters, is less difficult than the double diode model, which has seven unknown parameters. The triple diode model (TDM) is a complex model with nine unknown parameters. The extraction of these unknown parameters has been a long-standing and common subject of research to this day(Mule & Sankeshwari, 2015).

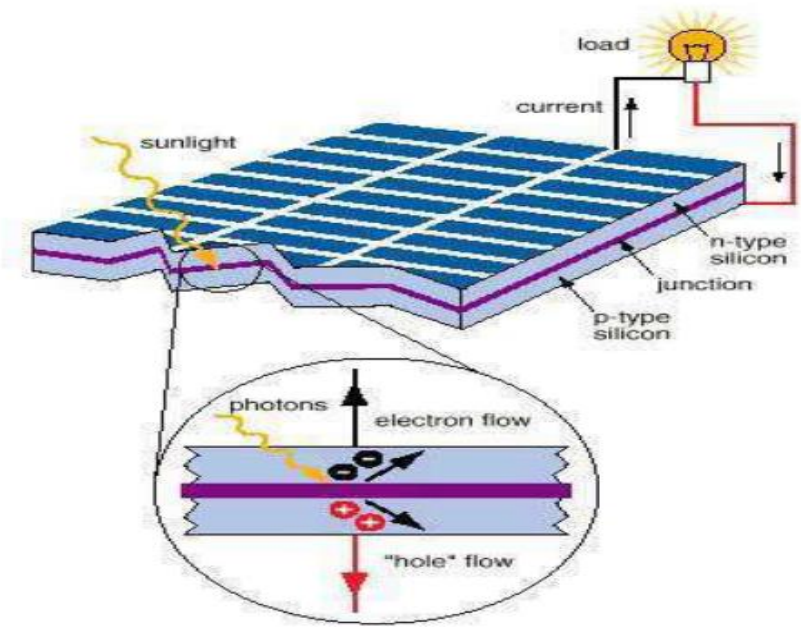

Figure 2.2 Basic Structure of PV Cell(Sethy & Maity, 2010)

For simplicity, the mathematical characterization and modeling of solar cells have been based on a single-diode equivalent circuit. The primary goal of modeling a solar module with a single diode equivalent circuit is to find the best parameters. In a single diode model, the main parameters to be determined are the photocurrent (I_{ph}), diode ideality factors (n), saturation current (I_o), series (R_s), and shunt (R_{sh}) resistances. There are several single-diode techniques that are based on five, four, or three parameter models(Reddy et al., 2020). These models have various mathematical derivations and degrees of accuracy. While both series and shunt resistances are ignored in the three-parameter model, the shunt resistance is considered in the four-parameter model since it is thought to be fundamentally high. The four-parameter model's neglect of the effects of shunt resistance is a significant flaw since it causes the model to not fit the experimental I-V curve under extreme temperature fluctuations. Given that it considers the parasitic effects of series and shunt resistances, the five-parameter model provides a comprehensive approach that is superior to the four- and three-parameter models.

2.5 Conventional Techniques for MPPT of A PV System

Perturb and observe (P and O) is one of the conventional methods widely used in research and industrial solar PV MPPT due to its simplicity and ease of implementation using both digital and analog technology. Despite its popularity, the technique fails to track MPP when solar irradiance fluctuates, and it often oscillates near MPP even in steady-state conditions, leading to power losses.

2.6 Classification of MPPT Techniques

In a photovoltaic (PV) system, maximum power point tracking (MPPT) is used to continually maximize the power output from the PV panel. Due to atmospheric factors, the panel's power output is nonlinear(Narendiran, 2016).

MPPT means measuring the power of the solar panel at given intervals and making sure it is always at its maximum power. A measurement is taken from the solar panel, and the power is calculated. After a specified interval, another measurement is taken. These two measurements, namely current and voltage, are compared, and adjustments are made to the solar panel to ensure that the most recent measurement will lead to the maximum power.

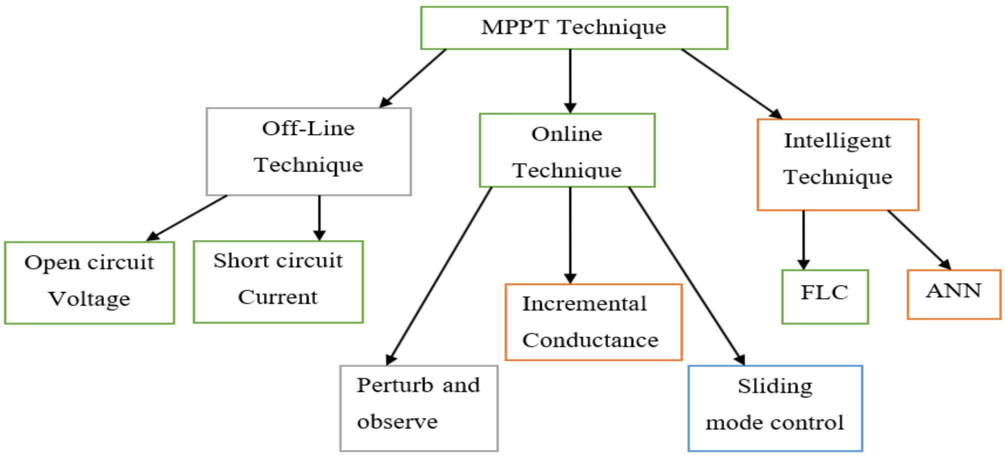

Figure 2.3 Classification of Commonly Used MPPT Technique

2.6.1 Offline Technique

The control signal utilized to manage the output power panel during system operation has been estimated using offline methods based on primary data and input variables of solar panels such as light intensity, temperature, open circuit voltage, and short-circuit current (Rihani & Ghandchi, 2015).

The offline technique is commonly called the indirect technique since this algorithm is worked offline, such that not in real time. In this technique, there is a necessity for prior knowledge of particular PV panel data, such as the mathematical modeling, I-V, P-V curve, etc. The open circuit voltage and short circuit current approaches are the fundamental indirect MPPT methods(Rodrigues et al., 2018). In both methods, a DC-to-DC converter with the driver circuit is controlled by the controller D and operates either in buck or boost mode. The duty cycle of the switching converter can be varied based on the computation of the open circuit voltage or short circuit current to track the maximum power point (MPP). The drawback of indirect techniques are that they use predetermined values and are not real-time based.

2.6.1.1 Open Voltage Circuit

The open circuit voltage method is one of the simplest offline methods presented, based on an approximately linear relationship between open circuit voltage and maximum power voltage in different weather conditions(Rihani & Ghandchi, 2015).

$$V_{mpp} \approx kV_{voc}$$

Where k is a constant value that is less than one (between 0.7 and 0.8), it depends on the solar panel and is calculated empirically by measuring the quantity and taking into account the various weather conditions. To calculate the best operating voltage using this method, the open-circuit voltage of the solar system generated from the source is used to extract the most power possible. It is easy and economical, and it doesn't cause the power loss that the short-circuit current approach does. The fact that the reference voltage stays constant between samplings is a drawback of this method.

2.6.1.2 Short Circuit Current

The short-circuit current method uses an approximate linear relationship between the short-circuit current Isc and the maximum power MPP Impp (k is between 0.8 and 0.9)(Rihani & Ghandchi, 2015). Although this method does not have oscillations like those appearing in the standard perturb and observe method, the power loss may increase since short-circuit current flows whenever MPPT control is performed. Furthermore, it becomes difficult to perform MPPT control during periods of low solar radiation because short-circuit current decreases with solar radiation.

$$I_{mpp} \approx kI_{sc}$$

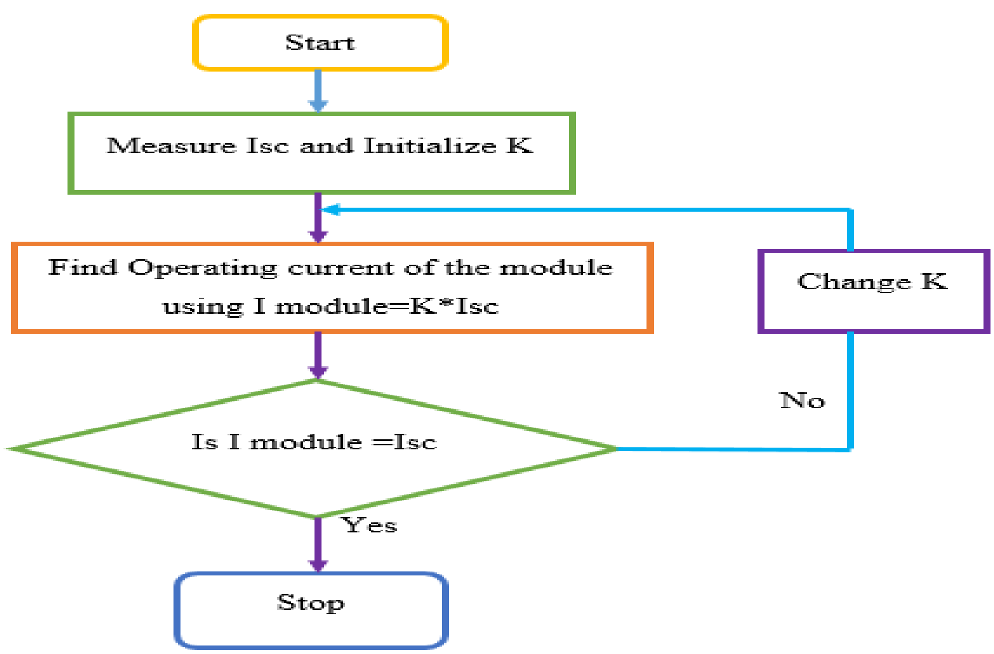

Figure 2.4 Flowchart For Short Circuit Current Technique(Subbarao & Kalyan, 2021)

2.7 Perturb and Observe (P&O)

The incremental conductance (INC) approach, which employs the features of the solar cell's power-voltage curve to locate the highest power point, is another classic method. When the slope of the power-voltage curve reaches zero, the maximum power point is reached. Under quickly varying situations, the INC can enhance tracking accuracy and dynamic performance. However, there are still some disturbances at the maximum power point. Sliding-mode control (SMC) is a strong tool for controlling uncertain systems. The sliding-mode control system exhibits flexibility in the face of both internal and external parameter uncertainties. Sliding-mode control has been widely employed in power electronic equipment, and numerous algorithms based on sliding-mode control have been developed for tracking the maximum power points of power electronic equipment.

The PV array voltage would be perturbed in the same way by the P&O method. If the PV array is shifted away from the MPP by the change in operating point and the P&O algorithm reverses the direction of the perturbation, this procedure continues until the MPP point is reached. It is based on the fact that at MPP, the power derivative with respect to voltage equals zero. Although this approach has a downside, it fails to quickly change the atmospheric conditions. It also has additional drawbacks, such as a sluggish reaction time and oscillation around the MPP. Rather than being set at the exact MPP point, the operational point oscillates significantly around it. During periods of low solar energy, it is unable to follow the MPP.

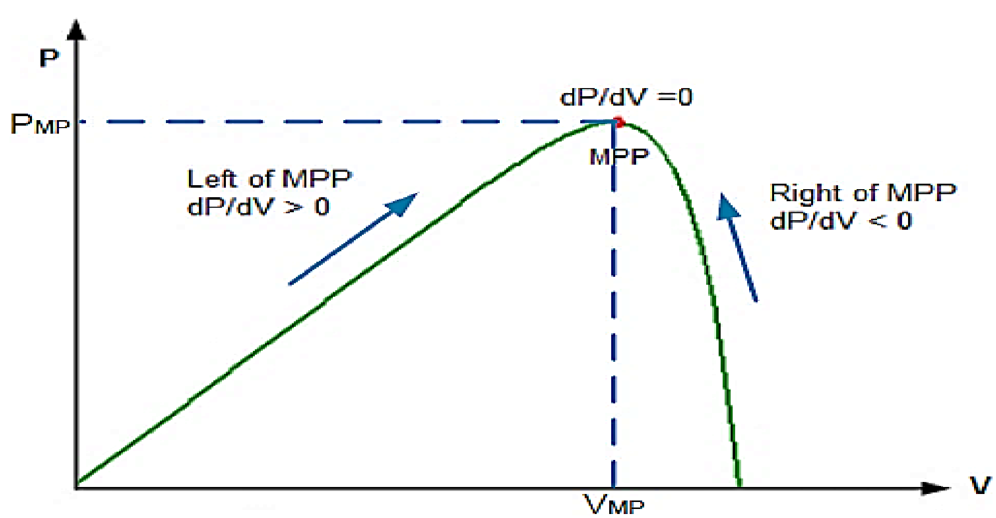

Figure 2.5 P-V Characteristics Curve of PV Module(Situmorang et al., 2019)

2.8 Convergence Speed

Convergence speed is the time taken to reach the MPP. The time needed to converge to the necessary operating voltage or current should be short for a high-performance MPPT system. The system must keep the load at the MPP in accordance with how quickly must accomplish this and tracking system's criteria. The shorter duration and more frequent tuning required to obtain the MPP minimize power losses and maximize efficiency(Islam et al., 2018).

As the solar irradiation is not uniform for the whole day, it will also vary according to the climatic changes. There is a chance of an increase in the formation of partial shading. Due to this partial shading, the PV characteristics will have a multiple peak formation. Generally, the literature review summarized as table below 2.1.

Table 2.1 General description of Solar MPPT algorithm and its limitations

References	MPPT Algorithm	Advantage	Limitations or Gaps
Singhal et al., 2021	P and O	Easy to implement Easy to model and calculate based on current and voltage	Low tracking speed. More losses, during rapid change. Fail to track Under rapidly changed weather condition. High oscillation around MPPT. It has Less efficiency. It has Less accuracy. Oscillation problem is Unavoidable.
Zhang et al., 2021	ANN	It is having high accuracy	It is based on the input and output data. More input and output data give more tracking but, it takes more training or more time.
Kchaou et al., 2017	SMC	It is robust It has high stability It has High accuracy	Main limitation of this algorithm is chattering problem around MPPT.
ingh & Mishra, 2015	IM	IM is Cheaper than BLDC	Less efficient than BLDC An inverter would be required to converter DC electricity produced by solar panels to AC. This increase complexity and cost, it reduces efficiency

CHAPTER THREE

MODELLING AND DESIGN OF SOLAR MPPT ALGORITHM

3.1 METHEDOLOGY

The methodologies that we followed in this thesis are listed by the following chart

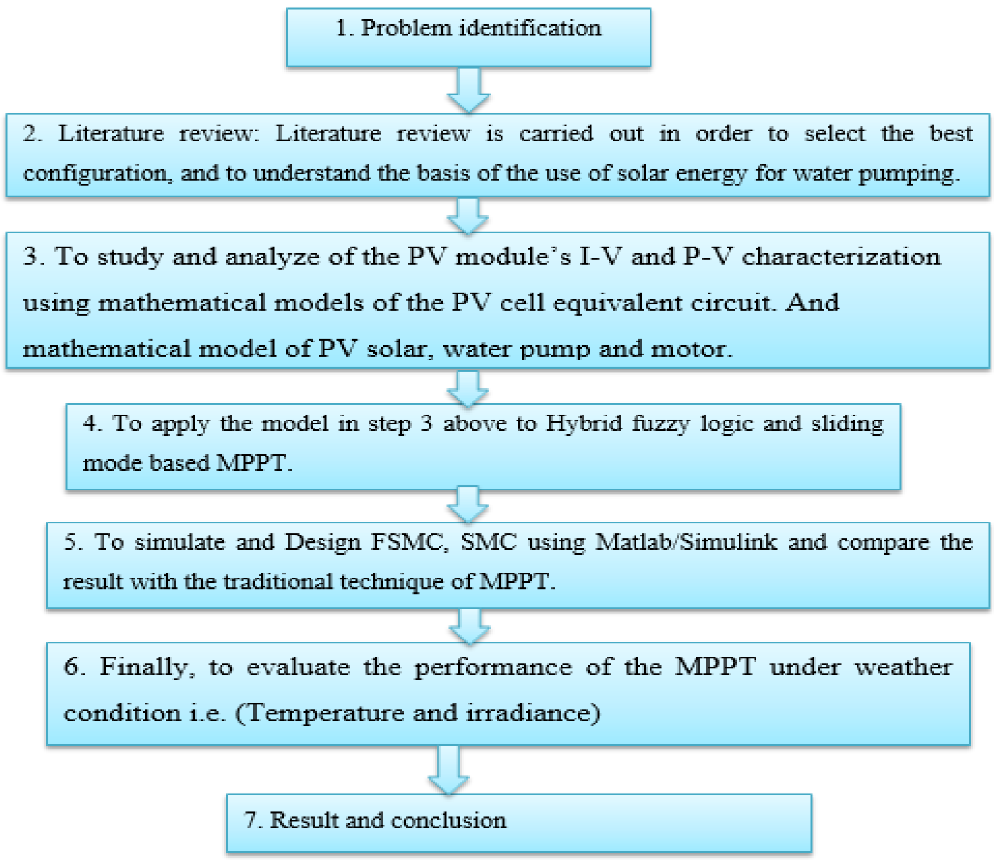

Figure 3.1 Methodology for the thesis

3.2 WATER PUMPING SYSTEM DESIGN

Solar water pumps are powered by solar PV technology, which uses solar panels to convert solar energy into electrical energy. The electrical energy received from the PV panels are converted into mechanical energy by a DC or AC motor, which then transforms that mechanical energy into hydraulic energy.

Perfect Sun Hours:

Number of equivalent daily hours that provide solar radiation energy equal to 1000W/m^2.

Controller: The pump is equipped with a little device that is placed in between the panels and the pump to enable the pump to turn on when it gets dark outside. The controller serves two purposes. First, it balances the input power from the solar panels with the output power that the pump receives. Second, a controller typically has a low-voltage protection feature that turns the system off if the voltage falls outside of the pump's operational voltage range. This lengthens the pump's life span and decreases the need for maintenance.

Water Storage: Water is stored in a large tank, usually set on a hill at a point that is high relative to other locations in the village. It is best if the well is located close to the location of the tank. Excess water is pumped to the tank to provide water when the pump is being serviced or cloud cover prevents electricity from being generated. Storage is generally provided for at least two to three days of projected use.

3.3 Power Source for Pumps

Solar energy, electric, gasoline, or diesel engines are commonly used as power sources for pumps. The power source will be designed to cope with the peak running load and the increased load during starting.

The power source, photovoltaic (PV) panels: A panel is rated in terms of the amount of power it can produce. A pump will require a certain amount of power to produce a certain amount of pressure and flow. By using a suitable-sized PV array, a pump can be operated at an economical cost.

A photovoltaic (PV) array is a stationary object mounted at a particular location to absorb sunlight and convert it to electricity. A maximum amount of irradiance is received when the solar panel is perpendicular to the sun. However, the sun is not stationary; it is constantly changing its relative position to the earth from morning to night and season to season, making it impossible to have an orientation where the solar panel will always receive maximum irradiance.

3.4 Design population and daily water demand

3.4.1 Determination of Hydraulic power

For the determination of water demand, it is necessary to consider the final use of water and/or user requirements. In this case, the aim is to supply drinking water to the community on a small scale (human consumption in liters per day).

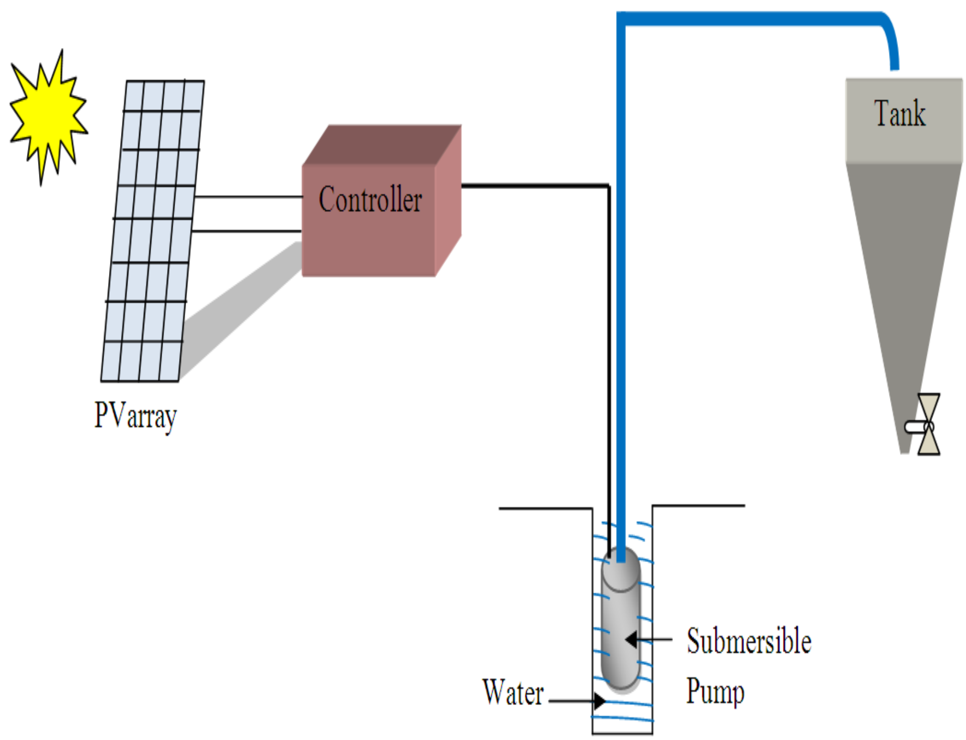

Figure 3.2 A Solar Water Pumping System with Submersible Pump(Salim, 2018)

Table 3.1 Water requirement assumptions in a day per person in a family and animals(De Buck et al., 2015)

Activities	Quantity	Water Used L/day	Total
Drinking	-	3	
Cooking	-	3	
Personal washing	-	12	
Food preparing	-	10	
Cleaning home	-	4	
Average no of family members (4), but assume 550 house hold		4x32=128	128x550=70,400
ANIMALS			
Goats	120	360	1,526
Sheep	55	165	
Milk Cows	35	455	
Chickens	100	9	
Horses	24	264	
Donkeys	13	273	
TOTAL			71,926L/day or 71.926m^3/day

It should be noted that 128 litres of water per day is required for a four-person family. For one goat and one sheep, the water required per day is six litres. That means three litres for one goat and three litres for one sheep. For one cow, horse, and donkey, the water required per day is thirty litres, eleven litres, and twenty-one litres, respectively. According to the above given table, the amount of water required per day is 71,926L/day or 71.926m^3/day.

Step 1: Calculate the daily water requirement in (m^3/day).

Daily water requirement = 71.926m^3

The flow rate or discharge capacity is calculated as the given below equation or Pump capacity or flow rate can be calculated as; Q $_{day}$=71.926m^3 (water required per day).

If the pump works 12 hours per day and also peak sunshine hours (PSH) are 6h.

$$q(l/s) = \frac{Q(l)}{pump\ operating\ hrs(h)} = \frac{71,926l}{6hr} = \frac{71,926l}{6 \times 3600\sec} == 3.33l/s \quad (3.1)$$

Where q-is flow rate in L/sec

PSH- peak sun hour

Therefore, the flow rate through the pipe is 3.33 litre per second.

Determination of Hydraulic Energy Required Per day (KWH):

$$E_h = \frac{\rho \times v \times g \times TDH}{3.6 \times 10^6} \quad (3.2)$$

Where,

E_h -hydraulic energy

V - Volume of the water require per day is 71,926 L/day or 71.926m^3/day.

ρ - is supply water density (1000kg/m^3)

g -is the increase of velocity due to gravity (9.81m/s^2)

TDH - is total dynamic head (m)

$$P = \frac{w}{t} \Rightarrow w = p \times t \quad (3.3)$$

However, 3.6MJ=1KWh, where W-energy in joule, P- Power in Watt

Step 2: Calculate the Total Dynamic Head (TDH) required for pumping the water.

To understand this simply let us design where we need 71.926 m^3 water per day from a depth of 45m. Assume, the elevation, standing water level, and drawdown of the solar water pump is given as 25m, 40m, and 8m respectively.

Total Dynamic Head=Total vertical lift +friction loss

Total vertical lift=Elevation +standing level +drawn down

Total vertical lift=25m+40m+8m=73m

Frictional loss = 5 % of the total vertical lift = 73 × 0.05 = 3.65 m

Then, TDH=Total Vertical lift +friction loss=73m+3.65m=76.65m≈77m

Vertical lift is the vertical distance between the water surface at the intake point (the stream's water surface) and the water surface at the delivery point (the tank's water surface).

Friction loss is the loss of pressure due to the friction of the water as it flows through the pipe.

Step 3: Calculate the total hydraulic energy required per day (Watt-hour/day) for pumping the water.

$$E_h = \frac{\rho \times v \times g \times TDH}{3.6 \times 10^6} \tag{3.4}$$

$$E_h = \frac{1000 \times v \times g \times TDH}{3.6 \times 10^6}$$

$$E_h = \frac{1000kg / m^3 \times 71.926m^3 / day \times 9.81m / s^2 \times 77m}{3.6 \times 10^6 Kwh} = 15091.87Whr / day$$

Therefore,

$$E_h = 15.09187 Kwhr / day \approx 15 kwhr$$

Determination of the Power Required for The Motor:

Sizing of pump motor:

$$P = g \times q \times TDH \tag{3.5}$$

$$= 9.81m / s^2 \times 3.33l / s \times 77m$$

$$= 2,515.3W \text{ or } 2.5153\text{kW}$$

Where:

P-power (kW)

g- Acceleration due to gravity

q- Flow rate of the water (L/s)

TDH- Total Dynamic Head (m)

Power of the electrical motor(Brahmi et al., 2018):

$$P_m = \frac{P_p}{\eta_p} \tag{3.6}$$

Where, η_p efficiency of the motor pump, in most case $\eta_p = 60\%$

P_m : Electric motor power

Then,

$$P_m = \frac{2,515.38}{0.6} = 4,192.3 \simeq 4.2kW$$

Step 4: Calculate the solar radiation available at the site.

The amount of solar radiation at the location (in peak sunlight hours per day) is 6 hours (1000 W/m^2 equivalent).

Step 5: Calculate the size and number of PV modules required.

The PV generator power (kW) necessary can be written as:

$$P_{pv} = \frac{E_h}{G_t \times P_e \times F} (kw) \tag{3.7}$$

Where,

G_t - is the day-by-day sun energy on PV plane in kwh/m^2 (6h/day)

F - is the mismatch factor values range between 0.85 and 0.9

P_e -is the everyday subsystem effectiveness which has a typical significance in between 0.20 and 0.60

Then, I have selected F =0.88 and P_e =0.5

$$P_{pv} = \frac{E_h}{G_t \times P_e \times F} = \frac{15kwhr}{6h \times 0.88 \times 0.5} = 5.682\text{kw}$$

The motor needs to be powered to drive the pump that delivers water to the tank or to the point of use. In the case of an SPWPS, the motor is powered using electricity generated by the PV generator. For this thesis, the KC200GT module, which contains 54 cells, has been chosen. The wattage power of this solar panel is 200Wp. Then I can calculate the number of panels based on the calculated power of the sizing array from the above and on the selected module.

$$\text{Solar panels} = \frac{5682W}{200W} = 28.41 \approx 28 \quad = \frac{5682}{200} = 28.41 \approx 28$$

So, 28 solar panels are needed for this thesis on solar water pumping. The number of modules in series and parallel is selected to be seven series modules and four parallel strings, respectively. In the most general case, a PV generator is made up of several standard PV modules combined in a series-parallel matrix. Scaling rules are required to connect the characteristics of the PV plant or generator to the individual PV module characteristics.

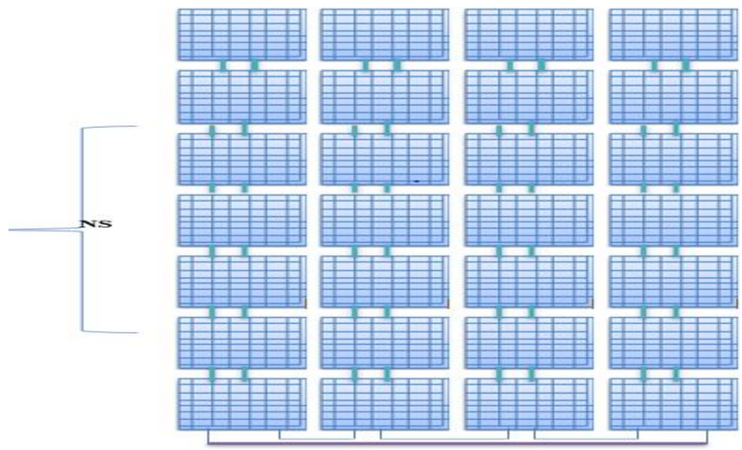

Figure 3.3 Numbers of Seven Series Modules and Four Parallel String of PV Array(Deshpande & Bodkhe, 2017)

3.4.2 Pump Selection

The 4kW medium submersible solar pump kit, which consists of a pump end, a motor, a controller, and equipment, is designed to offer the greatest degree of flexibility in accordance with borehole yield, daily water needs, and available solar energy. The required amount of solar power will be determined by the amount of sunlight available (irradiation), the required flow, and head requirements(Range, n.d.).

Although pump or motor size can be determined as shown above, because pump or motor choices available in the market are limited to certain sizes, it is recommended that pump designers consult water pump system charts from major manufacturers including Grundfos, Lorentz, and Kyocera to select the pump that closely matches their calculated value. Therefore, the type of pump selected for this thesis is the Lorentz pump.

Water Storage: The system’s total water storage capacity should be sufficient for a minimum of two days' water use.

$$71,926 = 71,926 \times 2 = 143,852l \approx 150,000l \text{ or } 143.852\text{m}^3$$

3.4.3 PV Panel Structure

Solar panels can be ground-mounted, roof-mounted, or post-mounted, depending on the site conditions. Metallic structures are normally used to hold the panels; these structures are designed to withstand high winds and stormy weather. The structure itself needs to be properly coated and protected against environmental factors such as rain, humidity, and other conditions.

3.4.4 Water Storage versus Battery Storage

Solar energy can only be used during the day, and it might occasionally be missing on cloudy winter days, necessitating storage for some uses. In theory, batteries might be employed as a form of energy storage, but the expense, maintenance, and replacement needs make this a difficult task.

Water can be pumped using a system like this, especially for drinking. If we need water during the night, we can use the battery's stored energy to pump the water. Batteries, however, can only be recharged in the sunlight, as we are all aware. On the other hand, we are aware that batteries are expensive and that a power electronics circuit, like a charge controller, would be necessary for them, adding to the cost. The expense and space needed for the battery and charge controller in this standalone application may be eliminated by using the solar energy that is immediately available during the times of sunshine to pump the water. Due to this, many photovoltaic power applications prefer to employ water storage instead; in these applications, water is pumped when there is enough solar power available and stored in raised tanks from which water may be retrieved as needed.

When the system is designed correctly, water storage is quite useful. Since pumping is free on sunny days, the system can supply more water than is needed for a day. This extra water can be stored in water tanks, which should be sized to have an appropriate storage volume depending on the weather and how much water is used.

3.4.5 AC versus DC pump

DC pumps have an added benefit over AC pumps since PV generates power in this form, which avoids the additional expenses associated with using an inverter (a device that converts DC to AC) and the resulting loss of efficiency. DC pumps, however, are only appropriate for applications requiring power pumps of 4 kW or less and smaller. There should always be a significant preference for brushless DC pumps over AC ones when the power of the pump in a particular system is 4 kW or less(Solar & Initiative, 2017).

3.5 Relationship among PV Cell, Module and Array

Photovoltaic cells serve as the fundamental building blocks for PV power systems. Due to surface area restrictions, a PV cell can typically provide no more than a few watts of electricity. This little power is insufficient to achieve hundreds of watts. As a consequence, to create a PV module, PV cells are linked either in series or in parallel. Similar to this, it is possible to connect a collection of PV modules (in series, parallel, or both) to generate the necessary current and voltage, resulting in PV arrays whose power ranges from kilowatts to megawatts(B.Eteiba et al., 2013).

3.5.1 Photovoltaic Cell

Silicon and a P-N semiconductor connection are used to construct the most common type of PV cell. A thin semiconductor material is precisely treated to produce an electrostatic attraction that is positive on one side and negative on the other. An electrical field is produced when sunlight strikes a solar cell that is attached to an electrical load, causing a current to flow. This solar energy to electricity conversion is brought about via a photovoltaic reaction. Due to the low voltage produced by a PV cell, which is about 0.5V, many PV modules are often connected in series for high voltage and in parallel for high current.

3.5.2 Photovoltaic Module

A PV module, a collection of PV cells sealed in an environmentally friendly laminate, may generate a sizable quantity of electrical power. A collection of cells is referred to as a PV module, sometimes known as a panel. Since there are no moving parts, there is no noise or pollution, which is the main benefit of PV modules. PV modules are created by joining PV cells in parallel or series, as seen in Figure 3.3, to produce the desired output.

In actuality, a home or company cannot produce enough power with only one module to suit their needs. A PV array can have its modules connected in series to achieve the appropriate voltages or in parallel to increase the system's current output.

3.5.3 Photovoltaic Array

Several PV cells are arranged in series or parallel to form a photovoltaic array, which is a collection of modules. One PV module is rarely enough for commercial applications. As a result, the PV array is made up of several modules. These modules can also be linked in series or parallel to enhance voltage or current on a single rack or a number of racks. The PV array therefore satisfies the need for electricity.

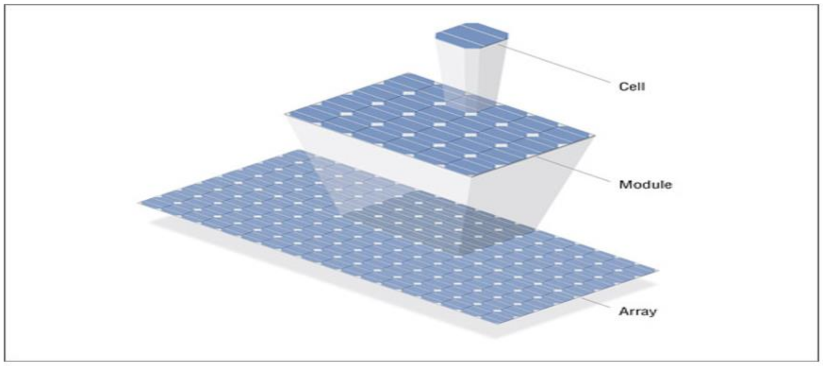

Figure 3.4 Relationship among PV Cell, Module and Array

3.6 Working Principle of PV Cell

A PV cell's operation is based on the photoelectric effect, which is the conversion of solar energy into electricity. A photoelectric impact is a phenomenon that occurs when an electron is ejected from the conduction band as a result of sunlight absorption. An electron and a hole pair are produced when sunlight is absorbed. Following that, the device's structure separates the electron and hole pair. Holes travel to the positive terminal, whereas electrons travel to the negative terminal. Standard Test Conditions is the name of the industry benchmark that all PV modules are evaluated against and can be compared. An STC is a predetermined set of laboratory test settings that simulate real-world usage scenarios for solar panels or PV modules. Although there are various standards that provide more accurate real-world approximations, STC is the most general standard. The same standard is also used to evaluate potential installation locations, since it is the basis for values.

3.7 MODELING OF PHOTOVOLTAIC SYSTEM

A solar cell, commonly referred to as a "photovoltaic" (PV) cell, is a technology that transforms solar energy into electricity. Photovoltaic cells may be joined to create a module, and connecting a number of modules can help create a solar array. Numerous modules are connected in series or parallel topologies inside the PV array. The output of the array might vary greatly depending on the day's varying amounts of irradiation. Numerous PV modules that are joined in parallel and series to form photovoltaic arrays are mostly made up of PV cells.

The kind of connection depends on the voltage and current levels that the PV array power treatment system should run at. Solar, or PV, cells are the fundamental component of a PV system. A PV module is created by connecting the pre-wired cells in series. The voltage rating of the modules is then increased by connecting them in series, and the current rating by connecting them in parallel. The term PV array refers to such a series and parallel arrangement of modules.

A single PV cell is a photodiode. Typically, the single-cell equivalent circuit can be modeled by a current source dependent on irradiation and temperature in parallel with an inverted diode that conducts reverse saturation current. However, no solar cell is ideal, and that means shunt and series resistances are added to the model as shown in Figure 3.4. Series resistance (R) is due to a hindrance in the flow of electrons from the n to p junction, and it has intrinsic series resistance whose value is small. Shunt resistance (R) is due to the leakage current, which has a very high value.

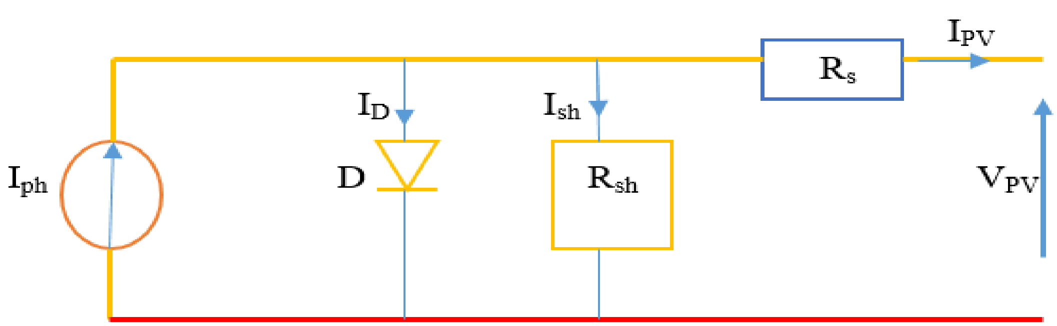

Figure 3.5 Equivalent Circuit Model of a Solar Cell(Reddy et al., 2020)

The Rs is the current path's series resistance, which is a loss caused by the Joule effect and is mostly caused by metal grids, semiconductor materials, collecting buses, and their connections. The Rp is a type of parallel resistance. Shunt resistance is the amount of current that leaks out of a circuit because of the thickness and shape of the cells(Magaji et al., 2022). In the generalized model of a PV module as shown in Figure 3.5, the current source is used to model the incident solar irradiance, a diode for the polarization phenomenon, and a series and parallel resistances to represent the power losses. The mathematical equations describing the behavior of the cases in Figure 3.5 are given by the following equations:

Using Kirchhoff's law (KCL), the current in the circuit can be calculated by:

$$I_{ph} - I_D = I_{Rsh} + I_{Rs} \tag{3.8}$$

And using Kirchhoff's voltage law (KVL), the output voltage (V) can be expressed as:

$$V = V_{ph} - V_{Rs} = V_{Rsh} - V_{Rs} = V_D - V_{Rs} \tag{3.9}$$

The Shockley's diode has an exponential current-voltage relation given as:

$$I_D = I_o(\exp\frac{qV_D}{nkT} - 1) \tag{3.10}$$

Where

I_o -Dark or Saturation current of Diode (A)

I_{ph} - Photo generated current (A)

V -Terminal voltage of PV module (V)

n-Diode ideality factor

k - Boltz Mann's constant = 1.3806503 e−23 J/K

T-Temperature (K)

q -Charge of electron = 1.602e−19 C

The equation of the PV cell can be represented with I-V characteristic as:

$$I = I_{ph} - I_s\left[e^{\frac{(V+IR_s)}{nV_t}} - 1\right] - \frac{V + IR_s}{R_p} \tag{3.11}$$

Mathematically, the thermal voltage is given as:

$$V_T = \frac{n \times K \times T}{q}$$

$$I_{photo} = \left[I_{ref,sc} + k_i \left(T - Tref \right) \right] \frac{G}{G_O} \tag{3.12}$$

The saturation current Isat depends on the cell temperature, which is given by:

$$I_{sat} = I_{r,sat} \times \left[\frac{T}{T_{ref}} \right]^3 \exp\left[\frac{q \times E_g}{n \times K} \left\{ \frac{1}{T_{ref}} - \frac{1}{T} \right\} \right] \tag{3.13}$$

The reverse saturation current Ir, sat is expressed as follows:

$$I_{r,sat} = \frac{I_{ref,sc}}{\exp(\frac{qV_{oc}}{N_s nKT}) - 1}$$

The output current I of the solar PV module is given as:

$$I = N_p I_{photo} - N_p I_{sat} \left[\exp(\frac{q(V + IR_s)}{N_s nKT}) - 1 \right] - \frac{V + IR_s}{R_p} \tag{3.14}$$

Where is the temperature coefficient for short-circuited current, and what are actual and reference temperatures, respectively. is the ideality criterion, G is the solar irradiation (W/m^2), and G_0 is the nominal irradiation, i.e., 1000 W/m^2. Is the module short-circuit current taken from the reference model's datasheet and measured under standard test conditions (T = 250°C and G = 1000 W/m^2)(Nguyen & Nguyen, 2015). Ir,sat is the module's reverse saturation current, q is the charge of an electron, Voc (VPV) is the module open-circuit voltage, Eg is the semiconductor's bandgap energy, and NS and NP are the number of cells connected in series and parallel, respectively. RS and RP are the equivalent series and parallel resistances of the module, respectively.

Maximum power point current and Maximum power point voltage are the terms used to describe the photovoltaic current and voltage at the maximum power point, respectively. The abbreviations Impp and Vmpp, which stand for maximum power point current and voltage, respectively. Solar cells employ semiconductor components to transform solar energy into electrical energy. When these materials are exposed to light, photons with energies greater than their band gap materials' energies will be absorbed. When a photon is absorbed, it works to remove an electron from its atom, allowing it to pass across the cell junction and generate electricity. The photovoltaic effect is the mechanism by which light energy (photons) is transformed into electrical energy (voltage).

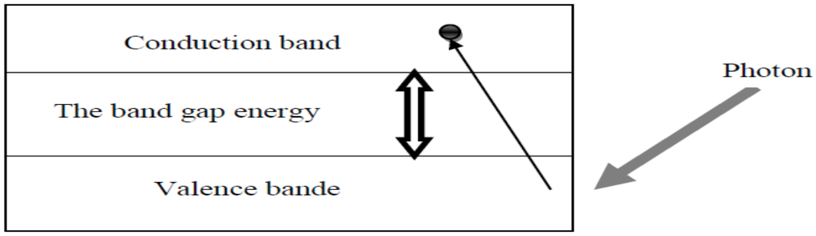

Figure 3.6 The Semiconductor of Converting Light Energy(Salim, 2018)

The operation of a solar cell can be represented by a simple p-n junction diode where the electrons flow from the n layer side to the p layer side of the photovoltaic cell via an external wired connection. In general, the module comprises a group of cells connected in series and parallel to supply the desired output power and voltage as depicted in Figure 3.6. Generators or arrays are made up of some combination of series and parallel modules to increase power. The connection of cells in series will directly multiply the voltage handling capability of the system, and connection in parallel will directly multiply current production.

3.7.1 Photovoltaic Characteristics under Varying Irradiances

Short-circuit current and open-circuit voltage both increased proportionally as the amount of sunshine increased, and this resulted in an overall rise in power.

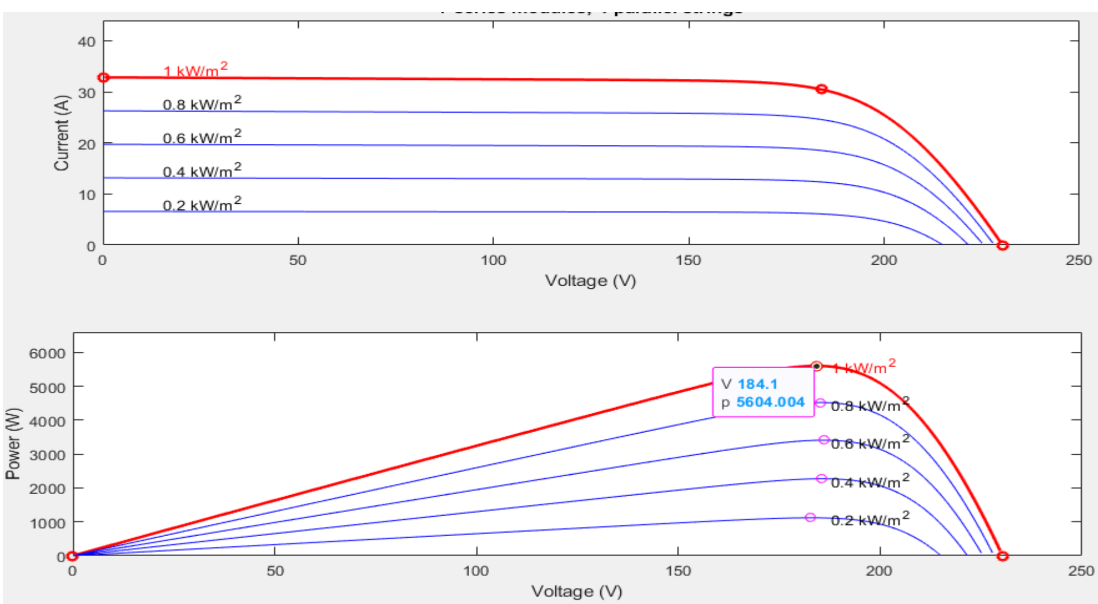

Figure 3.7 I-V and P-V characteristics at constant temperature STC 25^{0}C

3.7.2 I-V and P-V Characteristics under Varying Temperatures

The open circuit voltage decreased with huge values as the temperature rose, but the short circuit current increased with very small values, resulting in a complete loss of power.

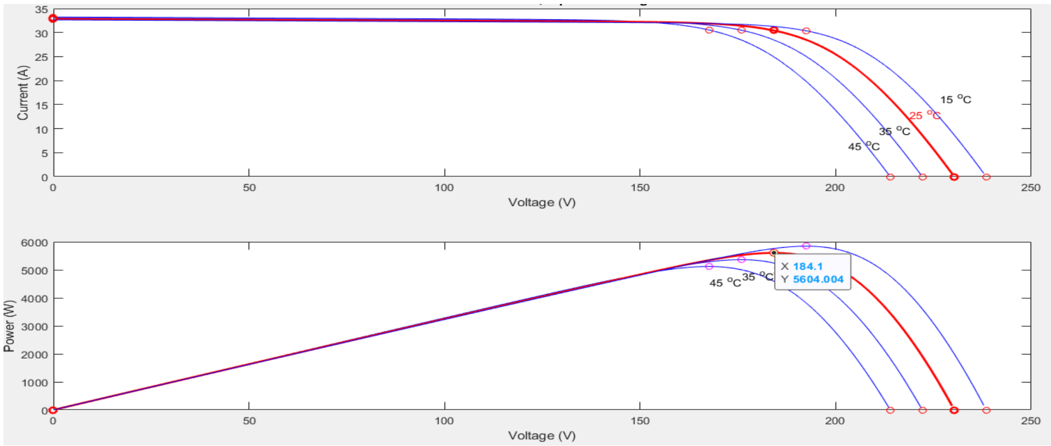

Figure 3.8 I-V and P-V at constant Irradiance 1000W/m^2 but at different temperature

$$P_{mpp} = I_{mpp} \times V_{mpp} \tag{3.15}$$

$$\mathrm{I}_{mpp} = \frac{P_{mpp}}{V_{mpp}}$$

$$I_{mpp} = \frac{5604.004W}{184.1V} = 30.44A$$

$$R_{mpp} = \frac{V_{mpp}}{I_{mpp}} = \frac{184.1V}{30.44A} = 6.0479\Omega$$

The numbers of modules required to connect in series are as:

$$N_s = \frac{V_{mpp}}{V_m} = \frac{184.1V}{26.3V} = 7 \tag{3.16}$$

The numbers of modules required to connect in parallel are as:

$$N_s = \frac{I_{mpp}}{I_m} = \frac{30.44A}{7.61A} = 4 \tag{3.17}$$

3.8 Effects of Partial Shading on PV or Mismatch Factors

In a PV power system, partial shadowing of PV modules is the most frequent mismatch phenomenon. Temperature, solar insulation, shading, and array arrangement all have an impact on PV power systems. Trees, passing clouds, towering buildings, or other obstacles may completely or partially shadow a PV system, causing irregular insolation conditions.

Under conditions of homogeneous irradiation, the P-V characteristics of a photovoltaic string exhibit one peak that corresponds to the P-V characteristics in Figure 3.7. The peak, which serves as the overall peak, represents the solar string's maximum power. Using a bypass diode results in many peaks on the P-V characteristics when partial shading occurs. The photovoltaic string's maximum power is represented by the highest peak, known as the global peak. The adjacent peaks of the other mountains(Teo et al., n.d.).

The performance of the PV array, which consists of parallel and series-connected PV panels, depends on the properties of each individual cell. Individual cells' properties differ due to mismatch loss (dust, chemical aging, partial shading, and radiation). The minimum radiation-receiving cell determines the maximum current flow in the string for PV cells linked in series. The partially shaded cell absorbs and produces heat from the excess power produced by the unprotected cells.

The power output of a PV module is decreased by shading, but it also results in voltage and string mismatches between parallel strings, as well as current mismatches within a PV series. A bypass diode is linked in parallel with the PV module to offer a different current path, minimizing power damage to the panel. On the other hand, the current flowing through a module's cells has changed.

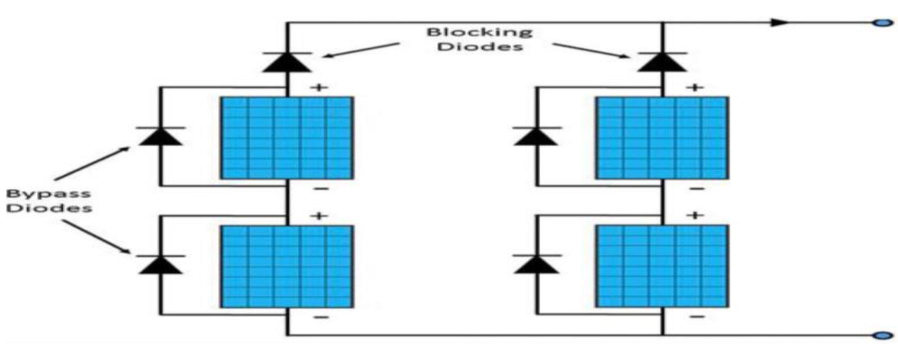

Figure 3.9 Shaded PV Cell(Sameeullah & Swarup, 2016)

In this case, the shaded cell stops generating electrical energy and starts acting more like a semi conductive resistance. The shaded cell produces significantly less current than the other two cells, which reduces the series string's ability to produce energy. As a result, the power that the sunny cells were generating is now being lost by the shaded cells, which could eventually lead to the bad cell's departure due to overheating (hot spots).

When a PV cell is shaded, the generated current cannot pass through the cell. Therefore, bypass diodes are connected externally and in reverse parallel with the PV cell to provide an alternative electrical path. This keeps the series string functioning properly by limiting the reverse bias voltage that may be generated across any partially shaded cell and, as a result, lowering the amount of electrical power that the cell can lose.

3.9 Identification of PV Model Parameters

For simplicity, in this thesis, the single diode, known as the "five-parameter model" (Iph, Is, n, Rs, Rp), is used as a model for the identification of photovoltaic cell parameters. A simplified calculation of the value of the parallel resistance (Rs is much less than Rp) shows that it is high enough that it can be neglected. However, the equation whose parameters need to be identified is (3.18). The aforementioned unknown parameters can be determined as follows:

$$I = I_{sc} - I_s \left[e^{\frac{(V+IR_s)}{nV_t}-1} \right] \tag{3.18}$$

Photovoltaic module parameters determination: The PV panel output current Ipv depends on many parameters such as the type of materials from which the PV panel is made (ideality factor n), shunt and series resistance, number of parallel and series solar cells (Ns and Np), temperature, and irradiation variations. These are the main factors in PV panel models used to gate the required voltage, power, or current.

Number of cells to be used: I must build a 200Watt PV module starting with the aforementioned specifications and estimates. Only 0.5–0.6V and a few watts of power, which are little value, produced by a single cell. Multiple prewired cells are connected in series to provide a bigger voltage, and the entire module is housed in a robust, weatherproof container. A module is made up of cells arranged either in series or parallel. The needed number of series-connected cells for a typical module may be 36, 54, 60, 72, or 96. The same current flows through each solar panel when they are connected in series, and their voltages add up.

$$V_{module} = N_s(V_{oc} - I_{sat}R_s) \tag{3.19}$$

Where, N_s : number of cells in series, V_{oc} : open circuit voltage, I_{sat} saturation current and R_s Series resistance.

Table 3.2 Single solar data sheet

Description	Value	Unit
Open Circuit Voltage (Voc)	0.5-0.6	V
Irradiation (G)	1000	Watt/m^2
Quality factor	1.5	-
Saturation current (Is)	2.3246*e^{-10}	A
Series resistance (Rs)	0.34483	Ω

To raise voltage, multiple cells can be wired in series; to increase current, they can be wired in parallel. In this instance, I want to create a design that will produce 200 watts of power at 7.61 amps of current, identify the necessary cells, and compare their values to those on the data sheet. As a result, Vmodule = 200/7.61A = 26.3V using Table 3.2. Ns=26.30/0.5= 54 cells in series where 7.61A is the required current to produce by the photon.

Table 3.3 Electrical characteristics data of PV module taken from the datasheet

Electrical Characteristics	
Maximum Power (*Pmax*)	200.143W
Voltage at Vmax (Vmp)	26.3V
Current at Imax (Imp)	7.61A
Open-circuit voltage (Voc)	32.9V
Short-circuit current (Isc)	8.21A
Series resistant	0.34483 Ω
Shunt resistance	150.6921 Ω

Then the photo-induced current is calculated straightforwardly because it is significantly higher than the diode current, so it is assumed to be equal to the short-circuit current in STC:

$$I_{ph} \approx I_{sc} \tag{3.20}$$

3.9.1 Fill Factor

PV arrays are often characterized by a parameter known as the fill factor (FF). FF actually measures the quality of the PV array. We call the maximum power point (MPP) the point where the solar cells work by receiving the light intensity and transmitting the maximized power. When considering the I-V curves, the Vmpp and Impp values can be calculated from Voc and Isc(Aurairat & Plangklang, 2022).

$$V_{mpp} \approx (0.75-0.9)V_{oc}$$

$$I_{mpp} \approx (0.85-0.95)I_{sc}$$

The fill factor (FF) is the value considered properties of the solar cell with the following values.

$$FF = \frac{V_{mpp} \times I_{mpp}}{V_{oc} \times I_{sc}} \tag{3.21}$$

The fill factor value refers to the value that represents the quality of the solar cell. Typically, silicon cells are approximately 0.7–0.8.

Assume

$V_{mpp} = 0.8 \times V_{oc} = 0.8 \times 32.9V = 26.32V$ And $I_{mpp} = 0.9 \times I_{sc} = 0.9 \times 8.21 = 7.39A$ for single PV module.

Then, $FF = \frac{26.32V \times 7.39A}{32.9V \times 8.21A} = 0.72$

High performance cells feature low series resistance values and high parallel resistance values to achieve the ideal circumstance where the current is kept up to the short circuit value, then abruptly decreased to zero at the MPP, and has an FF of unity. It goes without saying that real cells that rely on particular PV array types do not attain this value.

3.9.2 The Effect of Temperature

The two main ways that temperature impacts solar cell characteristics are directly through the value of Temperature in the exponential and indirectly through its impact on the reverse-diode saturation current and the photo-generated current.

Table 3.4 The Proposed Module and Array Value

Parameters	Modelled Module value	Proposed array Value	Unit
Open circuit voltage (Voc)	32.9	230.3	V
Short circuit current (Isc)	8.21	32.84	A
Maximum current (Imax)	7.61	30.44	A
Maximum voltage (Vmax)	26.3	184.1	V
Number of cells (Ns)	54	1,512	-

3.10 Maximum Power Point Tracking Controller

The following factors have been taken into consideration when developing the proposed MPPT algorithm:

- The dynamic response speed of the system is important since a fast-dynamic response can increase the system's output power.
- Steady-State Power Oscillation: As reducing the power oscillation around the MPP can considerably reduce power losses.
- Tracking direction: in cases of rapidly changing weather conditions, most of the MPPT algorithm can be confused and track in the wrong direction.
- Partial shading: Partial shading: Under these conditions, MPPT controllers perform less effectively. The bulk of MPPT controllers are based on the principle that the PV module can only produce its maximum power at one point along the P-V characteristic. But, when PSC happens, the module will have many MPPs, which will affect the controller's performance and lower the system's overall output power.

The Maximum Power Point Tracking (MPPT) approach is used to track the maximum power point (MPP), which ensures that the maximum power can be extracted regardless of the daily changes in irradiance and temperature.

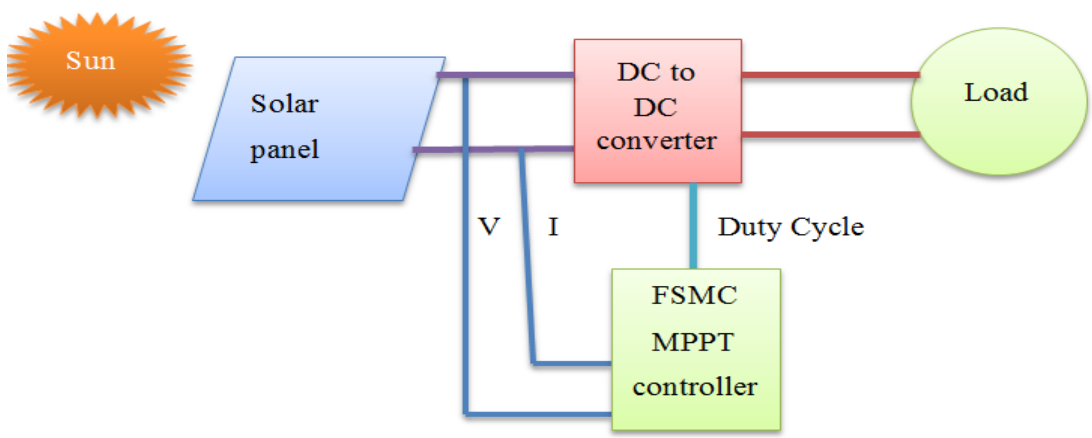

Figure 3.10 Maximum Power Point Tracking System Using FSMC (El, 2017)

3.11 Performance specifications of MPPT control algorithm

Maximum Power Point Tracking - is a technique used commonly with wind turbines and PV solar systems to maximize power extraction under all conditions(Ravi & Sultana, 2019). The dynamic response, steady-state error, and tracking efficiency should be considered for a successful design when evaluating the performance of a new or modified MPPT control algorithm.

3.11.1 Dynamic Response

In order to follow the MPP during the rapid changes in atmospheric conditions, an MPPT control algorithm must be quick to react (to solar irradiation and temperature). The system's loss of solar energy is inversely proportional to the MPPT algorithm's tracking speed.

3.11.2 Steady-State Error

Once the MPP is found, the MPPT control algorithm should stop searching for it, forcing the system to operate as long as possible at this ideal operating point. However, due to the active perturbation process in MPPT algorithms with set tracking step-size and the ongoing variation in solar insolation and temperature, this is practically hard to achieve in an actual MPPT system. The efficiency of the PV system is negatively impacted by this phenomenon.

3.11.3 Tracking Efficiency

To quantify how successfully an MPPT control procedure tracks the MPP and to what extent it contributes to increasing the overall performance of the PV system compared to other methods is a very significant step. Accordingly, tracking efficiency is defined as the ratio between the actual power of the PV array and the theoretical power during the same time period. The atmospheric conditions (irradiation and temperature) are changeable and differ over a wide range. Hence, each MPPT algorithm must be evaluated over a range of different operating conditions when comparing MPPT algorithm performance. A well-designed MPPT control system should provide good performance in different atmospheric conditions.

3.12 DC-DC Converter Used for the MPPT System

An MPPT extracts and transmits the maximum power from the solar PV module to the load. A DC-DC converter's objective is to transfer as much power as possible from the solar PV module to the load. No MPPT systems are created without a dc-dc converter, so we may consider it to be an interface between the load and the module.

The MPPT function regulates a DC-DC converter, which takes a DC input and produces a DC voltage that is either greater, lower, or equal to the input voltage. The DC voltage output of a boost converter will be greater than the input voltage. These converters utilize inductors and capacitors as intermediate energy storage components, which regulate the energy flow from the PV module to the load by repeatedly opening and closing switches(Prabhakaran & Mathew, 2016).

3.12.1 Boost Converter

A power converter that controls the average output voltage at a level greater than the input or source voltage is known as a DC-to-DC boost converter. The boost converter is hence frequently referred to as a step-up converter or regulator(Kurian, 2014). A converter is used to transfer the energy from the PV panel to the resistive load. The electrical configuration is a boost type that targets a voltage step up from the source to deliver a suitable end-used voltage.

A type of converter called a DC-DC boost converter is utilized in applications where a greater output voltage is needed than an input voltage. The IGBT switch, diode, capacitor, inductor, and resistance are the passive elements that make up a DC-DC boost converter(Gonal, 2016). The IGBT switch is fired in the ON state of the boost converter operator, and the switch is off in the off state.

The DC-DC converter is the component in charge of keeping the PV array at its maximum power point (MPP). The boost converter was chosen from a range of alternatives. This converter can increase voltage and regulate the MPPT, and it is relatively straightforward in its construction, design, and operation. Additionally, it provides a constant current at the input.

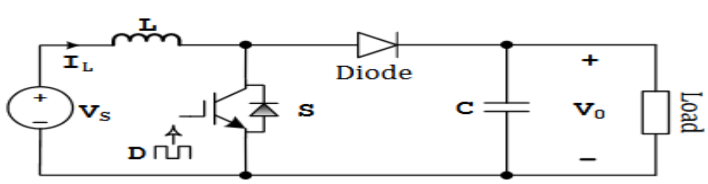

Figure 3.11 DC-DC Boost Converters(ÇELİKEL & GÜNDOĞDU, 2021)

The boost converter is in charge of monitoring the maximum power available at the PV array. Thus, the MPPT controller works effectively if the DC bus voltage remains constant. The formula in a boost converter relates the output voltage to the input voltage.

3.12.2 Boost Converter Design

A boost converter's output voltage is greater than its input voltage. The input voltage is increased until the output voltage reaches the desired level. A form of switched-mode power supply (SMPS) requires at least two semiconductors (diodes or transistors) and one energy storage component (inductor or capacitor). The input voltage source is coupled to an inductor. The solid-state device that acts as a switch is connected across the source.

A diode is utilized as the second switch. The boost is regarded as a constant-current input source since the inductor attached to the input source produces a constant input current. Pulse-width modulation (PWM) is used to turn on and off the controlled switch. PWM can be frequency- or time-based. The drawback of frequency-based modulation is that a wide range of frequencies must be used to regulate the switch in order to produce the required output voltage. In DC-DC converters, time-based modulation is frequently employed. This sort of PWM modulation keeps the frequency constant.

Step 1: Calculation of duty cycle:

$$\frac{V_{out}}{V_{in}} = \frac{1}{1-D}$$

$$D = 1 - \frac{375V}{184.1V} = 0.51$$

Where, V_{out} is the output voltage of the converter, V_{in} is the input voltage of the converter from PV, D is the duty cycle of the converter.

Step 2: Determine of ripple current:

Current Ripple Factor (CRF): According to the international electro technical commission(IEC) harmonics standard, CRF should be bound within 20% to 40%(Ramachandra Rao et al., 2019).

$$CRF = \frac{\Delta I_L}{I_{out}} = 30\% \tag{3.22}$$

$$\Delta I_L = 0.25 \times \frac{P_{out}}{V_{out}} = 0.25 \times \frac{5604W}{375V} = 3.376A$$

Step 3: The inductor voltage can be determined as follows:

$$L = \frac{(1-D)^2 \times D \times R}{2 f_s} \tag{3.23}$$

$$= \frac{(1-0.51)^2 \times 0.51 \times 27\Omega}{2 \times 20{,}000} = 0.0836mH$$

Step 4: Calculation of voltage ripple factor is determined by(Ramachandra Rao et al., 2019):

$$VRF = \frac{\Delta V_o}{V_o} = 5\%$$

$$V_r = 0.05 \times 375V = 18.75V$$

Step 5: Calculation of the minimum capacitor value is also determined by:

$$C_{out} = \frac{D}{2 \times R \times f_s} \tag{3.24}$$

$$C_{out} = \frac{0.51}{2 \times 27 \times 20000} = 0.4722\mu F$$

Table 3.5 Boost Converter Parameters

Power Rating (Pmax)	5.682kW
Input Voltage Range (Vin=Vpv)	32.9-184.1V
Output Voltage (Vdc=Vout)	375V
Max, Input Current (Ipv=Pmax/Vin)	30.88A
Max, Load Current=Pmax/Vout	15.15A
Switching Frequency	20kHZ
Vout Ripple(ΔVout)	1%-50%
Iin Ripple (ΔIin)	20%-40%
Inductance (L)	1.0188mH
Output Capacitance (Cout)	0.4722µF

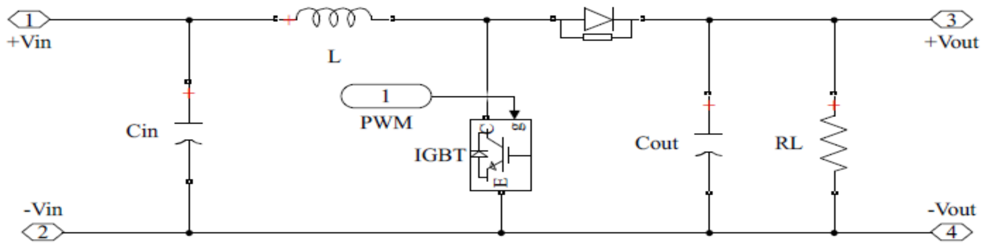

Figure 3.12 Matlab Simulink of Dc-to-Dc Boost Converter

3.13 Perturb and Observation Based MPPT Technique

This approach causes a small amount of system disturbance. The power of the solar module changes as a result of this disturbance. If the disturbance causes an increase in power, the perturbation will continue in that direction. The perturbation then reverses as a result of the power at the next moment decreasing once the peak power is attained. The approach oscillates about the peak point when a steady state is reached. The magnitude of the perturbation is kept extremely maximal to minimize the power variation. The technique is designed to set a reference voltage for the module that corresponds to the peak voltage of the module(Kute, n.d.). Applied to the PV system, the perturbation is generated through a change in the voltage $V_{in}(k)$ and current $I_{in}(k)$, such that the power of the PV is measured. This implies that the slope dP/dV can be calculated, which helps with knowing whether the MPP is achieved.

Table 3.6 Control Actions for Various Operating Points in the P & O Method

Case	ΔV	ΔP	ΔP/ΔV	Tracking Direction	Voltage Control Action
1	+	+	+	Good Direction	Increase V by ΔV
2	-	-	+	Bad Direction	Increase V by ΔV
3	-	+	-	Good Direction	Decrease V by ΔV
4	+	-	-	Bad Direction	Decrease V by ΔV

In this perturb and Observe technique by measuring the current and voltage, can get the power. The voltage value is perturbed by small value to be increased and the corresponding power is observed.

If the change in voltage is positive and the change in power is also positive, then $\frac{dP}{dV}$ is positive then the perturbation of voltage and observation of power is continued till reaching the maximum value where $\frac{dP}{dV}$ will change to zero then to negative value; where the process is stopped. The P&O method continuously controls the current or voltage in the direction of increasing power by perturbing the PV voltage or current and observing power. The P and O operation starts by sensing panel current I_k and V_k voltage then the solar panel power can be computed as $P_k = V_k \times I_k$ and compared with the previous rating P_{k-1} continuously.

$$\Delta P = P_k - P_{k-1} \tag{3.25}$$

$$\Delta V = V_k - V_{k-1} \tag{3.26}$$

$\Delta P = 0$, at MPP

$\Delta P < 0$ and ΔV< 0 at the left of MPP

$D(k) = D(k-1) - \Delta D(k)$ dec*rease* Vout

$\Delta P < 0$ and $\Delta V > 0$, at the right of MPP

$D(k) = D(k-1) + \Delta D(k)$ increase Vout

$\Delta P > 0$ and ΔV<0 at the right of MPP

$D(k) = D(k-1) + \Delta D(k)$ increase Vout

$\Delta P > 0$ and ΔV>0 at the left of MPP

$D(k) = D(k-1) - \Delta D(k)$ decrease Vout

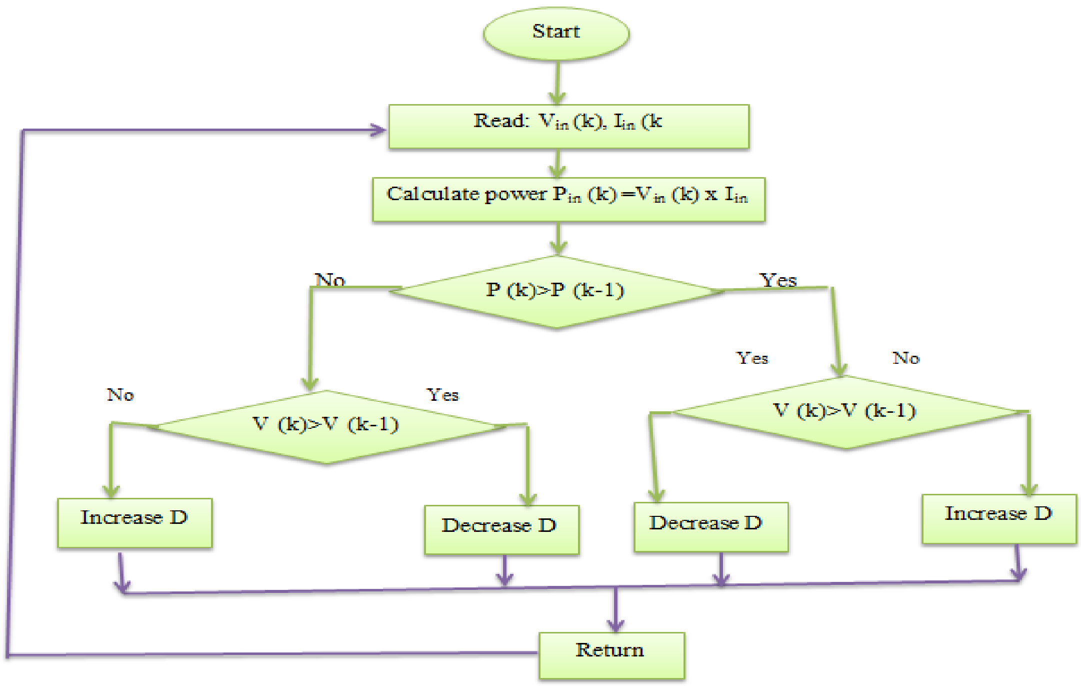

Figure 3.13 Flow Chart of Perturbation and Observation(Aurairat & Plangklang, 2022)

The photovoltaic system's voltage is adjusted using perturbation and observation techniques in accordance with the characteristic curve to move in the direction of steadily increasing power. The voltage is continually shifting and oscillating near the maximum power when it is attained. This method works well for gradual changes in temperature and irradiance. An output oscillation at full power is a drawback. Additionally, the step size affects how quickly a maximum power point converges (D delta of duty cycle). Low oscillations at maximum power and long tracking times are characteristics of short step sizes. Big step size has low tracking time and high oscillations at maximum power point(Aurairat & Plangklang, 2022).

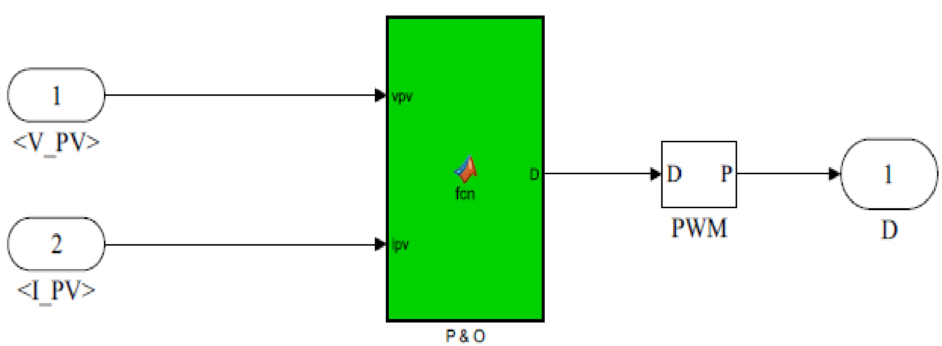

Figure 3.14 Matlab / Simulink of Perturbation and Observation

3. 14 Fuzzy Maximum Power Point Tracking Method

Fuzzy control is one of the most popular methods for MPPT control because it offers the benefit of supporting nonlinear systems without the need for precise mathematical modeling. Fuzzification, rule-based control, and defuzzification are the three main components of fuzzy control. Based on the membership function, fuzzification transforms numerical input into linguistic input variables. The opposite of fuzzification is called defuzzification(Kadeval & Patel, 2020).

This method is reliable in use and can handle inaccurate data because it doesn't require precise mathematical expressions while designing the controller. The fuzzy inference system serves as the base for the fuzzy logic controller (FLC). The duty cycle (D) is the system's output, and its inputs are errors (E) and changes in errors (CE). A linguistic variable, or a variable whose values are words rather than numbers, is the fundamental idea of fuzzy logic (such as small and large).

Fuzzification, logic judgment, and defuzzification are successive stages of a FLC. At the stage of fuzzification, the numerical ratio, E (a change in solar power to a change in solar voltage, P/V), is translated into a linguistic variable via membership functions, as well as the numerical error, CE, which is the perturbation intensity, V. E and CE are two input linguistic variables of the FLC.

$$E = \frac{\Delta P(k)}{\Delta V(k)} = \frac{P(k) - P(k-1)}{V(k) - V(k-1)}$$

$$CE = E(k) - E(k-1)$$

Where, the E(k) -Error shows if the operating point at the instant k is located on the left side or on the right side of the MPP on the P-V characteristic, while CE(k)-change in error expresses the displacement direction of this point. The change in duty ratio of the DC-DC converter is used as the output of the controller. Therefore, the control is done by changing this duty ratio according to the slope E (k) in order to bring back the operation point on the optimal point where the slope is zero.

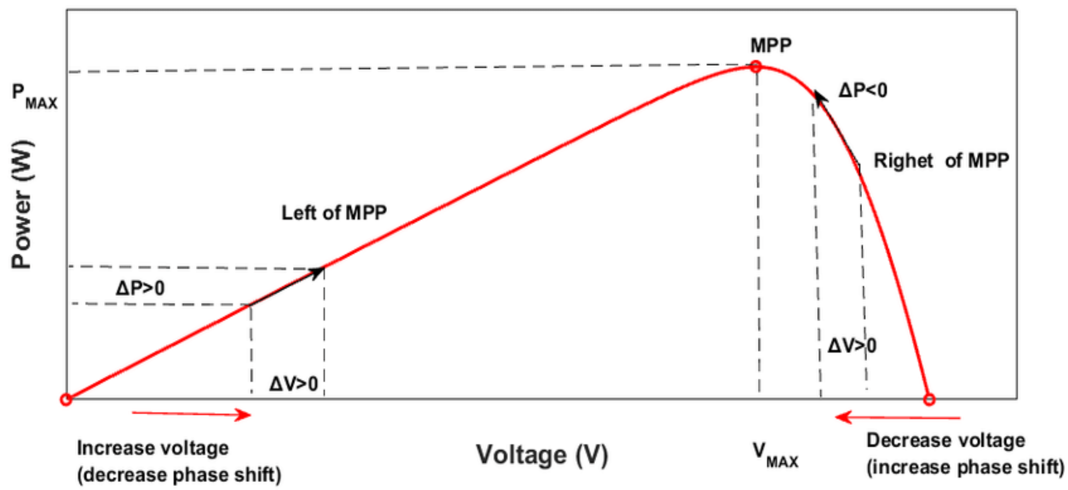

Figure 3.15 Tracking of the MPPT by FLC(Kadeval & Patel, 2020)

3.14.1 Rules of Fuzzy Logic Controller

1. When **E(k) < 0** and **CE(k) < 0**, P from the left side of the MPP, D should be positive, to reach the MPP.

2. When **E (**k) < 0 and **CE (k) > 0**, P from the left side far away from the MPP**, D** should be positive, to reach the MPP.

3. When **E (k) > 0** and **CE (k) < 0**, P from the right side close to the MPP, **D** should be negative, in order to return to the MPP.

4. When **E (k)** > **0** and **CE (k)** > **0**, P from the right side far away from the MPP, **D** should be negative, in order to return to MPP.

Fuzzy systems perform better for particular applications due to two key properties:

- Fuzzy systems are appropriate for uncertain or approximate reasoning, particularly for a system with a challenging mathematical model.
- Fuzzy logic enables estimation of values during decision-making with partial or uncertain information.

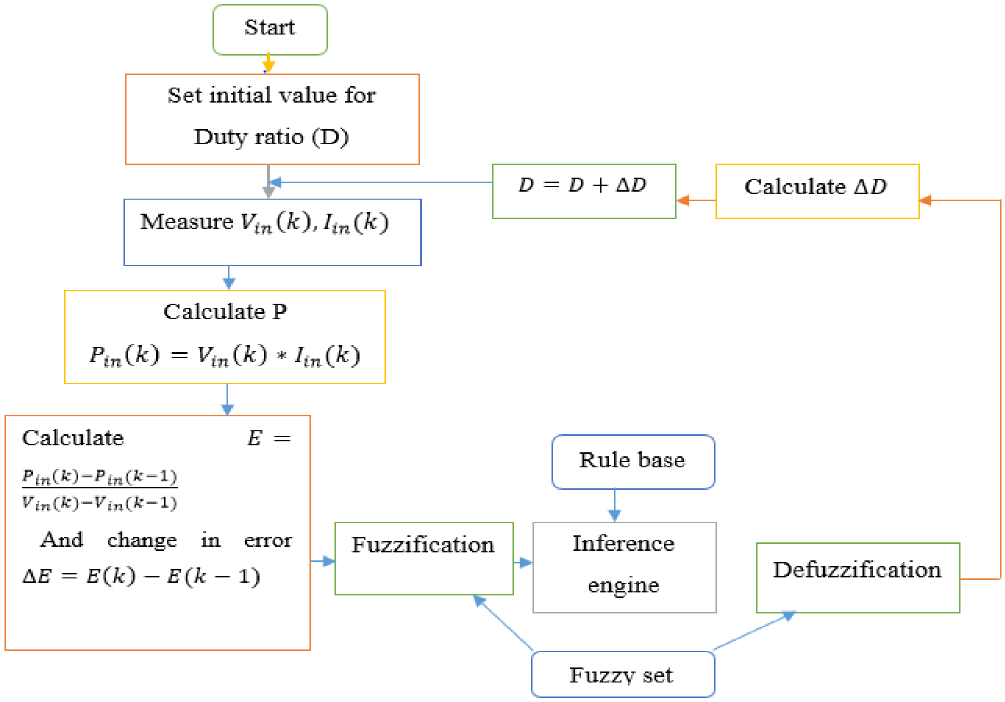

Figure 3.16 Flow Chart of Fuzzy Logic Controller(Baramadeh et al., 2021)

3.14.2 Fuzzy Logic Controller Structure

The general structure of a fuzzy controller and its main parts of the fuzzy logic controller consists of four components: fuzzification interface, knowledge base, interface engine, and defuzzification interface.

Inference: the inference method is the step of formulating the cartography using FLC of a given input to an output. It is associated with the basic types of rules: "If ... Then ..."The fuzzy inference step is carried out by Mamdani's method table shows fuzzy base rules.
Defuzzification: the defuzzification process computes the FLC crisp output.

3.14.2.1 Knowledge Base

The knowledge base is the heart of the fuzzy control system. It is the inference basis for fuzzy control. The knowledge base defines all relevant language control rules and parameters. The derivation of fuzzy control rules can be performed in four modes. These four modes are not mutually exclusive, and it is necessary to combine them to obtain an effective system.

- Expert experience and control engineering knowledge: the fuzzy control rule is based on information obtained from the controlled system.

- Operators' control actions: observation of a human controller's actions in terms of input-output operating data.
- Based on the fuzzy model of process: a linguistic description of the dynamic characteristics of a process.
- Based on learning: the ability to modify control rules such as self-organizing controllers such as neural networks and genetic algorithms.

The number of base rules can be defined based on the number of memberships in the fuzzy set and the inputs. The higher the number of memberships, the better the system efficiency will be, but the system implementation will become more complex.

3.14.2.2 Fuzzy Interface Procedure

Both the input and output variables' membership functions are divided into seven sets: big positive (BP), medium positive (MP), small positive (SP), zero (Z), big negative (SN), medium negative (MN), and small negative (NB) (Wasekar & Chamat, 2020). The table below lists the 49 rules that make up the fuzzy control rule. These guidelines are used to regulate the boost converter so that the output of the PV array produces the most power possible.

Table 3.7 Fuzzy Rule Base Table

$\frac{E \rightarrow}{CE \downarrow}$	**NB**	**NM**	**NS**	**ZE**	**PS**	**PM**	**PB**
NB	ZE	ZE	NS	MN	PM	PM	PB
NM	ZE	ZE	ZE	NS	PS	PM	PB
NS	ZE	ZE	ZE	ZE	PS	PM	PB
ZE	NB	NM	NM	ZE	PS	PM	PB
PS	PB	NM	NM	ZE	ZE	ZE	ZE
PM	NB	NM	NM	PS	ZE	ZE	ZE
PB	NB	NM	NM	PM	PS	ZE	ZE

3.14.2.3 Fuzzy Membership Functions and Rules

Membership function is a curve that defines how fuzzy value of the variable mapped to membership value between 0 and 1. Fuzzy memberships are based on the multiple input, single output (MISO) scheme with P and V and one Vref output. These appear as variables in the FIS membership editor, as shown in the figure below.

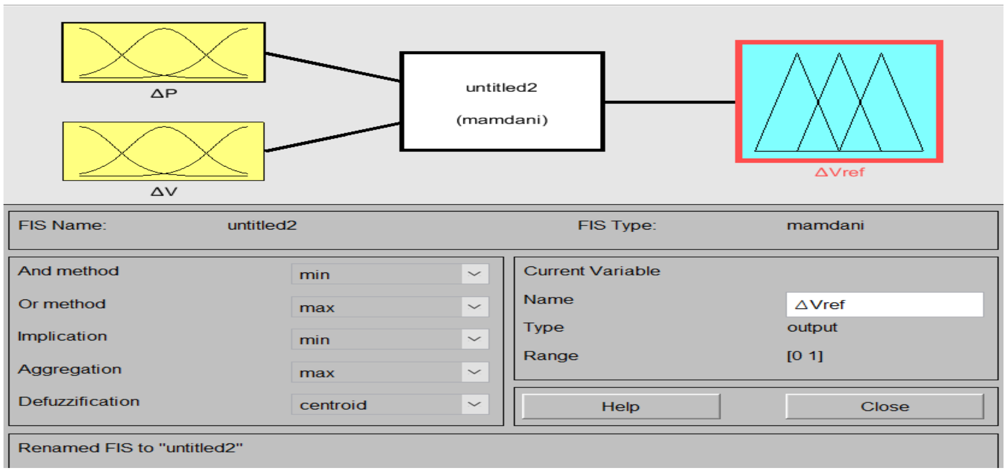

Figure 3.17 Fuzzy Logic Control Designer of Two input and one output

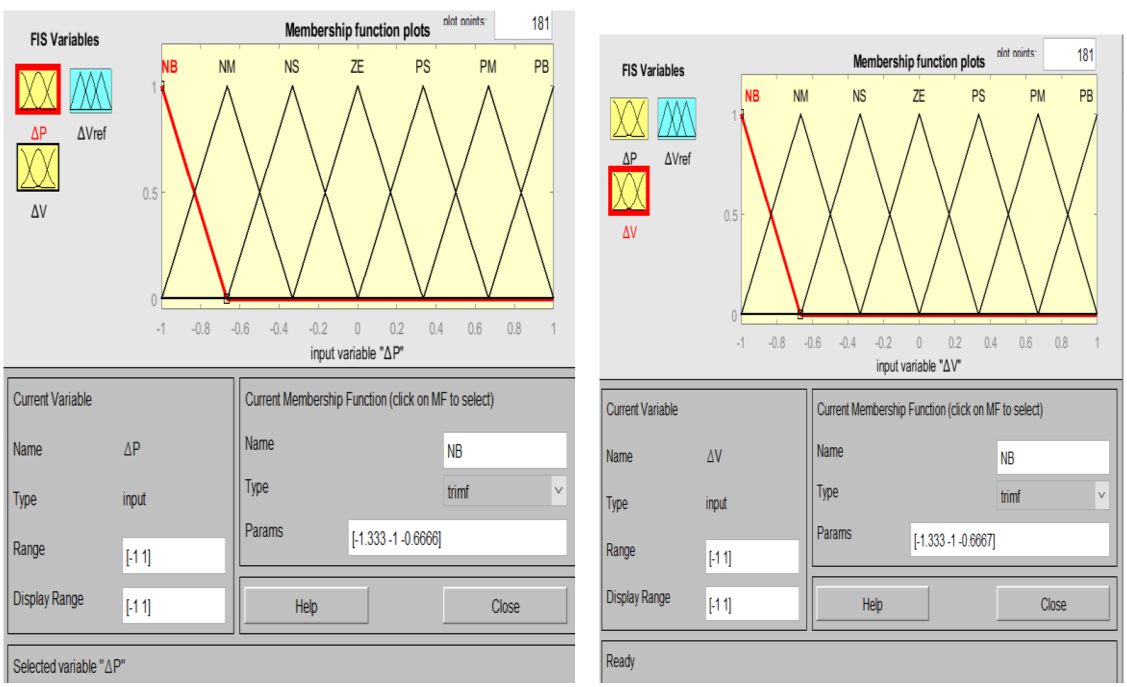

a) ΔP b) ΔV

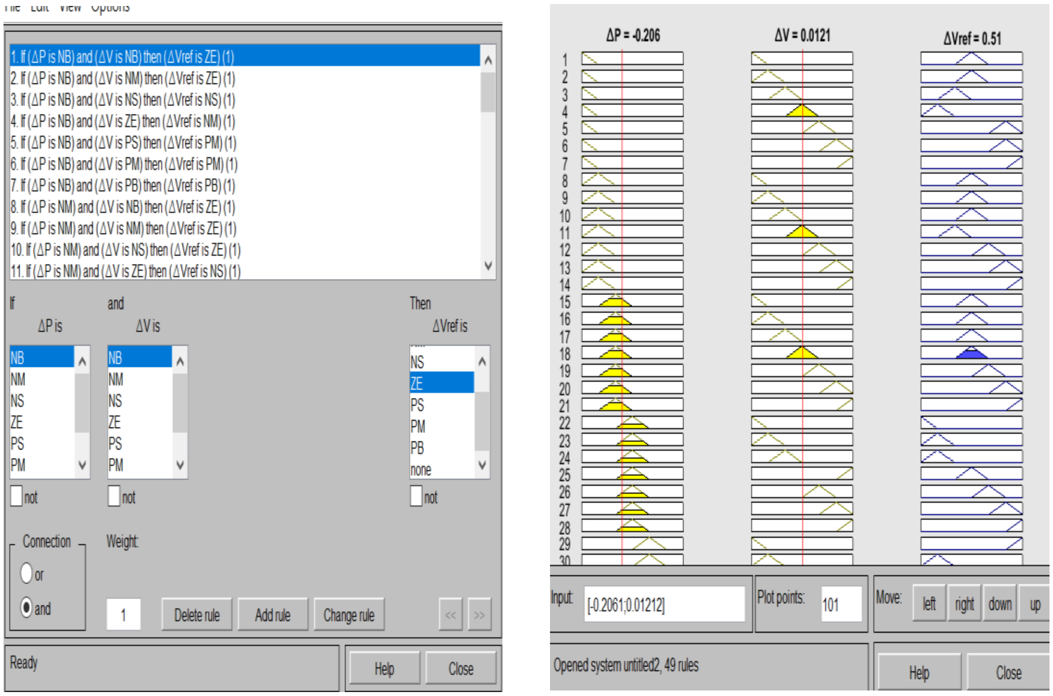

c) Rules d) Rule reviewers

Figure 3.18 Fuzzy Membership Functions (MFs) and Rules

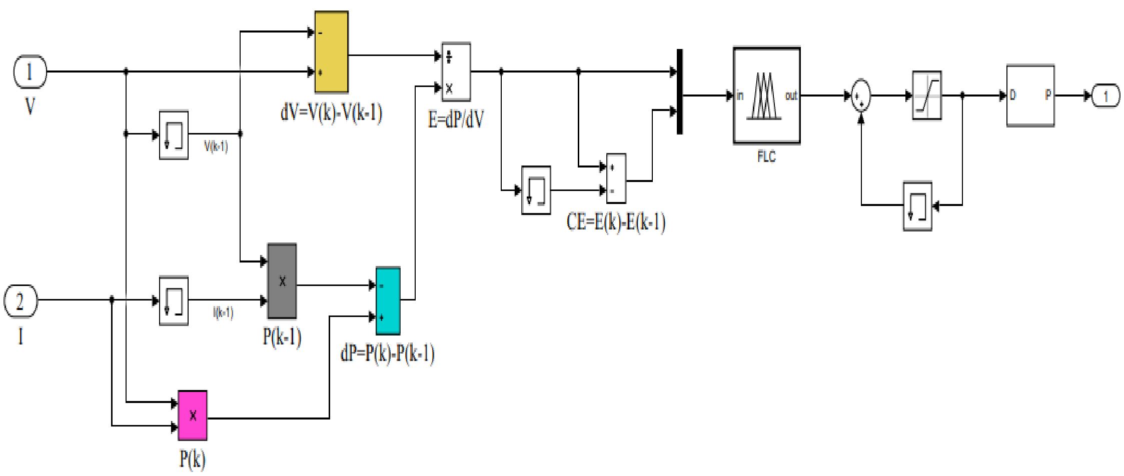

Figure 3.19 Matlab Simulink of fuzzy logic controller

3.15 Sliding Mode Controller Based Solar MPPT

Uncertain systems can be effectively controlled via sliding-mode control (SMC). The sliding-mode control system demonstrates robustness characteristics with regard to both internal parameter uncertainty and external disruptions. The DC-DC converter is managed by the

SMC-based MPPT controller, which enables MPP in varying weather conditions. With more switching, the MPP tracking speed is faster, but oscillations in the voltage output and power output are increasing (Meng et al., 2018).

A variable-structure control method based on feedback and high-frequency switching control is known as SMC. SMC provides various advantages, including a lack of susceptibility to load variations, disturbances, and changes in system parameters.

There are two stages to the SMC-MPPT algorithm. The first step is to calculate the real reference voltage (VMPP) value at which the system will operate at peak efficiency. The second is the voltage regulation of the SMC PVG at the VMPP voltage setting. These actions result in a PVG MPP functioning point. This controller's primary function is to create a command using a voltage reference (Vref) to force the system to operate at its maximum power point (MPP). The primary innovation in this method is the definition of the controller's input as Vp = VMPP.

MPP searching algorithm:

To achieve the maximum power operation the power slope $\frac{dP_{pv}}{dV_{pv}}$ can be expressed as:

$$\frac{dP_{pv}}{dV_{pv}} = 0 \tag{3.27}$$

$$\frac{dP_{pv}}{dV_{pv}} = \frac{d(I_{pv} \times V_{pv})}{dV_{pv}} = I_{pv} + V_{pv}\frac{dI_{pv}}{dV_{pv}} = 0 \tag{3.28}$$

When the power slope $\frac{dP_{pv}}{dV_{pv}} = 0$, i.e. $\frac{I_{pv}}{V_{pv}} = -\frac{dI_{pv}}{dV_{pv}}$ at MPP. Therefore, the maximum power-searching algorithm developed based on the following rules:

$$\text{For } \frac{dI_{pv}}{dV_{pv}} = -\frac{I_{pv}}{V_{pv}}, \quad \text{V}_{ref} = V_{pv}(k) \text{ at MPP} \tag{3.29}$$

$$\text{For } \frac{dI_{pv}}{dV_{pv}} > -\frac{I_{pv}}{V_{pv}}, \quad \text{V}_{ref} = V_{Pv}(k-1) + \Delta V_{ref}(k) \text{ at the left of MPP} \tag{3.30}$$

$$\text{For } \frac{dI_{pv}}{dV_{pv}} < -\frac{I_{pv}}{V_{pv}}, \quad \text{V}_{ref} = V_{pv}(k-1) - \Delta V_{ref}(k) \text{ at the right of MPP} \tag{3.31}$$

Where V_{ref} the reference maximum power voltage at k step, $\Delta V_{ref}(k)$ is the update parameter, which can be adjusted, based on fuzzy logic controller. V_{ref} is the control signal voltage used to adjust the operating point of the PV array to reach the voltage corresponding to the MPP(Hahm et al., 2015b).

MPP Stabilization:

Following estimation, the SMC was used to guide the regulation element in order to reduce the actual voltage error between the acquired PV voltage and the target VPV. The boost converter conducts the PV to operate at the targeted reference voltage value (Vref) and at the maximum power point.

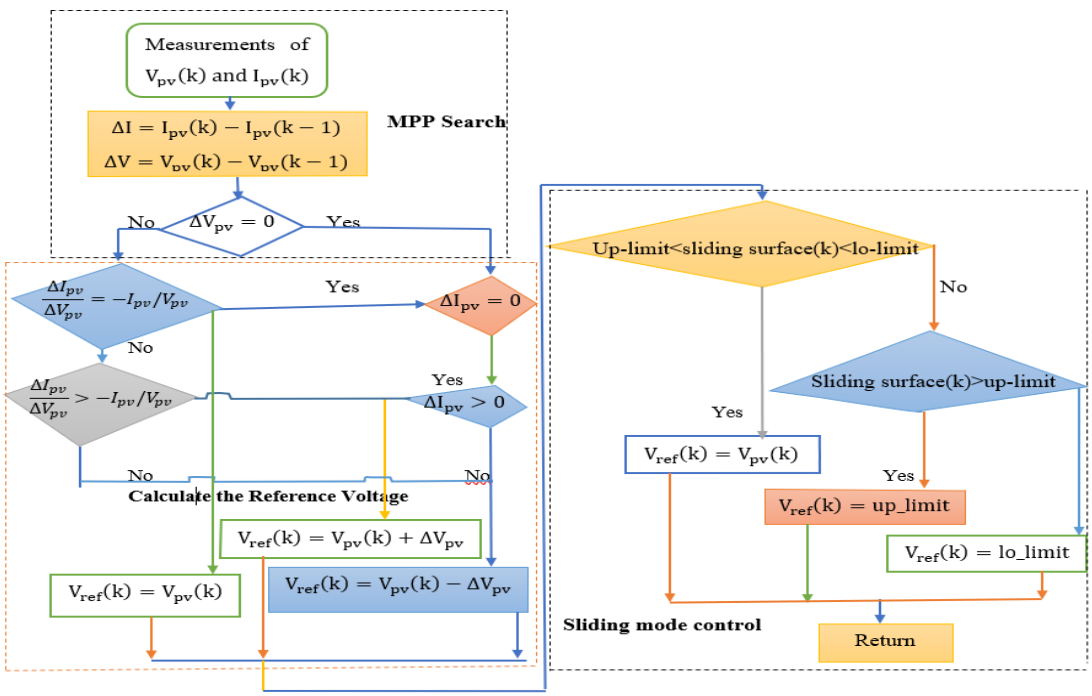

Figure 3.20 Sliding Mode Control Algorithm based on of the *V*ref (El, 2017a)

The change in PV voltage and the reference voltage are the controller's inputs; the change in duty cycle is the sliding mode control's output. Comparing the incremental conductance (Ipv/Vpv) to the instantaneous conductance (Ipv/Vpv) allows for the tracking of the MPP. Vref is the voltage of the control signal that is used to modify the PV array's operating point so that it reaches the MPP's voltage. Once the MPP voltage is reached, the PV array is kept at this operating point unless an alteration in ΔIpv is noted, indicating an alteration in the weather conditions and the MPP. The algorithm decrements or increments Vref to track the new MPP. To implement sliding mode control (SMC), we use a saturation function; the Up limit is the upper limit and the Lo limit is the lower limit of the saturation function. The output is Vref when the sliding surface is situated between the lower and upper saturation limits. Otherwise, the output will be one of these two possibilities (Hahm et al., 2015b).

The main role of this controller is to generate a command using a voltage reference (Vref) in order to force the system to work at the maximum power point (MPP). After the estimation of VMPP, the implemented SMC is used to drive the regulation element in such a way as to reduce the actual voltage error between the acquired PVG voltage and the target VMPP. The boost converter is forced to bring up the PVG to operate at the desired reference voltage value (Vref) and therefore at the maximum power working point(Farhat et al., 2016).

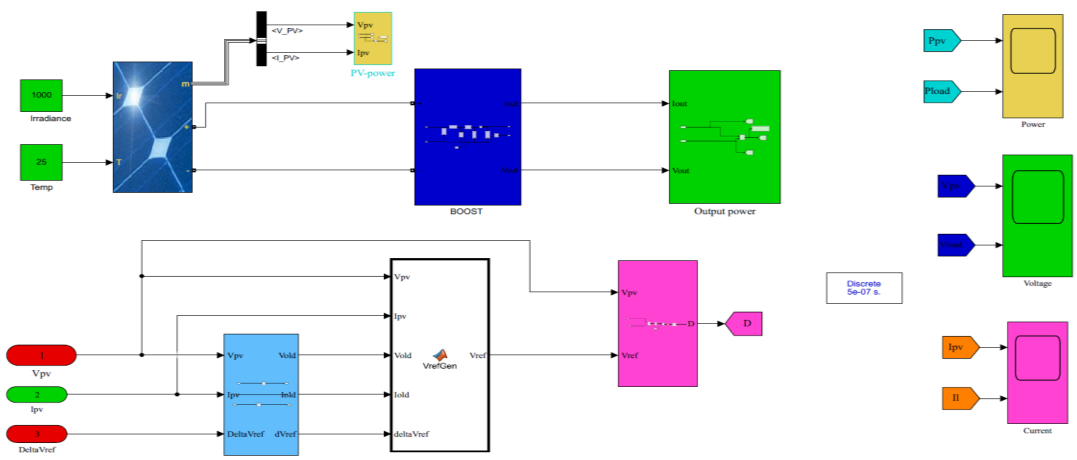

Figure 3.21 Simulink Model of Sliding Mode Controller

3. 16 Fuzzy Sliding Mode Control Algorithm

In this thesis, a new MPPT controller that combines two different and powerful tracking techniques in non-linear systems is introduced: sliding mode control (SMC) and fuzzy logic control (FLC). It is well known that SMC offers good robustness and transient performance. However, due to the discontinuous control action, chattering occurs, which is defined as oscillations around the sliding surface and degrades steady-state performance (El, 2017a).

The PV system operates as efficiently as possible under changing solar conditions and load. The fuzzy sliding mode control is used. In this study, a fuzzy sliding mode controller has been developed to offer smooth control action and stabilize system responses under significant disturbances. An interface consists of a DC-DC boost converter and a hybrid MPPT unit with sliding and fuzzy controllers. To turn the converter on and off, the MPPT unit produces a control signal for pulse width modulation (PWM). The boost converter increases the PV current and voltage that is sent to a grid-connected system with a DC-AC inverter or a standalone system.

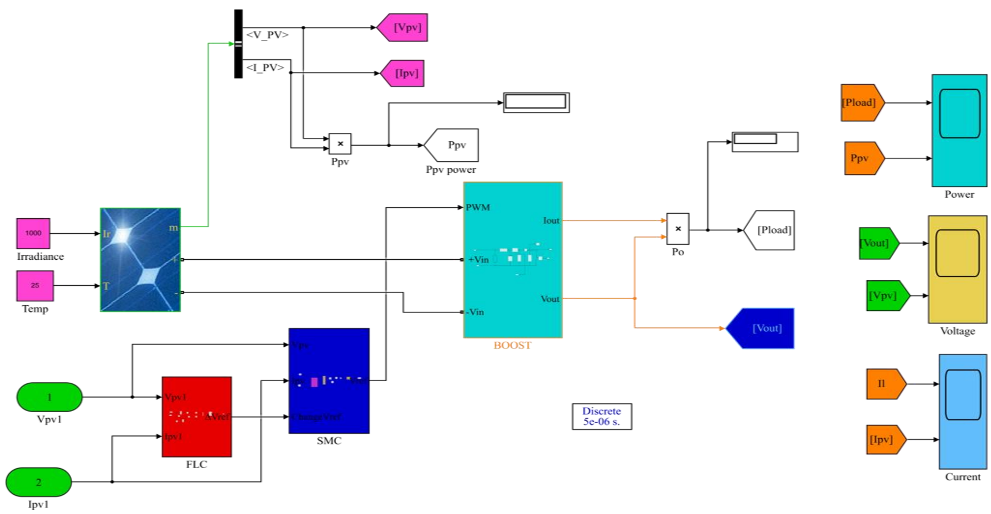

Figure 3.22 Simulink Model of Fuzzy-Sliding Mode Controller

3.17 Design of BLDC Motor for Solar Water Pumping System

In isolated rural locations where power transmission is either practically impossible or unaffordable even if it is possible, water pumping has emerged as the most attractive use of solar photovoltaic (SPV) energy(Singh & Kumar, 2016). As an example, a typical PV water pumping system accomplishes the following tasks: it eliminates the issue of pumping being impossible owing to a lack of grid availability and helps close the gap between power production and demand(Rayaguru & Sekar, 2017). A centrifugal water pump attached to the shaft of the BLDC motor is driven by it. The BLDC motor is chosen due to its advantages in the building of an appropriate water pumping system.

In this thesis, the PV array's MPPT is powered by a DC-DC boost converter. The advantages of this converter include its inherent features of lowest switching stress conceivable, highest conversion efficiency due to fewer components, excellent switch utilization, and the elimination of an input ripple filter because the input inductor itself serves as a ripple filter(Singh & Kumar, 2016). Because this converter is used in continuous conduction mode (CCM), its power devices and components are under less stress(Kumarasamy et al., 2017).

Positive displacement and centrifugal pumps are frequently employed in PV water pumping applications. Low-volume pumps often use positive displacement types since they are more affordable. The efficiency of centrifugal pumps is rather high, and they can move a lot of water(Krishnakant & Kulkarni, 2021).

3.17.1 Mathematical Model of a Brushless Direct Current Motor

BLDC motors are synchronous motors that operate on the same principles as DC motors. They are electrically commutated motors. Commutation is the process of energizing stator windings sequentially to start the rotor. To determine which winding will energies next, the location of the rotor is sensed by hall sensors(Shajilal & Julian, 2017). Since DC motors may be connected directly to PV arrays and simplify operations, many PV water pumping systems do so(S. Kumar & Kumar, 2020).

The model of armature winding for BLDC motor is expressed as follows:

$$V_a = Ri_a + L\frac{di_a}{dt} + e_a \tag{3.32}$$

$$V_b = Ri_b + L\frac{di_b}{dt} + e_b \tag{3.33}$$

$$V_c = Ri_c + L\frac{di_c}{dt} + e_c \tag{3.34}$$

Where:

$R_a = R_b = R_c = R$ Stator resistance per phase (Ω)

$L_a = L_b = L_c = L$ Stator inductance per phase (H)

V_a, V_b, V_c Stator phase voltages (V)

i_a, i_b, i_c Stator phase currents (A)

e_a, e_b, e_c Motor back emf (V)

The equivalent circuit of the brushless dc winding is shown below

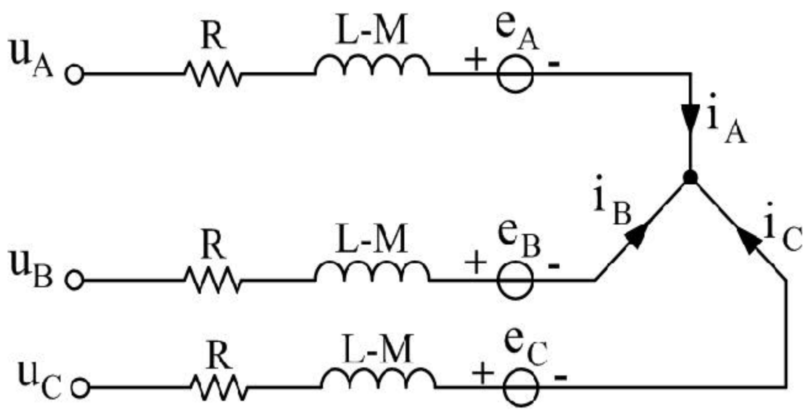

Figure 3.23 The equivalent circuit of BLDC Motor

A BLDC motor's windings generate a voltage during rotation that is the opposite of the main voltage applied to the windings. The source voltage's polarity is opposite that of the return electromagnetic field(Mondal et al., 2015).

The back EMFs generated are given by the following equations:

$$e_a = k.\omega.f(\theta) \tag{3.35}$$

$$e_b = k.\omega.f(\theta - \frac{2\pi}{3}) \tag{3.36}$$

$$e_c = k.\omega.f(\theta + \frac{2\pi}{3}) \tag{3.37}$$

where,

K is the Back EMFs constant (V/rad/s)

θ is the electrical angle

ω is the mechanical speed of the rotor (rad/s)

The Back EMFs are also related to the function of rotor position and each phase has a phase difference of 120^o. Back EMF is affected by these three main factors:

(i) Angular velocity of the rotor.

(ii) Magnetic field generated by the rotor magnets.

(iii) The number of turns in the stator windings.

So, the total torque equation can be defined as:

$$T_e = \frac{i_a e_a + i_b e_b + i_c e_c}{\omega} = \frac{ia.K.f(\theta) + ib.K.f(\theta - \frac{2\pi}{3}) + ic.K.f(\theta + \frac{2\pi}{3})}{\omega} \tag{3.38}$$

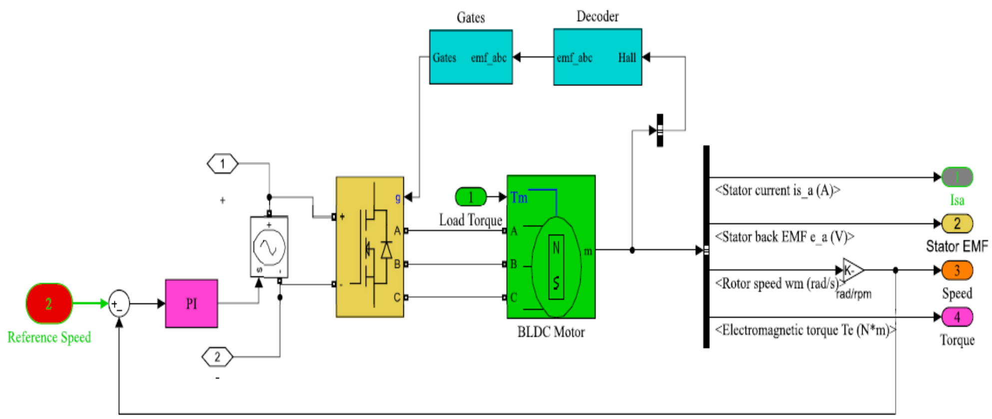

Figure 3.24 Model of the BLDC Motor

CHAPTER FOUR

RESULTS AND DISCUSSIONS

The functionality of the suggested MPPT controllers is tested and validated in this chapter using the Matlab Simulink models of the PV power systems. A PV system simulation in Matlab is used to illustrate the suggested perturb and observe, fuzzy sliding, and fuzzy sliding based on the MPPT modes of a water pumping system. A comparison of the effectiveness of the proposed controller to perturb and observe, sliding mode, fuzzy sliding mode, and fuzzy logic controllers has also been made.

4.1 Photovoltaic System Modeling Using MATLAB/Simulink

MATLAB 2019a/SIMULINK is used to model and simulate the system design. The major components of the modelled system are a model of the PV array and a model of the DC-to-DC boost converter that connects the PV output load to the PV array's maximum power. The 5.682 kW power PV array utilised in the simulation has four strings and seven 200-watt modules. or, under the predetermined standard conditions of (G = 1000 w/m^2) irradiation and (T = 25°C) temperature, 4 x 7 elements are coupled to produce the desired power.

The current-to-voltage, voltage-to-power, and current-to-power relationship curves of the simulated model are used to discover the influence of temperature and irradiation changes on the output characteristics of the PV panel. The output of the PV array is recorded at different levels of irradiation (1000, 750, 550, and 350 w/m2) at 25 °C, as well as at different environmental temperatures (25, 45, 55, and 65) at standard irradiation values or random values of temperature and standard irradiation level, and the result of the characteristic curves is plotted.

4.2 Effect of Irradiance on the Performance of a PV Module

While the temperature is maintained at 25^oC, the voltage and current output of a photovoltaic module is directly proportional to solar irradiation, as shown in figure 4.1.

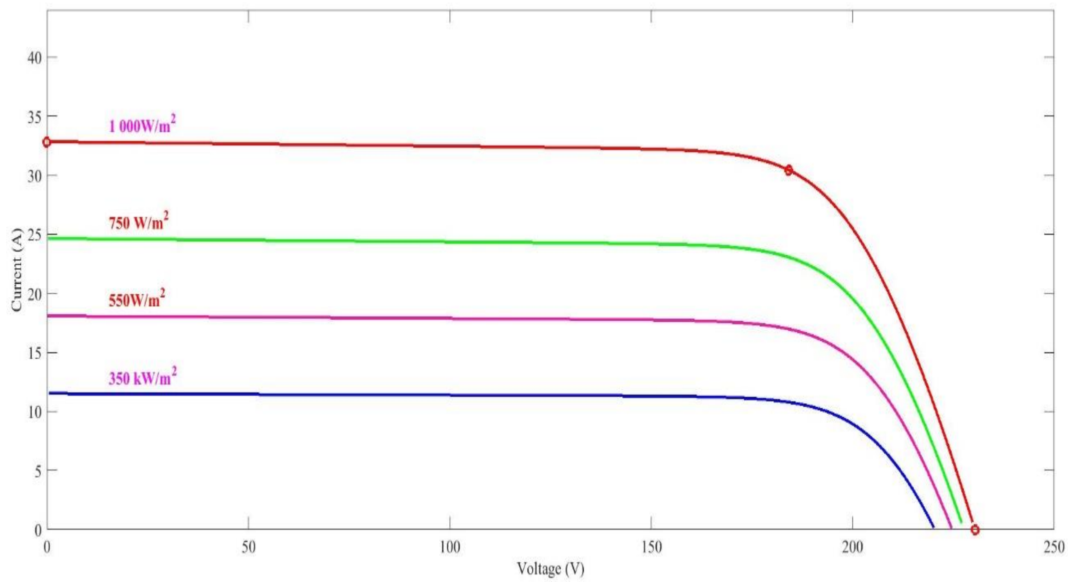

Figure 4.1 Effect of Irradiation on the PV voltage and current output

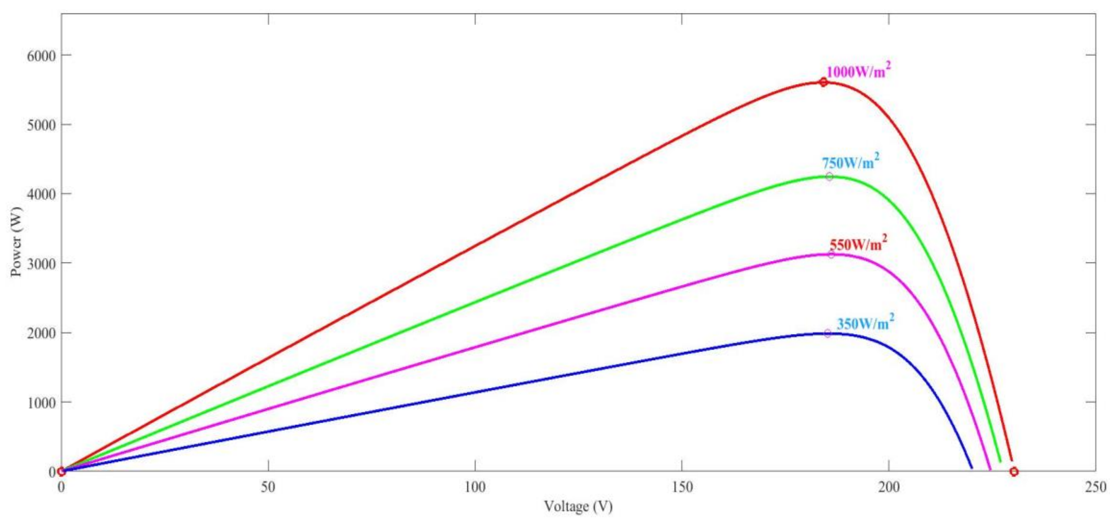

Figure 4.2 Effect of Irradiation on PV output Power

The curve shown in Figure 4.2 shows that the power produced by the solar panel is directly proportional to the solar radiation.

4.3 Effect of the Temperature on the Performance of a PV Module

When the irradiance is maintained at 1000W/m^2, the voltage and current of the panel is inversely proportional to the temperature as shown in figure 4.3 below.

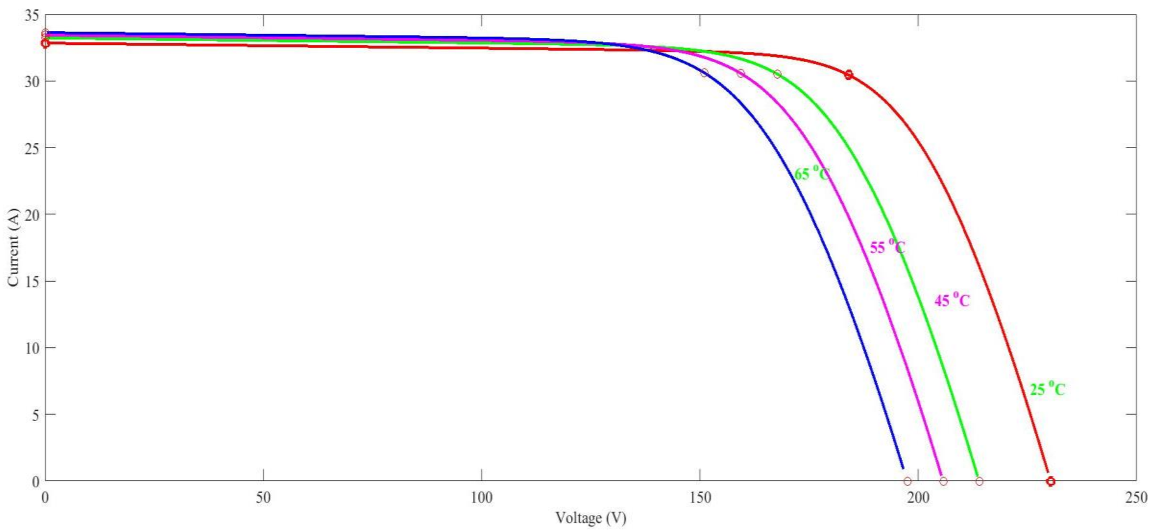

Figure 4.3 Effect of Temperature on output voltage and current

The power produced by the photovoltaic modules decreases with an increase in temperature because the band gap energy decreases and more photons have enough energy to create electron-hole pairs, which eventually reduces the efficiency of the panel.

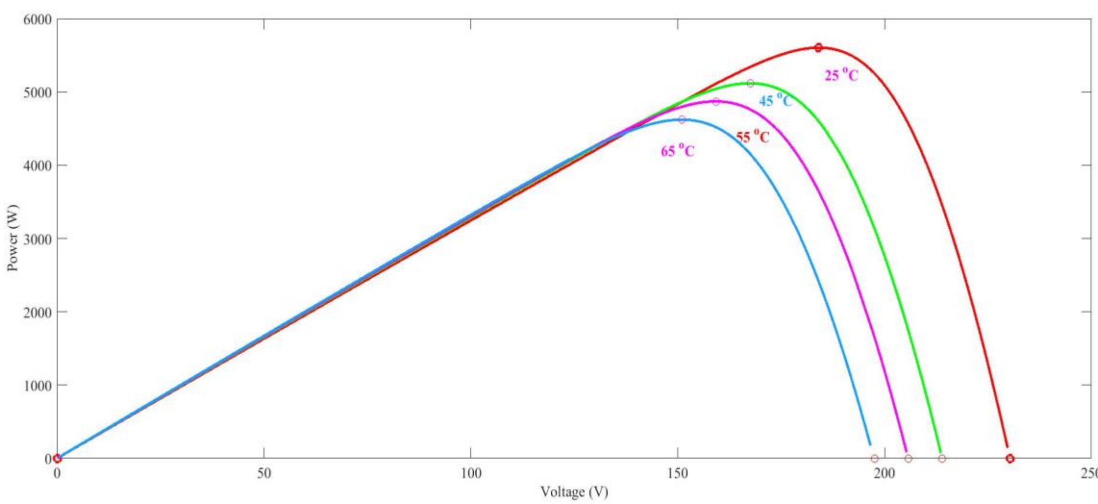

Figure 4.4 Effect of the temperature on solar power output

4.4 Current and Power Curves under Partial Shading

The incident of partial shading has been simulated using Matlab Simulink, as shown below under Appendix A, where the first solar panel has been subjected to an irradiance of 1000 W/m^2. The next set of panels has been subjected to an irradiance of 300 W/m^2, and the last set of panels has been subjected to an irradiance of 600 W/m^2. Figure 4.5 shows the current and power curves for the KC200GT module under partial shading conditions, where the modules partially received different irradiances of 1000 W/m^2, 300 W/m^2, and 600 W/m^2, respectively. The curves show multiple maximum power points. One global peak and two local peaks are observed, as shown in figure 4.5 below. The local peaks have different power results due to the variability of the irradiances.

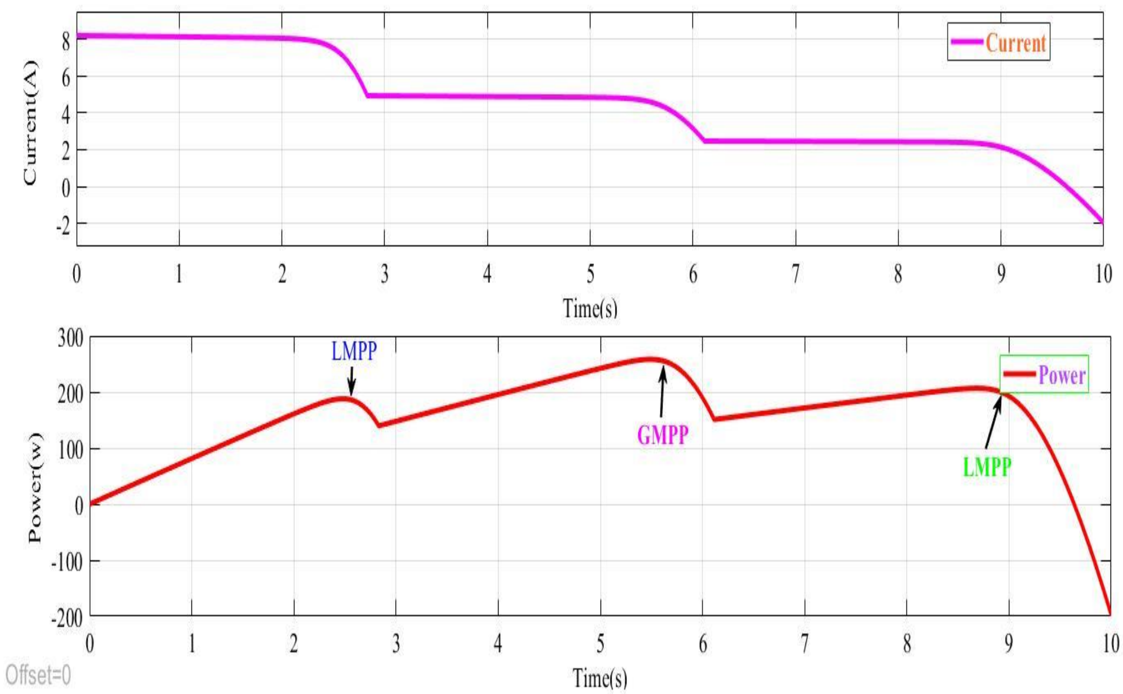

Figure 4.5 Current and Power Curve of under Partial Shading showing Local and Global MPP

4.5 Simulation Result of P and O with in different Disturbances

The performance of the proposed approach will be evaluated under conditions of uniform irradiation and temperature, rapid change in solar irradiation, rapid change in ambient temperature, and rapid change in load. I use three quick changes of illumination or irradiation, and Figure 4.6 shows one of the main drawbacks of the perturb and observe MPPT algorithm. That means at high irradiance, or around MPP, more oscillation occurs and it takes more time to track when compared with a sliding mode controller and an intelligent controller such as fuzzy logic.

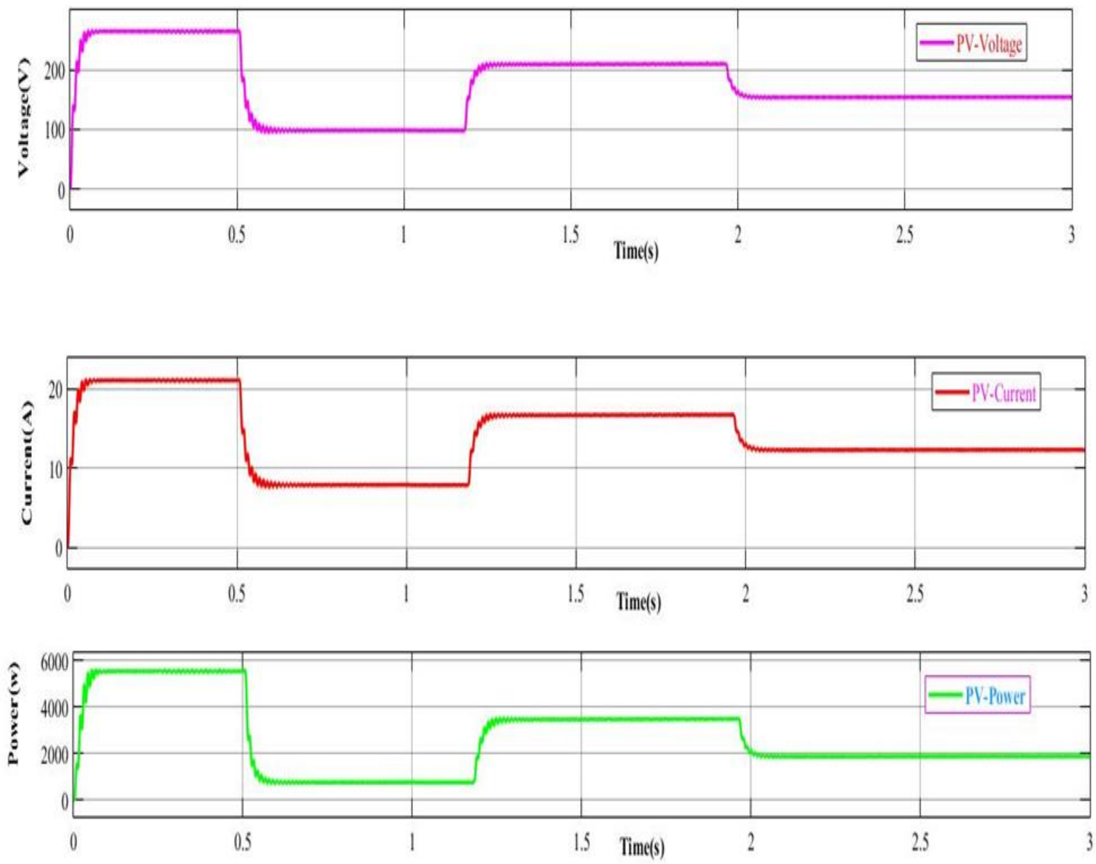

Figure 4.6 The PV-Voltage, PV-Current and PV- Power of P and O at 25°C Respectively

Figure 4.6 illustrates the output voltage, output current, and output power of the perturb and observe approaches under various illuminations. As the illumination is raised, the output increases, but the oscillation around the MPP is increased. The output voltage and output power are negatively impacted by the temperature. On the other hand, the output power tracks the power produced by the PV panel, maintaining the MPP as the operational point, proving the efficacy of this approach.

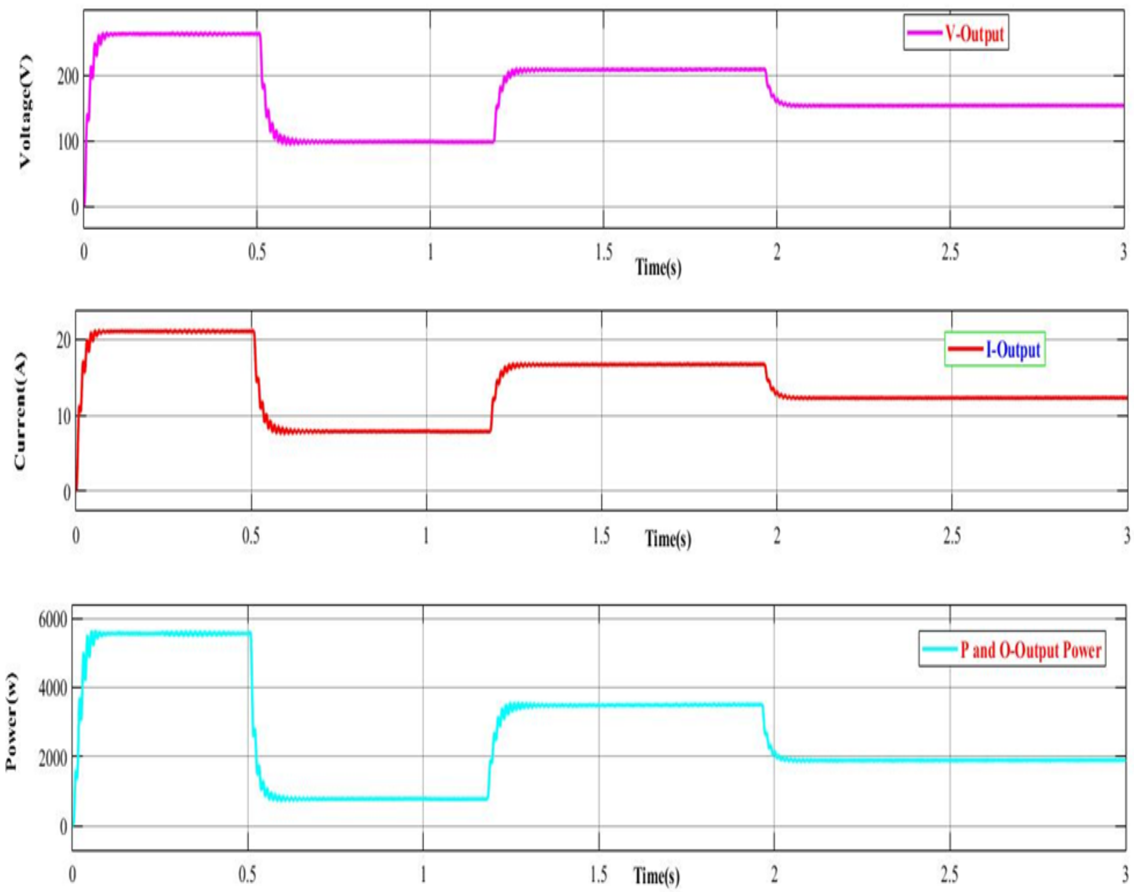

Figure 4.7 The Output-Voltage, Output- Power and Output-Current of P and O

In order to evaluate the performance of the proposed method, the efficiency of the P and O MPPT Algorithms are calculated in Table 4.1 below under different irradiances.

Table 4.1 Efficiency of Perturb and Observe Algorithm Temperature

Irradiance in w/m^2	Temperature (℃)	PV power PV(W)	Output power with P and O (W)	Tracking Efficiency (%) P_o / P_{pv}	
350	25	793	774	97.48	
550	25	1916	1879	98.07	
750	25	3549	3498	98.56	
1000	25	5598	5525	98.70	
				Average	98.20

According to table 4.1, the efficiency of the perturbation and observation depending on the irradiation at constant temperature will be evaluated. The efficiency or the performance of P and O is less when compared with other MPPT controllers.

4.6 Simulation of FLC Solar MPPT at Constant Irradiation and Temperature

The simulation has been carried out by the fuzzy logic controller algorithm. From the simulation results, it is clearly evident that the fuzzy logic controller's (FLC) maximum power point tracking is quite efficient in tracking the maximum power point (MPP). Moreover, it limits or reduces oscillations or chattering phenomena experienced when other MPPT techniques, such as sliding mode techniques, are used. The fuzzy logic controller maximum power point tracking techniques have the advantage of being implemented without the necessity of knowing the mathematical model of the system and can perform well in non-linear conditions. The fuzzy logic controller (FLC) shows smooth tracking.

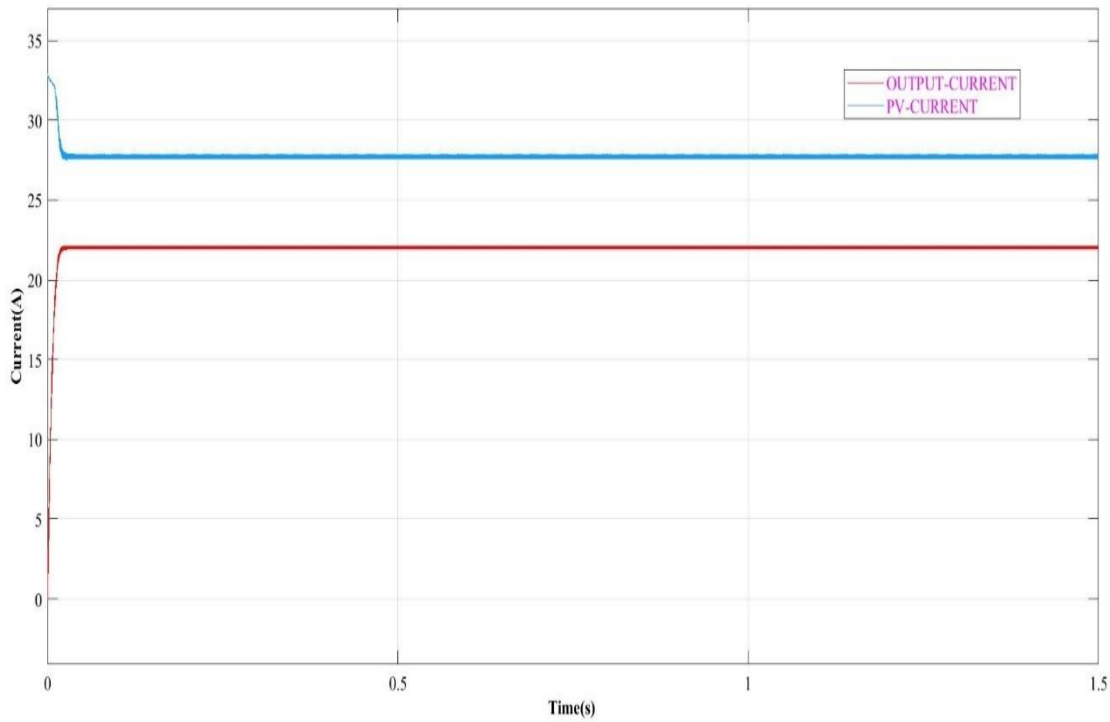

Figure 4.8 Output current and PV-Current of FLC under uniform Irradiation

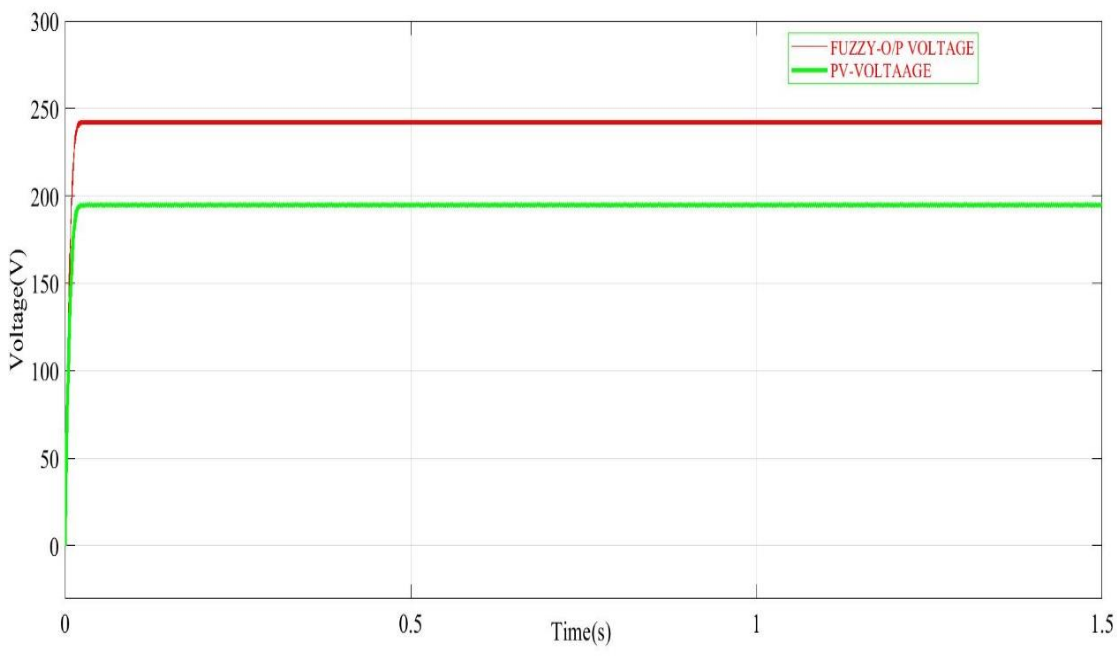

Figure 4.9 Output Voltage and PV-Voltage of FLC at uniform Irradiation

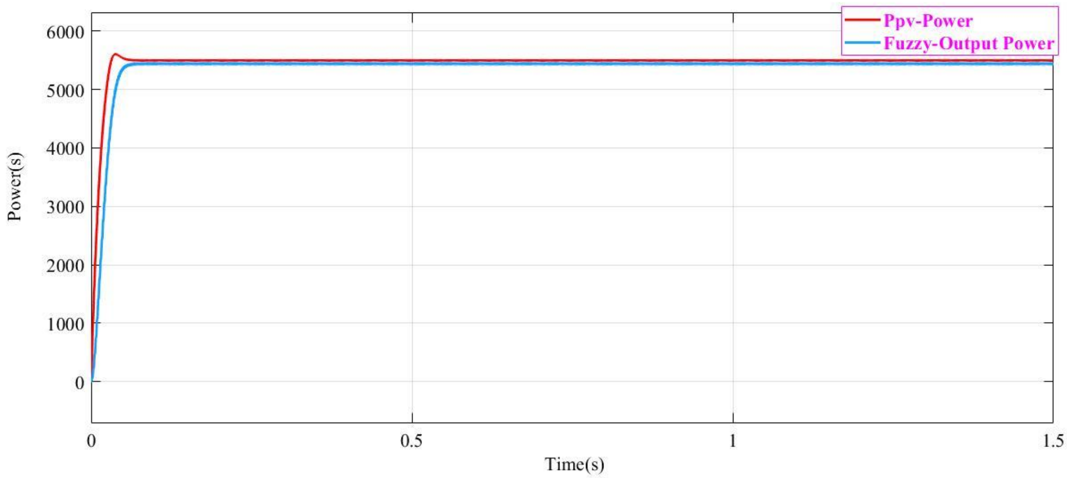

Figure 4.10 Output Power and PV-Power of FLC at uniform Irradiation

4.6.1 Simulation of the System at Variable Irradiation

In order to verify the effectiveness of the proposed and considered maximum power point algorithms, the system was also simulated under variable irradiance conditions. The simulation was applied at different irradiance levels and at a constant temperature, as shown in figure 4.11 below.

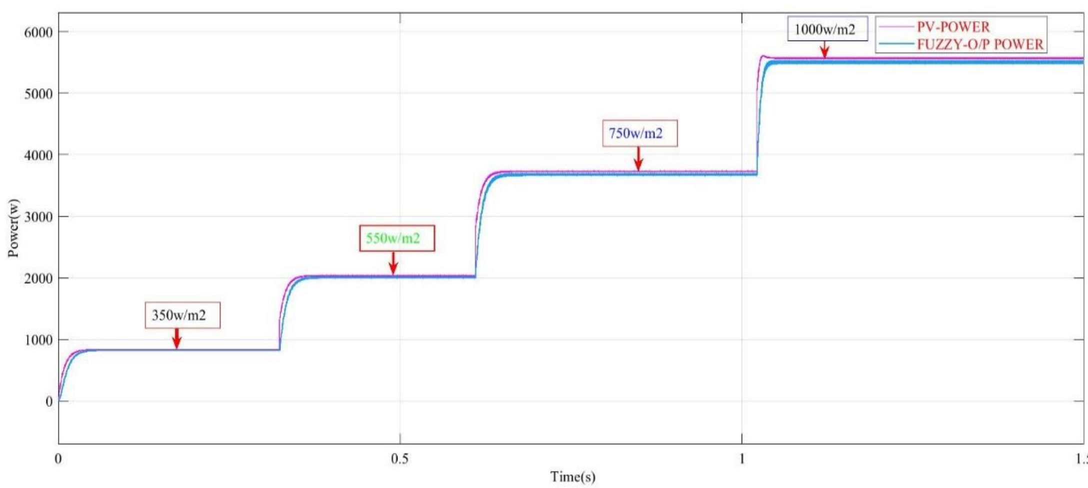

Figure 4.11 Output Power and PV-Power of FLC at different Irradiation

Table 4.2 Performance of FLC at different Irradiation and at 25 ^{0}C

Irradiance in W/m^2	Temperature (°C)	PV power Ppv(W)	Output power Po(W) with FLC	Tracking Efficiency (%) $\frac{P_o}{P_{pv}}$	
350	25	922	906	98.26	
550	25	2244	2211	98.53	
750	25	4037	4011	99.38	
1000	25	5556	5543	99.60	
				Average	98.69

Based on the result evaluated in Table 4.2 the efficiency increased with increasing irradiance, and when the radiation decreased, the efficiency decreased.

4.7 Simulation Results of Sliding Mode Controller at Uniform Temperature and Irradiation

The output of the PV array is recorded at different levels of irradiation, which are 350 W/m^2,550 W/m^2 ,750 W/m^2, and 1000 W/m^2 at 25^{o}C and the signal is shown in figure 4.12.

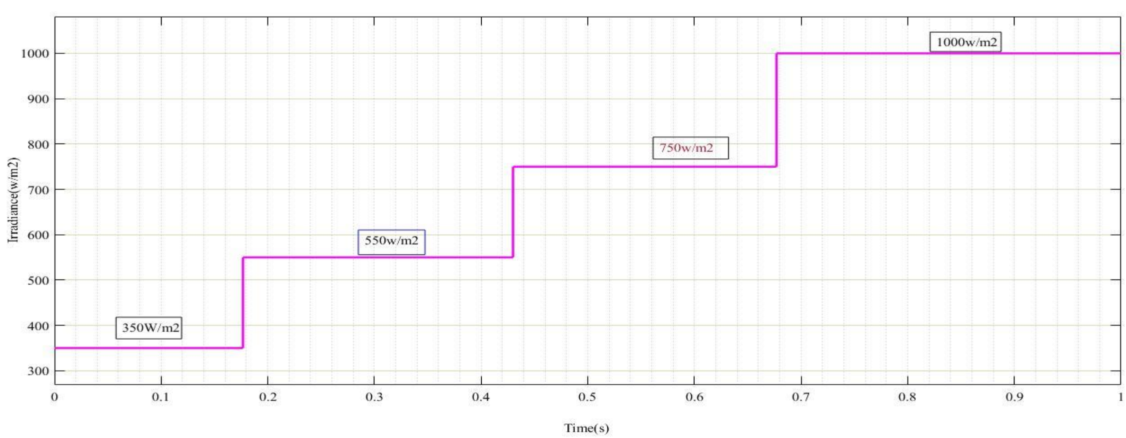

Figure 4.12 Signals at Variable Irradiations

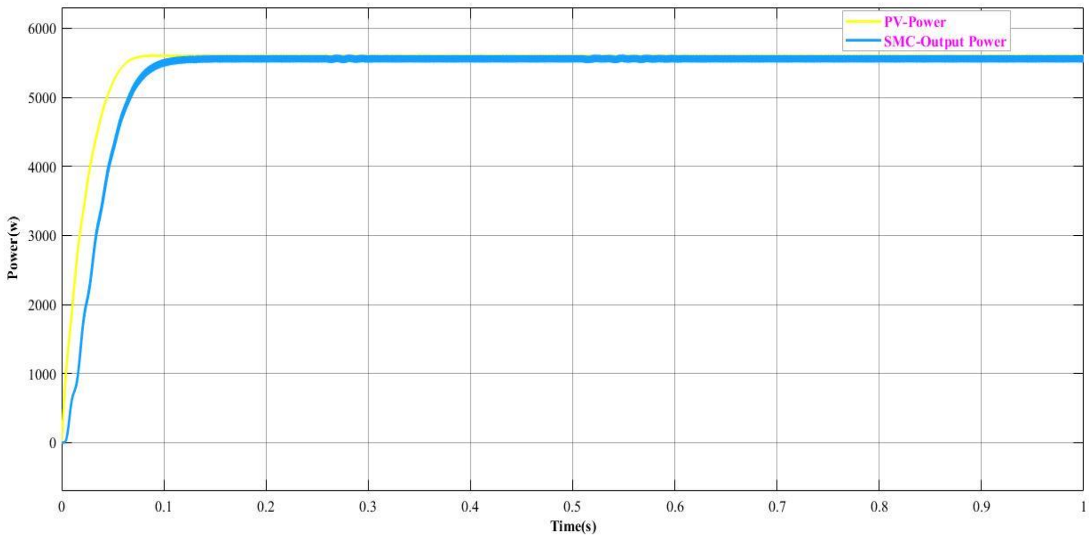

Figure 4.13 MPPT performance of SMC at 25^0C and 1000W/m^2

The simulation results in Figure 4.13 and Table 4.3 indicate that the sliding mode controller has better tracking performance compared to perturb and observe and fuzzy logic controllers, but there is a chattering problem around the maximum power point with irradiation variation. A fuzzy logic controller has smooth tracking speed at medium irradiation compared to a sliding mode controller. As shown in Table 4.2, the tracking efficiency of a fuzzy logic controller at irradiation levels of 350 and 1000 W/m2 is 98.26% and 99.60%, respectively. While the tracking efficiency of the sliding mode controller is 98.32 percent and 99.66 percent, respectively, as shown on table 4.3. But, at medium irradiation 550W/m^2 and 750W/m^2 tracking efficiency of the Fuzzy logic controller is 98.53% and 99.38%, while in tracking efficiency of the sliding mode controller is 98.60% and 99.44%, respectively.

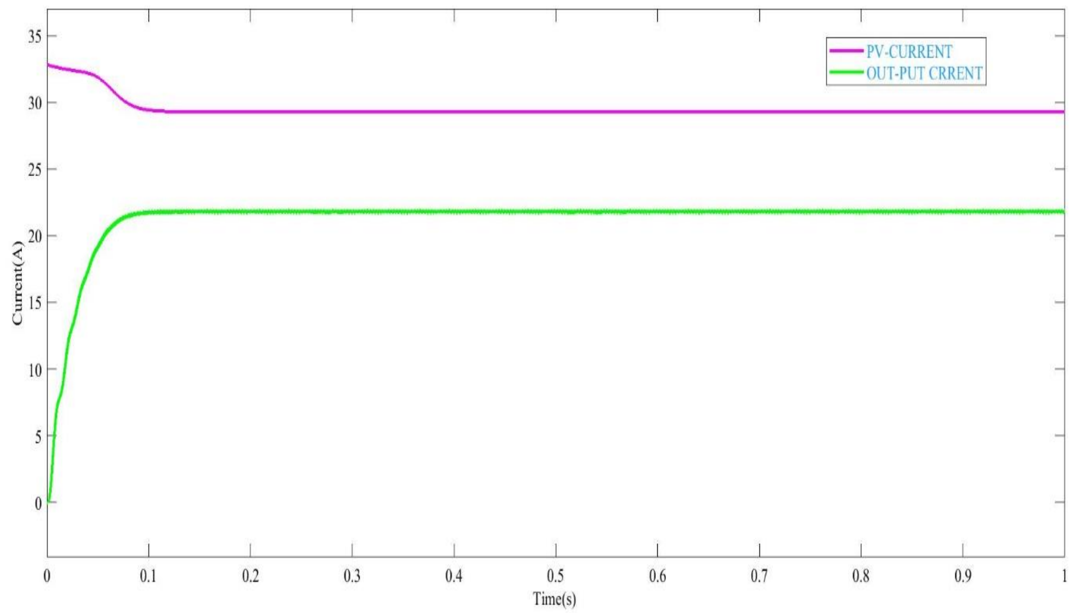

Figure 4.14 PV and Output-Current of SMC respectively

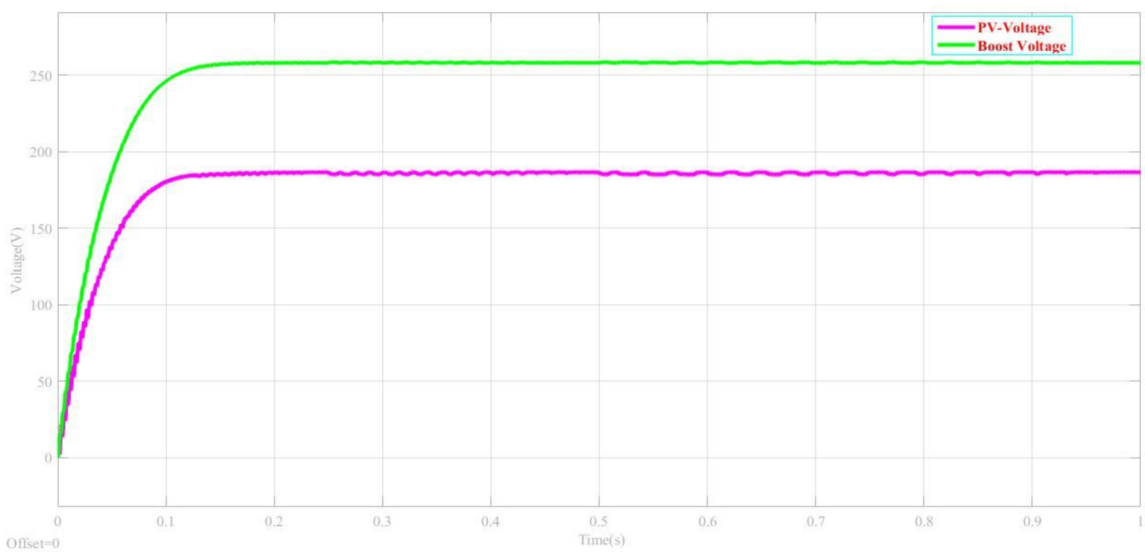

Figure 4.15 Output Voltage and PV-Voltage of SMC under uniform Irradiation

Table 4.3 Performance of SMC at different Irradiation and at 25^0C

Irradiance in W/m^2	Temperature (℃)	PV power Ppv(W)	Output power Po(W) with SMC	Tracking Efficiency (%) $\frac{P_o}{P_{pv}}$	
350	25	848.3	834.1	98.32	
550	25	2073	2044	98.60	
750	25	3776	3755	99.44	
1000	25	5576	5557	99.66	
				Average	99.01

Table 4.5 and figure 4.24 shows the performance of the controllers at different temperatures. The output power of a sliding mode controller and a fuzzy sliding mode controller decreases as the temperature rises from 25 degrees Celsius to 65 degrees Celsius. As the result indicates, all the controllers have better performance with sudden variations in temperature. But, the hybrid of fuzzy and sliding mode controllers provides maximum output power compared with the fuzzy logic, sliding mode controllers and perturb and observe techniques. The maximum power point tracking efficiency during temperature variations in the case of a fuzzy-sliding mode controller is 99.97%, in the case of a sliding mode controller it is 99.66%, and in the case of a fuzzy logic controller it is 99.60%.

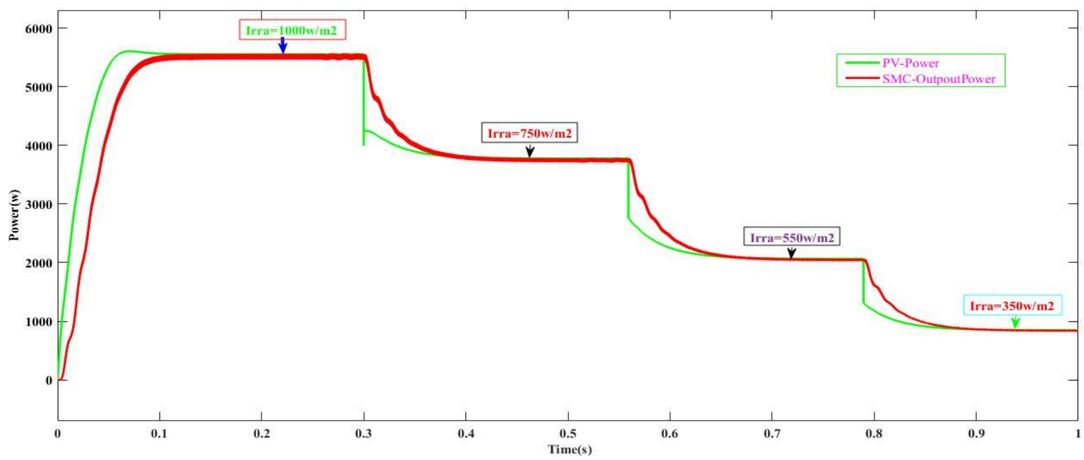

Figure 4.16 MPPT performance of SMC with sudden variation of irradiation

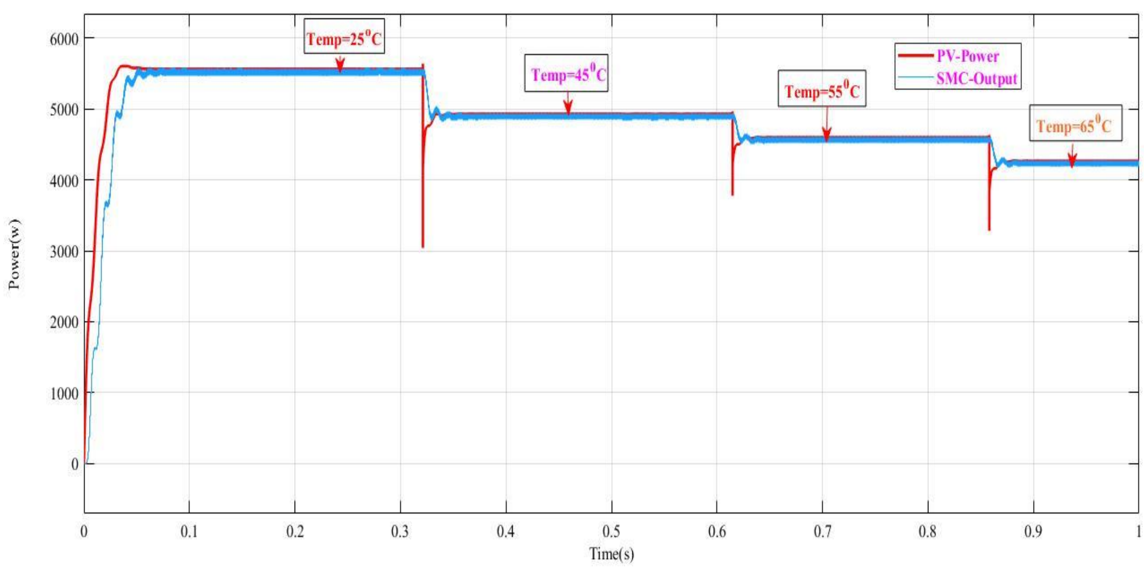

Figure 4.17 MPPT performance of SMC with sudden variation of Temperature

4.8 Simulation Result of a Fuzzy Sliding Mode Controller

The obtained result in figure 4.18 shows the good robustness of the fuzzy-sliding mode MPPT algorithm. It takes less time to track and maintain the output power at MPP all the time. The graph in 4.18 clearly shows that the FSMC technique overcomes the chattering problem or phenomenon and performs well when compared to P and O, SMC, and fuzzy logic. However, the perturb and observe method exhibits a hard oscillation, which reduces the output of the PV system. The algorithm consists of a single-diode equivalent circuit, which has been chosen due to the simplicity of simulation and modelling and because it provides fast convergence. To improve the power generated for a given set of climatic conditions, combine the performance of fuzzy logic and sliding mode control. The main advantage of FSMC is that it takes less time to track MPP, reduces the oscillation around the operating point, and also reduces chattering phenomena that can lead to a decrease in the efficiency of the PV system.

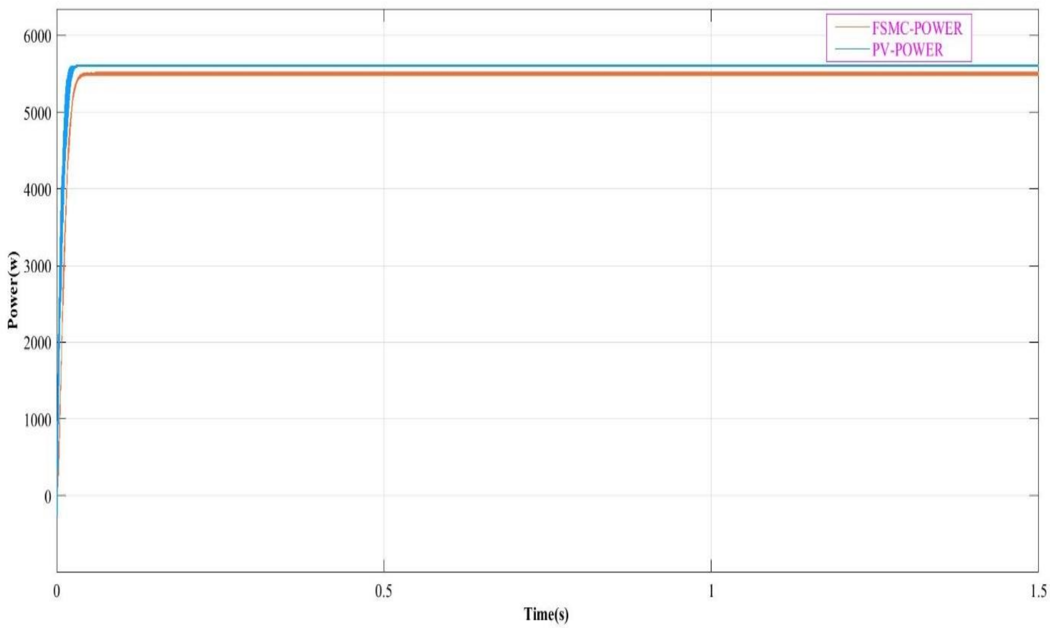

Figure 4.18 MPPT Output Power of FSMC with uniform Temperature and Irradiation

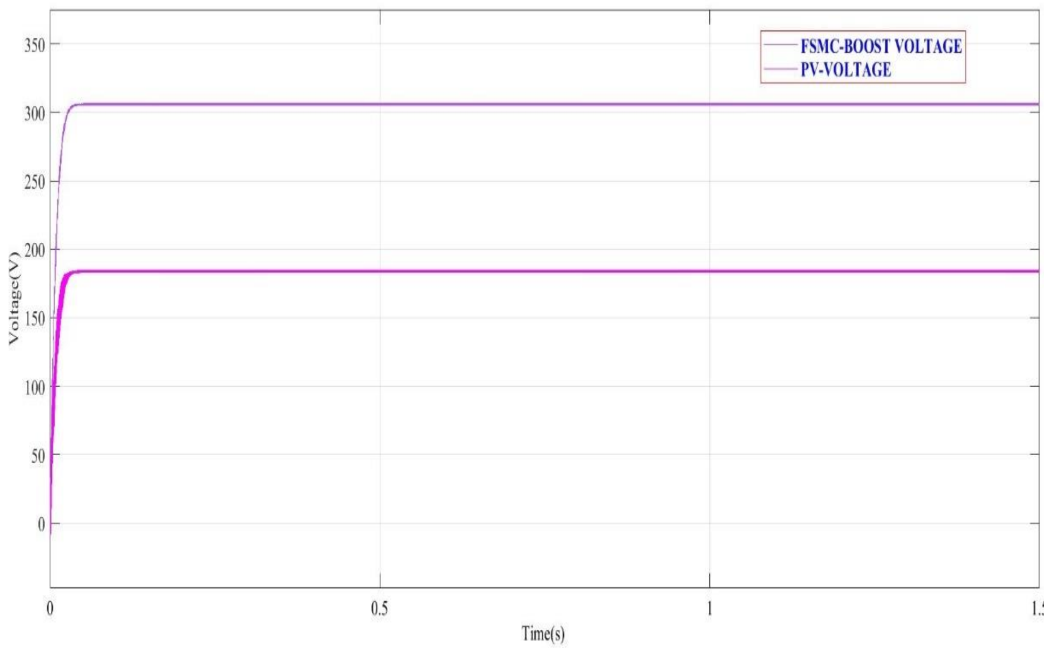

Figure 4.19 MPPT Output Voltage of FSMC with uniform Temperature and Irradiation

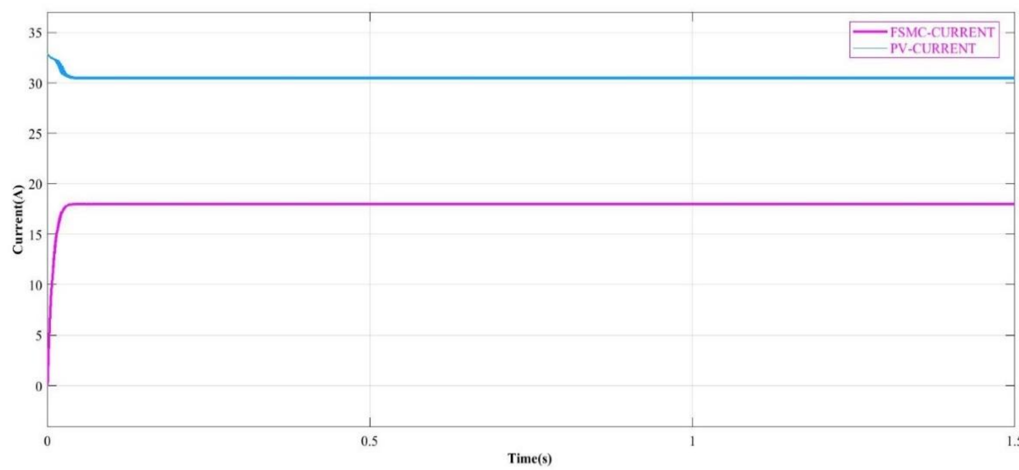

Figure 4.20 MPPT Output-Current of FSMC with uniform Temperature and Irradiation

The combination of fuzzy logic controller and sliding mode controller, known as the fuzzy-sliding mode controller, achieves the greatest benefits while minimizing the disadvantages of the sliding mode controller and the low efficiency of the fuzzy logic controller. The simulation result shown in figure 4.18 and table 4.4 confirms that the fuzzy-sliding mode controller has better tracking performance at all irradiation levels and reduces the oscillation or chattering phenomena around the maximum power point. Maximum power point tracking efficiency during sudden variations in irradiation is 99.97% in the fuzzy-sliding mode controller, 99.60% in the fuzzy logic controller, and 99.66% in the sliding mode controller. The fuzzy-sliding mode controller's method overcomes the chattering problem and yields very good performance compared to another algorithm.

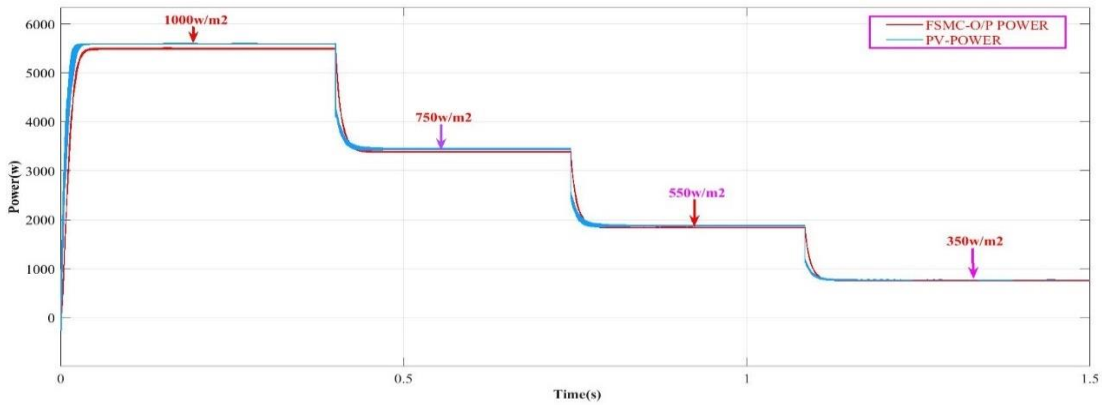

Figure 4.21 MPPT performance of FSMC with sudden variation of irradiation

Table 4.4 Performance of FSMC under different Irradiation and at 25^0C

Irradiance in W/m^2	Temperature (°C)	PV power Ppv(W)	Output power Po(W) with FSMC	Tracking Efficiency (%) $\frac{P_o}{P_{pv}}$	
350	25	765.3	756.6	98.86	
550	25	1879	1861	99.04	
750	25	3453	3441	99.65	
1000	25	5601	5599.5	99.97	
				Average	99.38

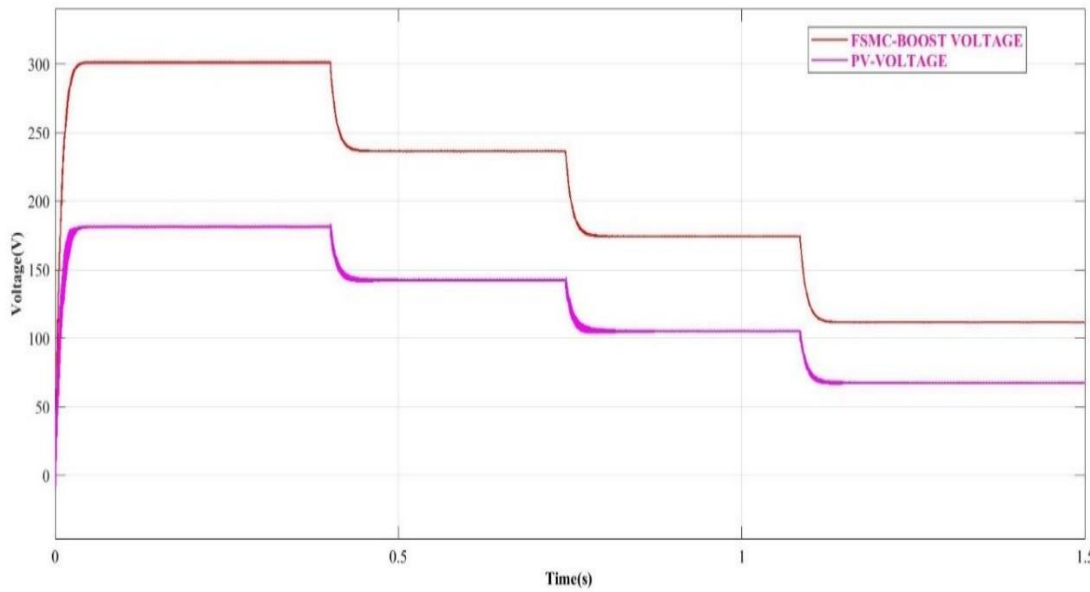

Figure 4.22 MPPT Voltage of FSMC with sudden variation of irradiation

In this thesis, a fuzzy sliding mode control (FSMC)-based maximum power point tracking strategy has been applied to a photovoltaic (PV) system. The main idea of the proposed technique is to combine the performance of fuzzy logic and sliding mode control in order to improve the generated power for a given set of weather conditions.

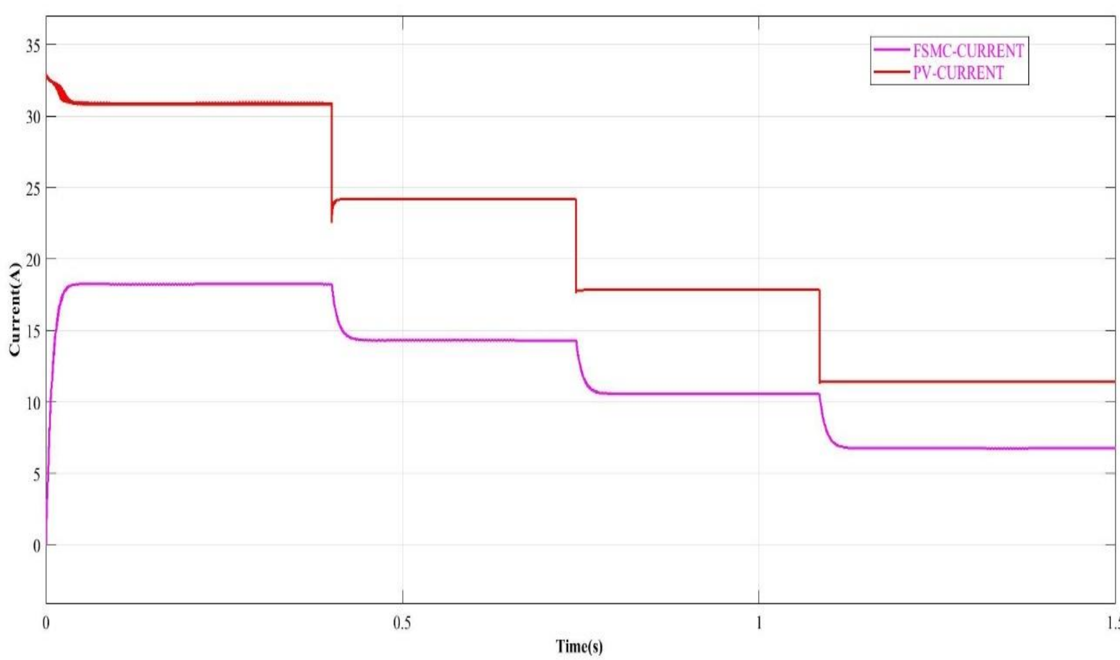

Figure 4.23 MPPT Current of FSMC with sudden variation of irradiation

Table 4.5 Performance of FSMC under different Temperature and at 1000W/m^2

Irradiance in W/m^2	Temperature (℃)	PV power Ppv(W)	Output power Po(W) with FSMC	Tracking Efficiency (%) $\frac{P_o}{P_{pv}}$
1000	25	5601	5599.5	99.97
1000	45	5056	5011	99.10
1000	55	4777	4712	98.64
1000	65	4450	4371	98.25
				Average 98.99

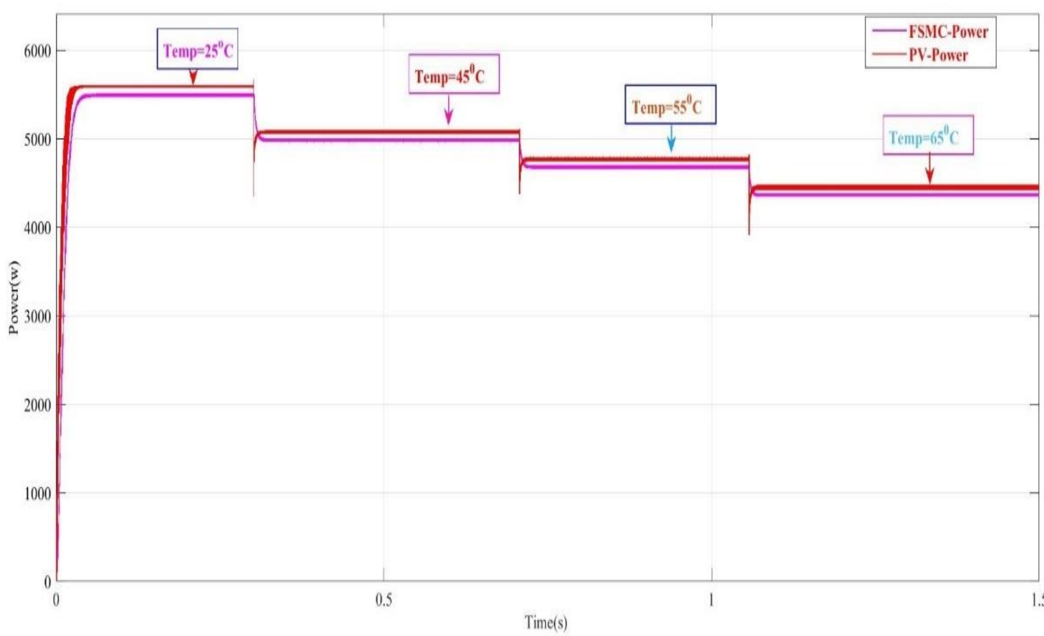

Figure 4.24 MPPT performance of FSMC with sudden variation of Temperature

Table 4.6 The performance MPPT algorithms at 25^0C and 1000W/m^2

MPPT	Temp(^{0}C)	Irradiance (W/m^2)	PV power Ppv(W)	Output power Po(W) with	Tracking Efficiency (%) $\frac{P_o}{P_{pv}}$
P and O	25	1000	5598	5525	98.70
FLC	25	1000	5556	5543	99.60
SMC	25	1000	5576	5557	99.66
FSMC	25	1000	5601	5599.5	99.97

Table 4.6 confirms that the fuzzy-sliding mode controller has better tracking performance at all irradiation levels and reduces the oscillation or chattering phenomena around the maximum power point. Maximum power point tracking efficiency during sudden variations in irradiation is 98.70% in the perturb and observe, 99.60% in the fuzzy logic controller, and 99.66% in the sliding mode controller and in the fuzzy-sliding mode controller 99.97%. The fuzzy-sliding mode controller's method overcomes the chattering problem and yields very good performance compared to another algorithm. The performance of the algorithms from table 4.6 are calculated using tracking efficiency output power over input power under STC(at 1000w/m^2 and at 25^oC).

Table 4.7 The performance of MPPT algorithms at different temperature and irradiance

MPPT	Tracking Efficiency (%) $\frac{P_o}{P_{pv}}$
P and O	98.20
FLC	98.69
SMC	99.01
FSMC	99.38

Table 4.7 confirms that the fuzzy-sliding mode controller has better tracking performance at all irradiation levels and reduces the oscillation or chattering phenomena around the maximum power point. Maximum power point tracking efficiency during sudden variations in irradiation is 98.20% in the perturb and observe, 98.69% in the fuzzy logic controller, and 99.01% in the sliding mode controller and in the fuzzy-sliding mode controller 99.38%. The fuzzy-sliding mode controller's method overcomes the chattering problem and yields very good performance compared to another algorithm. The performance of the algorithms from table 4.7 are calculated under different weather condition or this is the average of (350w/m^2, 550w/m^2, 750w/m^{2,} and 1000w/m^2) and temperature of (25^{o}C, 45^{o}C, 55^{o}C an 65^{o}C).

4.9 Simulation Result of BLDC Motor

The rotation speed of the motor is 1800 rpm, shown in figure 4.25 below.

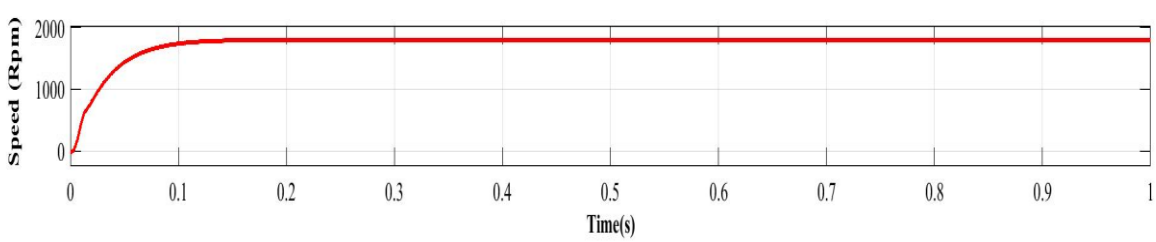

Figure 4.25 Rotation speed of motor

The 1800 rpm rotor speed of the BLDC motor is used as the set point, and the PI controller is given the error to adjust the real speed to this value. The decoder receives Hall Effect signals from the motor and transforms them into emf. The decoder's output from the gate pulse generator is used to create the gating pulse, which is then used to trigger the inverter.

Figure 4.26 shows the back emf generated by the motor pump group during operation. The variation of back emf is proportional to the rotational speed of the BLDC motor.

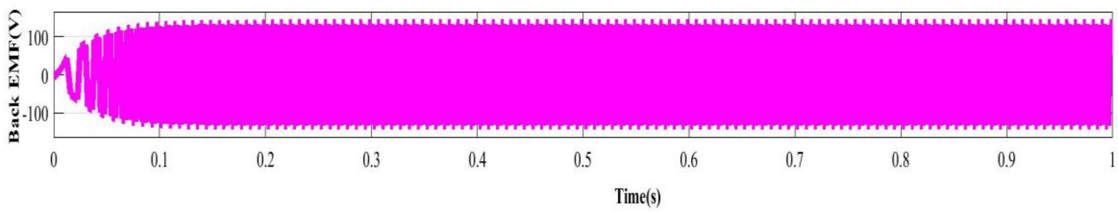

Figure 4.26 Back EMF

Figure 4.27 below shows the electromagnetic torque generated by the BLDC during the operation of the submersible pumps. Due to the type of electron commutation, which is based on Hall Effect sensors, the torque generated has ripples.

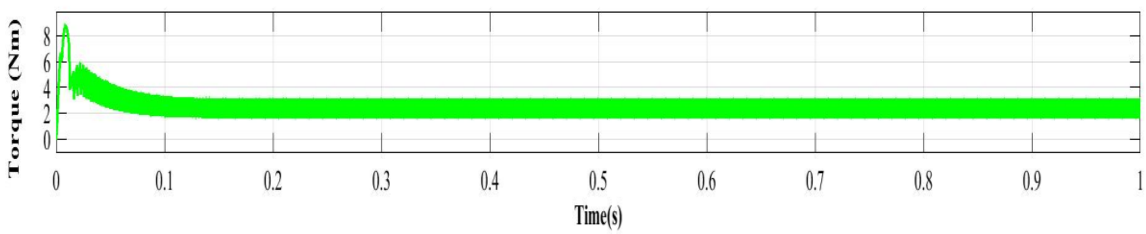

Figure 4.27 Electromagnetic Torque

The motor starts with a strong inrush current, but the steady current is approximately equal to 2.5 A, as seen in figure 4.28

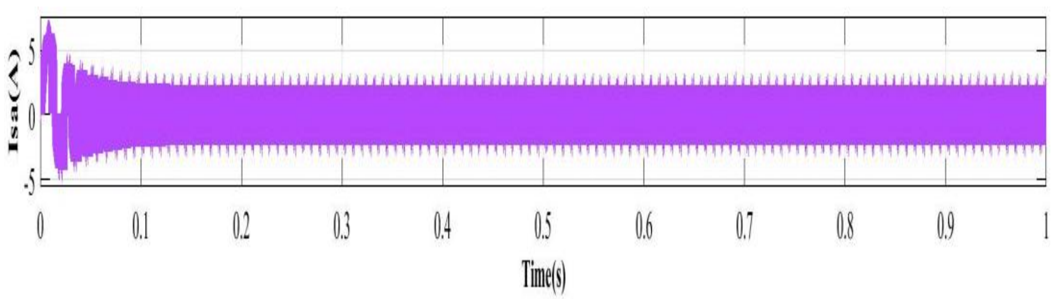

Figure 4.28 Stator Current

CHAPTER FIVE

CONCLUSION AND RECOMMENDATION

5.1 CONCLUSION

The best source of energy is solar energy, which naturally regenerates itself in a short amount of time and is referred to as renewable energy or sustainable energy. The Fuzzy Sliding Mode Controller for a Maximum Power Point Tracking Photovoltaic System for Water Pumping Applications is designed to increase the performance of solar MPPT and reduce the chattering phenomenon of sliding mode controllers. This thesis focuses mainly on how to improve the efficiency of solar systems by using an efficient MPPT algorithm.

A PV cell has a single operating point where the value of current and voltage results in the maximum power output. The MPPT process needs to be precise and quick in order to increase solar PV power extraction. The maximum power point (MPP) of solar panels, which is dependent on external parameters including temperature and irradiance, has a nonlinear voltage-current characteristic. Maximum power point tracking (MPPT), which maximizes the power output for a specific set of conditions, is crucial for PV power pumping systems in order to continually capture the maximum power from the solar panels. Using a fuzzy sliding control scheme, a standalone photovoltaic (PV) system can achieve maximum power point tracking. The main objectives of this controller are to increase the effectiveness of the PV power system and to achieve maximum power point operation without the requirement for atmospheric condition measurement.

A solar-cell array, a DC-DC converter, and a load comprise the PV water pumping system. The thesis focuses on increasing energy extraction by improving maximum Power Point tracking (MPPT). One of the most promising areas of photovoltaic applications is the use of photovoltaic energy as a source of energy for water pumping. From the simulation, the highest performance values of perturb and observe are 98.70%, and the highest performance or efficiency of SMC is 99.66%, the performance of fuzzy logic is 99.60% and the highest performance of fuzzy-sliding mode controller is 99.97%. Kyocera KC200G. In this thesis, 5.682 KW of power is designed for a BLDC solar water pumping system.

5.2 RECOMMENDATIONS AND FUTURE WORKS

In this thesis, simulation models were created and utilized to examine the effectiveness of the MPPT strategies employing P and O, the sliding mode controller, fuzzy logic, and fuzzy-sliding mode. The simulation results achieved in this work will hopefully incentivize future investigations involving the building of prototype models to test experimentally the developed MPPT techniques for the PV water pumping system, and among the proposed controllers, the hybrid controller shows better performance than the perturb and observe controllers, so it ought to be possible to apply these controllers in practical manners for PV water pumping systems. A final suggestion for future work is to connect the PV standalone system to the grid and make the necessary system adjustments to achieve a more comprehensive result of the actual generated electricity.

The boost converter serves as an interface in the present PV system, making it possible for the MPPT process to function. Future research could investigate some other converters such as buck-boost along with the proposed MPPT techniques to improve flexibility in the choice and configuration of PV array connections. Another point is to study the effect of changing both the temperature and irradiance at the same time, as that may occur in some instances, and its effect on the output power.

ACKNOWLEDGMENTS

This research thesis was funded by Adama Science and Technology University under the grant number ASTU/SM-R/565/22, Adama, Ethiopia.

REFERENCES

Abdul-Razzaq, I. K., Fahim Sakr, M. M., & Rashid, Y. G. (2021). Comparison of PV panels MPPT techniques applied to solar water pumping system. *International Journal of Power Electronics and Drive Systems*, *12*(3), 1813–1822. https://doi.org/10.11591/ijpeds.v12.i3.pp1813-1822

Aurairat, A., & Plangklang, B. (2022). *SS symmetry An Alternative Perturbation and Observation Modifier Maximum Power Point Tracking of PV Systems*.

B.Eteiba, M., T. El Shenawy, E., H. Shazly, J., & Z. Hafez, A. (2013). A Photovoltaic (Cell, Module, Array) Simulation and Monitoring Model using MATLAB®/GUI Interface. *International Journal of Computer Applications*, *69*(6), 14–28. https://doi.org/10.5120/11845-7579

Baramadeh, M. Y., Abouelela, M. A. A., & Alghuwainem, S. M. (2021). Maximum Power Point Tracker Controller Using Fuzzy Logic Control with Battery Load for Photovoltaics Systems. *Smart Grid and Renewable Energy*, *12*(10), 163–181. https://doi.org/10.4236/sgre.2021.1210010

Biadgie, G. (2021). *Design and Performance Analysis of Fuzzy Sliding Mode Controller for Maximum Power Point Tracking Photovoltaic Water Pumping System*.

Brahmi, A., Abounada, A., Chbirik, G., & Amrani, A. El. (2018). Design and optimal choice of a 1.5 kW photovoltaic pumping system for irrigation purposes. *AIP Conference Proceedings*, *2056*(December 2018). https://doi.org/10.1063/1.5084977

ÇELİKEL, R., & GÜNDOĞDU, A. (2021). Comparison of PO and INC MPPT Methods Using FPGA In-The-Loop Under Different Radiation Conditions. *Balkan Journal of Electrical and Computer Engineering*, *9*(2), 114–122. https://doi.org/10.17694/bajece.884815

Chinnamayan, V. (2020). *Design and Implementation of Sliding Mode MPPT and Fuzzy Logic MPPT in solar PV system DESIGN AND IMPLMENTATION OF FUZZY LOGIC AND SLIDING MODE MPPT CONTROLLER FOR SOLAR PV SYSTEM*. *December 2019*.

De Buck, E., Borra, V., De Weerdt, E., Vande Veegaete, A., & Vandekerckhove, P. (2015). A systematic review of the amount of water per person per day needed to prevent morbidity and mortality in (post-)disaster settings. *PLoS ONE*, *10*(5), 1–14. https://doi.org/10.1371/journal.pone.0126395

Derbeli, M., Barambones, O., & Sbita, L. (2018). A robust maximum power point tracking control method for a PEM fuel cell power system. *Applied Sciences (Switzerland)*, *8*(12). https://doi.org/10.3390/app8122449

Derri, M., Bouzi, M., Lagrat, I., & Baba, Y. (2016). *Fuzzy Sliding Mode Control for Photovoltaic System*. *7*(3), 964–973. https://doi.org/10.11591/ijpeds.v7.i3.pp964-973

Deshpande, V. P., & Bodkhe, S. B. (2017). Analysis of Various Connection Configuration of Photovoltaic Module under Different Shading Conditions. *International Journal of Applied Engineering Research*, *12*(16), 5715–5720. http://www.ripublication.com

El, A. (2017a). *Fuzzy sliding mode control for maximum power point tracking of a photovoltaic pumping system*.

Farhat, M., Barambones, O., & Sbita, L. (2016). A new maximum power point method based on a sliding mode approach for solar energy harvesting. *APPLIED ENERGY*. https://doi.org/10.1016/j.apenergy.2016.03.055

Gonal, P. V. S. (2016). *MPPT CONTROLLER USING SLIDING MODE CONTROL SCHEME FOR STAND ALONE PV SYSTEM*. *1*(8), 41–48.

Gouws, R., & Lukhwareni, T. (2012). *Factors influencing the performance and efficiency of solar water pumping systems : A review*. *7*(48), 6169–6180. https://doi.org/10.5897/IJPSX12.001

Hahm, J., Kang, H., Baek, J., Lee, H., & Park, M. (2015a). Design of incremental conductance sliding mode MPPT control applied by integrated photovoltaic and proton exchange membrane fuel cell system under various operating conditions for BLDC motor. *International Journal of Photoenergy*, *2015*. https://doi.org/10.1155/2015/828129

Hahm, J., Kang, H., Baek, J., Lee, H., & Park, M. (2015b). *Design of Incremental Conductance Sliding Mode MPPT Control Applied by Integrated Photovoltaic and Proton Exchange Membrane Fuel Cell System under Various Operating Conditions for BLDC Motor*. *2015*.

Islam, H., Mekhilef, S., Shah, N. B. M., Soon, T. K., Seyedmahmousian, M., Horan, B., & Stojcevski, A. (2018). Performance evaluation of maximum power point tracking approaches and photovoltaic systems. *Energies*, *11*(2), 7–9. https://doi.org/10.3390/en11020365

Kadeval, H. N., & Patel, V. K. (2020). *Comparison of Advanced MPPT Technique for*

Photovoltaic System. *7*(1), 14–26. https://doi.org/10.17148/IARJSET.2020.7103

Kayisli, K. (2023). Super twisting sliding mode-type 2 fuzzy MPPT control of solar PV system with parameter optimization under variable irradiance conditions. *Ain Shams Engineering Journal*, *14*(1), 101950. https://doi.org/10.1016/j.asej.2022.101950

Kchaou, A., Ayadi, A., Naamane, A., M'Sirdi, N., & Koubaa, Y. (2017). An Adaptive Sliding Mode Control based Maximum power point tracking method for a PV stand-alone system. *2017 6th International Conference on Systems and Control, ICSC 2017*, 69–74. https://doi.org/10.1109/ICoSC.2017.7958702

Khazane, J. El, & Tissir, E. H. (2018). *Achievement of MPPT by fi nite time convergence sliding mode control for photovoltaic pumping system*. *166*(March), 2017–2019.

Krishnakant, & Kulkarni, P. S. (2021). Design and Simulation of Solar Photovoltaic Water Pumping System. *3rd International Conference on Energy, Power and Environment: Towards Clean Energy Technologies, ICEPE 2020*, *3*(9), 2208–2213. https://doi.org/10.1109/ICEPE50861.2021.9404473

Kumar, B. S., Hora, B., Hora, B., & Hora, B. (2020). *SEPIC CONVERTER WITH PV SYSTEM BLDC MOTOR CONTROL FOR BIDIRECTIONAL POWER*. *7*(11), 3962–3967.

Kumar, S., & Kumar, S. (2020). Solar Pv Powered Water Pumping System Using Dc Motor Drive: a Critical Review. *International Journal of Technical Research & Science*, *05*(04), 1–8. https://doi.org/10.30780/ijtrs.v05.i04.001

Kumarasamy, K., I, K. S. R., M, B. N. S., & Mahesh, G. (2017). *BLDC Motor and Zeta Converter*. 3869–3877. https://doi.org/10.15680/IJIRSET.2017.0603157

Kurian, A. A. N. U. (2014). *Sliding Mode Control Based Power Point Tracking of*. *10*(August), 94–96. https://doi.org/10.9790/1676-10425863

Kute, U. T. (n.d.). *ISSN : 2278-6252 LITERATURE SURVEY ON MAXIMUM POWER POINT TRACKING (MPPT) TECHNIQUE FOR PHOTOVOLTAIC (PV) SYSTEM I . INTRODUCTION*. *2*(12), 13–29.

Magaji, N., Wazir, M., Mustafa, B., Lawan, A. U., Tukur, A., Abdullahi, I., & Marwan, M. (2022). *Application of Type 2 Fuzzy for Maximum Power Point Tracker for Photovoltaic System*. 1–25.

Miqoi, S., Ougli, A. El, & Tidhaf, B. (2019). *Adaptive fuzzy sliding mode based MPPT* *controller for a photovoltaic water pumping system*. *10*(1), 414–422. https://doi.org/10.11591/ijpeds.v10.i1.pp414-422

Mondal, S., Mitra, A., & Chattopadhyay, M. (2015). *Mathematical modeling and simulation of Brushless DC motor with ideal Back EMF for a precision speed control*.

Moussa, A. Y., Kuloba, P., & Kiplimo, R. (2019). *Assessment of Water Pumping System Powered By Solar Pump in Dry Areas*. *4*, 2859–2866. https://doi.org/10.35940/ijrte.D6950.118419

Mule, S. M., & Sankeshwari, S. S. (2015). *Sliding Mode Control based Maximum Power Point Tracking of PV System*. *10*(4), 58–63. https://doi.org/10.9790/1676-10425863

Muralidhar, K. (2021). *A review of various components of solar water-pumping system : Configuration , characteristics , and performance*. *June*, 1–33. https://doi.org/10.1002/2050-7038.13002

Nakuçi, L., & Spahiu, A. (2018). Saving Energy by Replacing IM with BLDC Motor in Fan Application. *European Journal of Electrical Engineering and Computer Science*, *2*(5), 31–37. https://doi.org/10.24018/ejece.2018.2.5.27

Narendiran, S. (2016). *Control and Analysis of MPPT Techniques for Maximizing Power Extraction and Eliminating Oscillations in PV System*. *16*, 107–118.

Nguyen, X. H., & Nguyen, M. P. (2015). Mathematical modeling of photovoltaic cell/module/arrays with tags in Matlab/Simulink. *Environmental Systems Research*, *4*(1). https://doi.org/10.1186/s40068-015-0047-9

Prabhakaran, A., & Mathew, A. S. (2016). *Sliding Mode MPPT Based Control For a Solar Photovoltaic system*. 2600–2604.

Raghuwanshi, S. S., & Khare, V. (2018). Sizing and modelling of stand-alone photovoltaic water pumping system for irrigation. *Energy and Environment*, *29*(4), 473–491. https://doi.org/10.1177/0958305X17752739

Ramachandra Rao, C. V., Siva Rama Ganesh, M., Sekhar, K. C., Pradeep Sudha, R., Dangeti, L. K., & Sarathbabu Duvvuri, S. (2019). A Generalized MPPT Controlled DC-DC Boost Converter for PV System Connected to Utility Grid. *2019 Innovations in Power and Advanced Computing Technologies, i-PACT 2019*, 1–5. https://doi.org/10.1109/i-PACT44901.2019.8960061

Ravi, A., & Sultana, S. (2019). *A Simulated Study on SOLAR PV Powered BLDC and*

Induction Motor Drive. 2601–2610. https://doi.org/10.15662/IJAREEIE.2019.0812002

Rayaguru, N. K., & Sekar, S. (2017). *Photovoltaic Fed Brushless DC Motor Aided Water Pumping System*. *10*(03), 245–255.

Reddy, K. H., Vijayasanthi, R., & Ramasudha, K. (2020). *Modeling and Performance Analysis of Perturb and Observe (P & O), Incremental Conductance (IC), Fuzzy Logic , and Model Predictive MPPT Controllers Using a Boost Converter*. *5*(12).

Rihani, A. T., & Ghandchi, M. (2015). *Increasing the Efficiency of Photovoltaic Systems by Using Maximum Power Point Tracking (MPPT)*. *4*(14).

Rodrigues, E. M. G., Godina, R., Marzband, M., & Pouresmaeil, E. (2018). Simulation and comparison of mathematical models of PV cells with growing levels of complexity. *Energies*, *11*(11). https://doi.org/10.3390/en11112902

Salim, D. (2018). *Performance Improvement of Photovoltaic Pumping System*.

Sameeullah, M., & Swarup, A. (2016). *MPPT Schemes for PV System under Normal and Partial Shading Condition : A Review*. *5*(2), 79–94. https://doi.org/10.14710/ijred.5.2.79-94

Sethy, B., & Maity, S. (2010). *Application of Sliding Mode Technology in Pv Maximum Power Point Tracking System*.

Shajilal, P. A. S., & Julian, N. (2017). *Torque Ripple Reduction Method for BLDC Motor for SPV fed Water Pumping System Employing Zeta Converter*. 1188–1195. https://doi.org/10.15662/IJAREEIE.2017.0603035

Shebani, M. M., & Iqbal, T. (2017). *Dynamic Modeling , Control , and Analysis of a Solar Water Pumping System for Libya*. *2017*.

Singh, B., & Kumar, R. (2016). Solar PV array fed brushless DC motor driven water pump. *2016 IEEE 6th International Conference on Power Systems, ICPS 2016*, 0–4. https://doi.org/10.1109/ICPES.2016.7584057

Singh, B., & Mishra, A. K. (2015). *Utilization of Solar Energy for Driving a Water Pumping System*. 1284–1288.

Singhal, A. K., Beniwal, N. S., Almutairi, K., & Dhanraj, J. A. (2021). *Experimental Analysis of Modified DC-P & O Technique with*.

Situmorang, M., Brahmana, K., & Tamba, T. (2019). Solar Charge Controller Using Maximum Power Point Tracking Technique. *Journal of Physics: Conference Series*, *1230*(1), 97–113. https://doi.org/10.1088/1742-6596/1230/1/012090

Solar, G., & Initiative, W. (2017). *SOLAR PUMPING GUIDELINES FOR SUDAN*. *March*, 1–19.

Solomon, Y., Rao, P. N., & Tadesse, T. (2021). *A Review on Solar Photovoltaic Powered Water Pumping System for off-Grid Rural Areas for Domestic use and Irrigation Purpose*. *10*(02), 258–269.

Spandana, T., & Kanchikere, J. (2018). *Grid Interfaced Solar PV Based BLDC Motor Driven Water Pump*. *5*(4), 5–7.

Subbarao, K. V, & Kalyan, K. J. V. S. P. (2021). *Comparitive Analysis of a MPPT Control Techniques*. *4*(11), 163–167.

Teo, J. C., Tan, R. H. G., & Tan, C. (n.d.). *Impact of Partial Shading on the P-V Characteristics and the Maximum Power of a Photovoltaic String*. https://doi.org/10.3390/en11071860

Wasekar, R., & Chamat, N. (2020). *Implementation of Simulink and Hardware System of MPPT by using Fuzzy Logic Control in Solar*. 2045–2049.

What is a Solar Pump : Working & Its Applications What is a Solar Pump ? (2021). 8051.

Zhang, M., Zhong, N., & Ma, M. (2021). Sliding mode control of SEPIC converter based photovoltaic system. *Systems Science and Control Engineering*, *9*(S2), 112–118. https://doi.org/10.1080/21642583.2021.1872043

APPENDIXES

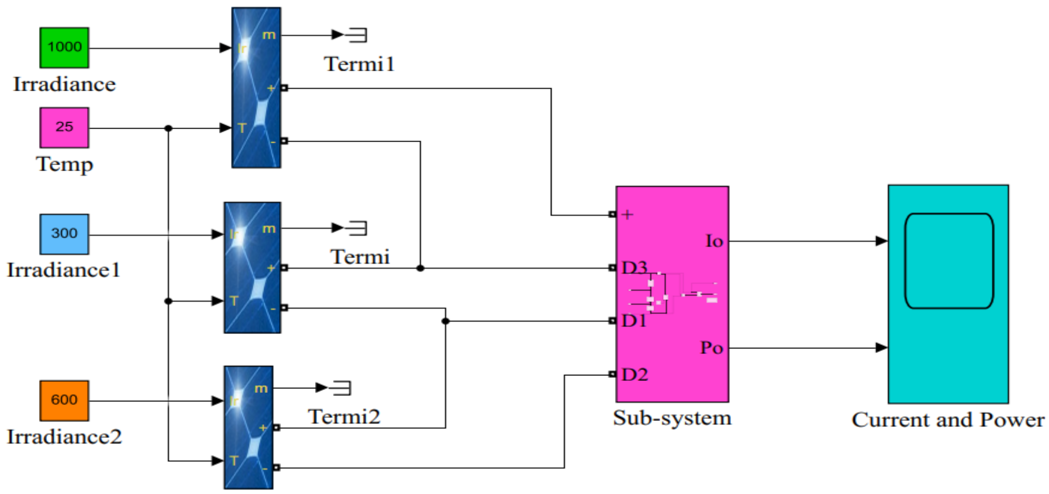

Appendix A: Matlab /Simulink Model of Partial Shading

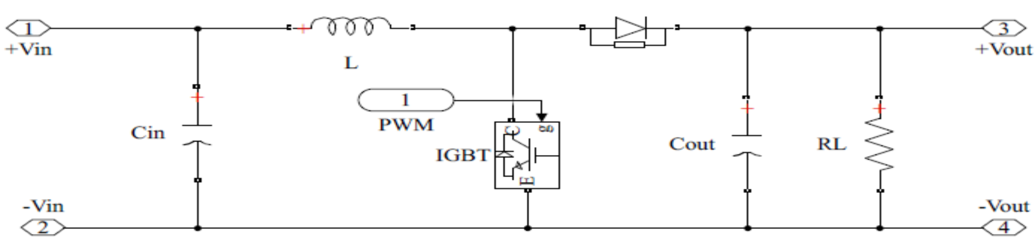

Appendex B: Figure of Boost Converter

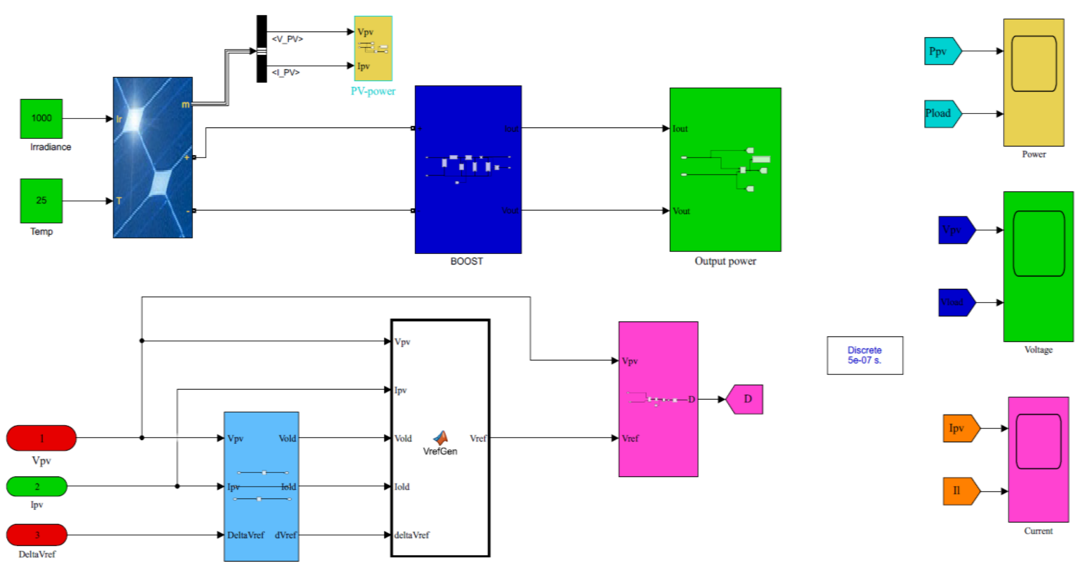

APPENDEX C: Simulink Model Sliding Mode Controller

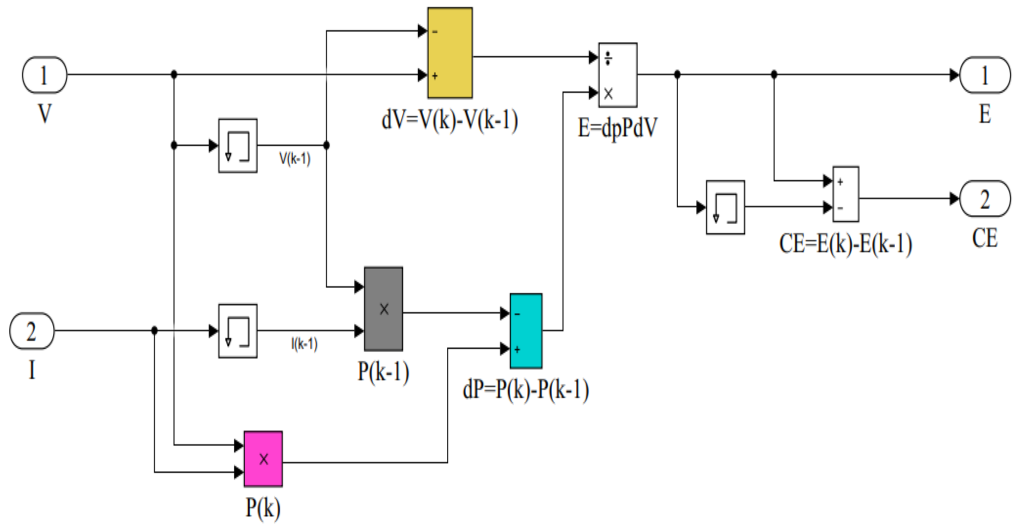

Appendix D: Figure Simulink model E and CE

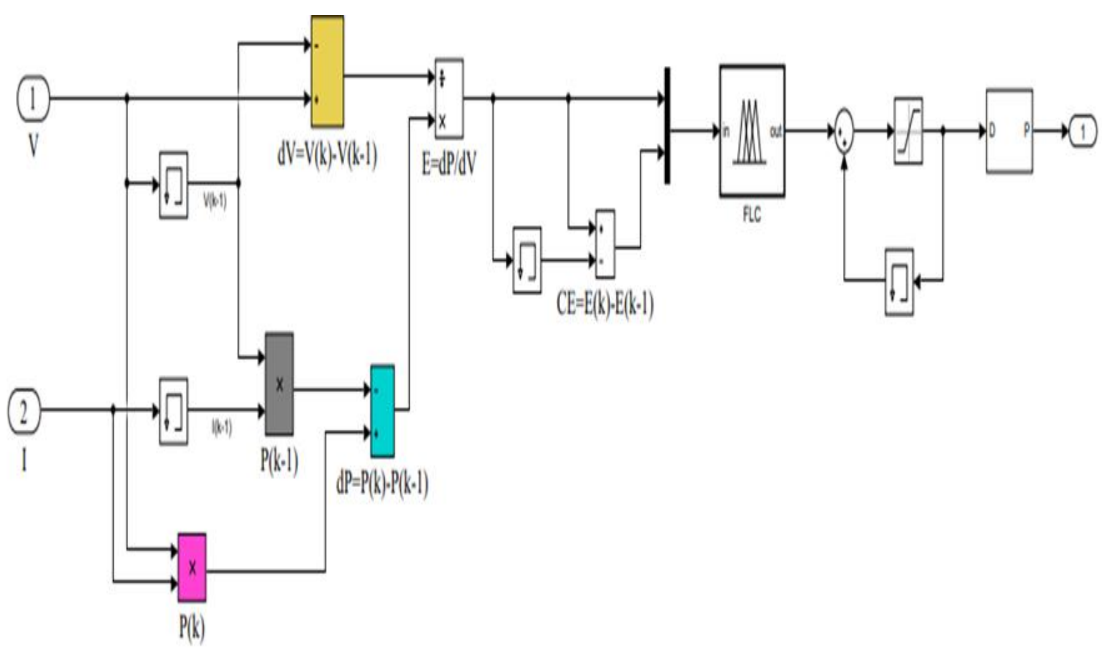

APPENDEX E: Matlab Simulink of Fuzzy Logic Controller

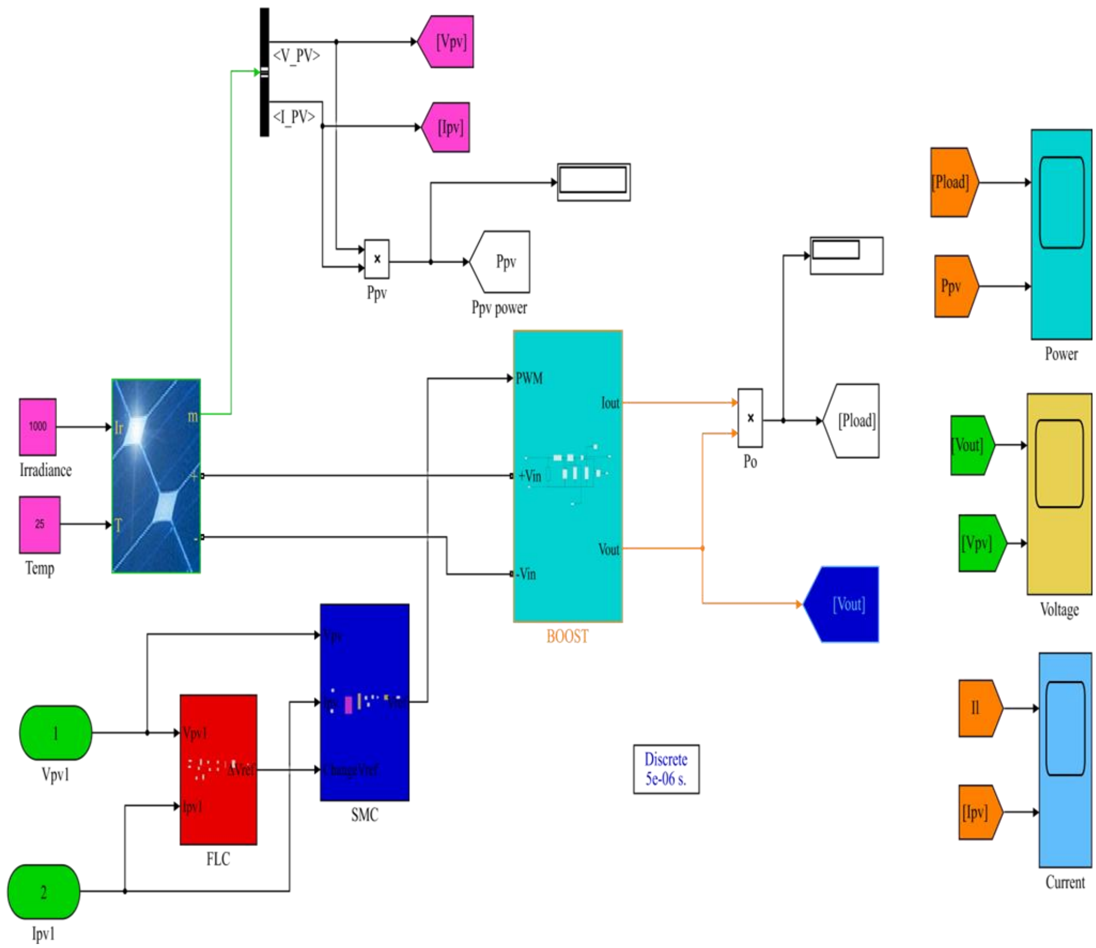

APPENDEX F: Figure for Model of Fuzzy-Sliding Mode Controller

APPENDEX G: Matlab Code of Perturb and Observe MPPT Algorithm

```
function D = fcn(vpv,ipv)
Dinit=0.4;
Dmax=0.51;
Dmin=0.1;
deltaD=0.001;
persistent Vold Pold Dold
dataType="Double";
if isempty(Vold)
   Vold=375;
   Pold=5604;
   Dold=Dinit;
end
P=vpv*ipv;
dV=vpv-Vold;
dP=P-Pold;
if dP~=0
   if dP<0
      if dV<0
         D=Dold-deltaD;
      else
         D=Dold+deltaD;
      end
   else
      if dV<0
         D=Dold+deltaD;
      else
         D=Dold-deltaD;
      end
   end
else D=Dold;
```

```
end
if D>=Dmax|D<=Dmin
   D=Dold;
end
Dold=D;
Vold=vpv;
Pold=P;
```

APPENDEX H: Matlab code for MPP Searching

```
function Vref= VrefGen(Vpv,Ipv,Vold,Iold,deltaVref)
Vrefmax=184.1;
Vrefmin=0;
Vrefinit=133;
dV=Vpv-Vold;
dI=Ipv-Iold;
if(dV==0)
if(dI==0)
Vref=Vpv;
else
if(dI>0)
Vref=Vold+deltaVref;
else
Vref=Vold-deltaVref;
end
end
else
if(dI/dV==(-Ipv/Vpv))
Vref=Vpv;
else
if((dI/dV)>(-Ipv/Vpv))
Vref=Vold+deltaVref;
else
```

```
Vref=Vold-deltaVref;
end
end
end
if Vref>=Vrefmax||Vref<=Vrefmin
Vref=Vrefinit;
end
```